

Oxygen metabolism in restored eelgrass (*Zostera marina* L.) meadows measured by eddy correlation.

Jennie Elizabeth Rheuban  
Charlottesville, VA

B.A., University of Virginia, 2010

A Thesis Presented to the Graduate Faculty  
of the University of Virginia in Candidacy for the Degree of  
Master of Science

Department of Environmental Science

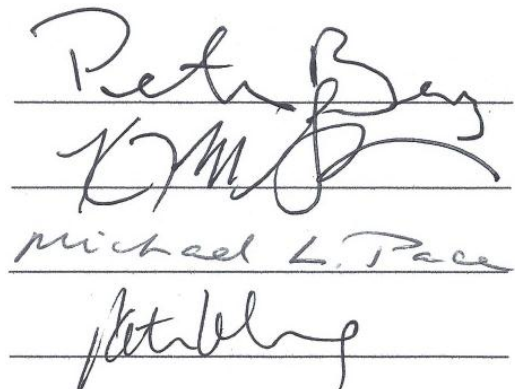
University of Virginia  
May, 2013

Peter Berg (co-advisor)

Karen J. McGlathery (co-advisor)

Michael L. Pace

Patricia L. Wiberg (Out of discipline representative)



The block contains four handwritten signatures, each on a horizontal line. From top to bottom: 1. 'Peter Berg' in cursive. 2. 'KJ McGlathery' in cursive. 3. 'Michael L. Pace' in cursive. 4. 'Patricia L. Wiberg' in cursive.

## **Abstract**

Primary productivity in seagrass meadows is an important factor to consider in coastal systems as it can support economically important industries such as finfish and shellfish fisheries. Seagrass meadows are significant to global carbon budgets and represent an important carbon sink through biomass and burial. They are declining worldwide, and restoration can return this important ecosystem to coastal environments. Therefore, studying the drivers of seagrass productivity and how net ecosystem metabolism (NEM) changes with colonization is warranted to understand the effects of restoration on the ecosystem services provided by seagrass meadows.

This thesis addresses the effects of seagrass restoration on oxygen metabolism using the eddy correlation technique (EC). Aquatic EC provides high temporal resolution measurements of NEM that integrates over a large spatial scale and does not alter the local hydrodynamics or light environment. As aquatic EC is relatively new, I investigated the capabilities of this method to incorporate heterogeneous fluxes using a 3-dimensional numerical model to provide guidance for measurements in patchy seagrass meadows. The results showed that by following certain empirical guidelines, heterogeneous fluxes are well-integrated, and eddy correlation measurements reflect ecosystem-scale fluxes. Using EC, I found that light, flow, and temperature were the major ecosystem-scale drivers of oxygen metabolism in seagrass meadows. From seasonal measurements, I found feedback processes occurring at multiple timescales – hourly, daily, and seasonal. Metabolism in both light and dark increased with seagrass colonization, suggesting that

seagrass meadows are hotspots of both autotrophic and heterotrophic production. From high temporal resolution data, annual NEM was modeled based on available light for every hour throughout the year and showed young seagrass meadows were autotrophic while older meadows were heterotrophic. The annual NEM combined with trajectories of seagrass shoot density since 2007 indicate that young meadows were becoming denser and accumulating biomass while older meadows may be maintaining a critical biomass. Although the older meadow was heterotrophic on an annual scale, it was not different from the unvegetated sediments. While this restoration has increased the magnitude of productivity and provided other important ecosystem services, it has not altered the net rates of benthic metabolism in the lagoons.

## Table of Contents

Abstract .....	i
Table of Contents .....	iii
List of Figures .....	vii
List of Tables .....	viii
Acknowledgements .....	ix
Introduction .....	1
O <sub>2</sub> metabolism in seagrass meadows .....	2
Light control on seagrass metabolism .....	2
Temperature control on seagrass metabolism .....	2
Epiphyte effects on seagrass metabolism .....	3
Sediment metabolism in seagrass meadows .....	4
Carbon budgets .....	5
Motivation .....	6
Research Questions .....	7
Chapter 1: How well do eddy correlation measurements integrate heterogeneous fluxes and how quickly will rapid changes in the O <sub>2</sub> flux be registered in eddy correlation fluxes? .....	7
Chapter 2: What are the primary drivers of ecosystem production and respiration in seagrass meadows and how do they change seasonally? .....	8

Chapter 3: How does ecosystem metabolism change with seagrass colonization?.....	9
References .....	10
 Chapter 1 : The effects of spatial and temporal variability at the sediment surface on aquatic eddy correlation flux measurements.....	16
Acknowledgements .....	17
Abstract .....	18
Introduction .....	19
Materials and Procedures .....	19
Numerical Solution.....	21
Heterogeneous fluxes .....	21
Response Time .....	22
Regression Analysis .....	24
Example from Glud et al. 2010 .....	24
Assessment .....	25
Numerical solution .....	25
Heterogeneity.....	25
Response Time .....	27
Example from Glud et al. 2010 .....	28

	v
Discussion .....	28
Comments and Recommendations .....	31
References .....	33
Figures .....	36

## Chapter 2 : Seasonal oxygen metabolism in restored *Zostera marina* L. (eelgrass)

meadows measured by eddy correlation .....	45
Acknowledgements .....	46
Abstract .....	47
Methods .....	50
Study site .....	50
Results .....	55
Eddy correlation analysis.....	55
Ecosystem metabolism in eelgrass meadows .....	56
Discussion .....	58
References .....	64
Figures .....	72

Chapter 3 : Ecosystem metabolism along a colonization gradient of eelgrass ( <i>Zostera marina</i> L.) measured by eddy correlation. ....	80
Acknowledgements .....	81
Abstract .....	82
Introduction .....	83
Methods .....	85
Study site .....	85
Data Collection .....	86
Data analysis .....	89
Results .....	91
Discussion .....	94
Productivity and Respiration .....	94
Modeling net ecosystem metabolism .....	94
References .....	103
Figures .....	111
Significance.....	122
Appendix 1 – Water column metabolism .....	125
Appendix 2 – Benthic Chlorophyll A .....	127

	vii
Appendix 3 – Waves.....	129
Appendix 4 – Data .....	131

## List of Figures

Figure 1.1 Conceptual model of heterogeneity effects. ....	36
Figure 1.2 Example model results. ....	37
Figure 1.3 Regression analysis for flux heterogeneity.....	39
Figure 1.4 Example model run for response time.....	41
Figure 1.5 Regression analysis for response time.....	42
Figure 2.1 Example deployment from June 2012.....	72
Figure 2.2 Two eddy correlation instruments side-by-side. ....	73
Figure 2.3 Example use of storage in flux calculation.....	74
Figure 2.4 Seasonal hourly fluxes and light.....	75
Figure 2.5 Flow stimulation of night respiration. ....	76
Figure 2.6 Hourly average O <sub>2</sub> flux vs. light for October 2011. ....	77
Figure 2.7 Daily gross primary production vs. respiration. ....	78
Figure 2.8 Seasonal average metabolism and shoot density.....	79
Figure 3.1 Seasonal metabolism across sites. ....	111
Figure 3.2 Late summer metabolism from South Bay from Hume et al.....	112



	viii
Figure 3.3 Photosynthesis-irradiance curves from 11 year site. ....	113
Figure 3.4 Photosynthesis-irradiance curves from 4 year site. ....	114
Figure 3.5 Light compensation vs. temperature.....	115
Figure 3.6 Incident light vs. canopy light. ....	116
Figure 3.7 Daily light and net ecosystem metabolism for 4 and 11 year sites. ....	117
Figure 3.8 Cumulative daily metabolism for all sites. ....	118
 Figure A.2.1 Benthic chlorophyll concentration with depth into sediment.....	 127

## List of Tables

Table 1.1 Model input parameters. ....	44
 Table 3.1 Site characteristics. ....	 119
Table 3.2. Comparison of sediment cores and eddy correlation technique. ....	120
Table 3.3 Measured vs. modeled seasonal NEM. ....	121
 Table A.1.1 Water column metabolism. ....	 125
Table A.3.1 Seasonal correlation of O <sub>2</sub> fluxes with wave height. ....	129
Table A.4.1 Daily fluxes from 11 year site.....	131
Table A.4.2 Daily fluxes from 5 year site.....	132
Table A.4.3 Daily fluxes from bare site.....	133

## **Acknowledgements**

I am grateful to the many individuals without whom this research would not have been possible. First, I would like to thank my advisors Peter Berg and Karen McGlathery, who have been instrumental in their support, generosity, design and implementation of this project. I would also like to thank my committee members Mike Pace and Pat Wiberg for their helpful advice in the data analysis of this project and others.

I am especially indebted to the staff of the Anhauser-Busch Coastal Research Center, for without their help, the data collection of this research would not have been possible. I specifically want to thank Chris Buck for his help and support in the field, especially during poor weather and winter months. I also want to thank Matt Long for his friendship and support, for teaching me the enjoyment of field work, for his countless hours of help in processing eddy correlation data, preparing for field excursions and for his help in writing and editing this manuscript.

I would also like to thank the members of the McGlathery and Berg labs for their support and friendship. They have also been invaluable in helping me write, edit, and prepare the manuscripts of this thesis for publication. I am also thankful for my parents, Karen and Bill, and my brothers, Jonathan and Andy, for their unending enthusiasm and support throughout this process.

## **Introduction**

Seagrasses are marine plants that are ubiquitous to nearly all shallow coastal systems across the globe. They provide numerous ecosystem services, including improving water quality by acting as a coastal filter for nutrient inputs off the land and reducing the potential for harmful algal blooms to occur (McGlathery et al. 2007). Seagrass meadows improve water clarity by preventing resuspension through sediment stabilization by a strong root/rhizome system, and by physically slowing currents and wave action by creating friction against the flow by the thick leaf canopy (Fonseca and Fischer 1986, Hansen and Reidenbach 2012). Their complex structure and calm environment also provides a nursery habitat for aquatic organisms, including many commercially important shellfish and finfish (Hemminga and Duarte 2000). Seagrass leaves also create a solid substrate for the growth of epiphytes which support lower trophic organisms (Mook 1977; Caine 1980; van Montfrans et al. 1984). Seagrasses have been shown to increase sediment bacterial respiration through higher labile organic stocks within the sediments and may in turn alter nutrient availability and turnover rates (Wetzel and Penhale 1983, Cole and McGlathery 2012). Seagrass ecosystems are declining in many systems globally (Orth et al. 2006, Waycott et al. 2009), thus understanding the environmental drivers of their productivity is important for predicting future seagrass abundance and the potential loss in essential ecosystem services.

## **O<sub>2</sub> metabolism in seagrass meadows**

### *Light control on seagrass metabolism*

Seagrass photosynthesis is dependent on available light, and can be described as a function of irradiance reaching the leaves by several different functions to describe the same general curvilinear shape (Aalderink and Jovin 1997). Photosynthesis-irradiance (P-I) relationships are well documented for many different seagrass species (Congdon and McComb 1979; Goodman et al. 1995; Mazzella and Alberte 1997; Gacia et al. 2005; Binzer et al. 2006; Staehr and Borum 2011). However, many of these studies were completed using lab incubations of components of plant tissues or whole plants and may not capture the variability due to in situ flow and light environments. Due to attenuation of light by the water column and self-shading by the leaf canopy, the surface of the canopy may be light saturated while the understory does not experience saturation or photoinhibition (Binzer et al. 2006, Sand-Jensen et al. 2007). Because of the complex nature of seagrass canopies, photon absorption and thus photosynthesis is higher at the canopy level than determined at the leaf level. Thus, the integrated ecosystem response to light may be much different from the single plant or tissue response.

### *Temperature control on seagrass metabolism*

Seagrass metabolic rates, in particular *Zostera marina* L., are also strongly dependent on temperature, and high temperatures can cause total mortality (Moncreiff et al. 1992; Olesen and Sand-Jensen 1993; Höffle et al. 2010; Ouisse et al. 2011; Staehr and Borum 2011). For example, where *Z. marina* can be found in Baja California, the seagrass avoids high summer temperatures by acting as a winter annual plant (Meling-

Lopez and Ibarra-Obando 1999). The strong dependence on temperature shown by *Z. marina* can be a key driver of metabolism at the cellular, plant, and community level. At the cellular level, deviations from optimal temperatures can cause slow enzymatic responses, reducing cellular metabolic rates (Staeher and Borum 2011). High temperatures can denature key proteins for photosynthesis, limiting metabolic rates during late summer (Staeher and Borum 2011). At the plant level, seagrass photosynthesis-irradiance relationships have been shown to be strongly seasonal, with plant respiration more sensitive to temperature than photosynthesis (e.g. Masini and Manning 1997; Staeher and Borum 2011). This increase in plant respiration with warmer temperatures causes a shift in the light compensation point such that the community may require significantly more light in order to maintain a positive carbon balance (Moncreiff et al. 1992; Olesen and Sand-Jensen 1993; Moore et al. 1997; Höffle et al. 2010; Ouisse et al. 2011; Staeher and Borum 2011). This process can cause large changes in areal coverage through either sloughing of aboveground tissue or complete die off annually.

#### *Epiphyte effects on seagrass metabolism*

Seagrasses are an important substrate for epiphytic algal growth in marine systems. A thin veneer of epiphytic algae can be beneficial for seagrass as a veneer of epiphytes may block harmful UV radiation from the seagrass leaves themselves and prevent photoinhibition (van Montfrans et al. 1984). However, in locations with high epiphytic growth on seagrass blades as is common in nutrient-enriched habitats, total light reaching the seagrass leaves may be significantly reduced, slowing growth, either through reducing uptake of bicarbonates for photosynthesis or increasing diffusive boundary layers inhibiting gas diffusion (Sand Jensen et al. 1977; van Montfrans et al.

1984). In some meadows, depending on local nutrient loading, epiphytic algae can be anywhere from 1 – 70% of the total biomass and from 8 – 56% of the total production found in seagrass meadows (van Montfrans et al. 1984; Moncreiff et al. 1992). Epiphytes also support lower trophic organisms residing within seagrass meadows, and grazing may be a significant control on epiphytic growth in many systems (Mook 1977; Caine 1980; van Montfrans et al. 1984).

#### *Sediment metabolism in seagrass meadows*

The presence of seagrass will alter sediment metabolic rates significantly through several processes. Seagrasses increase sediment carbon stocks (Duarte et al. 2011, McGlathery et al. 2012) by importing fine particulate matter through a reduction in water velocity that allows for particle settling (Fonseca and Fisher 1986, Hansen and Reidenbach, 2012) and by exuding dissolved organic matter (DOM) from the roots (Dillon 1971; Harlin 1973; Penhale and Smith 1977, Long et al. 2008). This exuded DOM is highly labile and can enhance a variety of microbial processes including oxygen consumption, nitrogen fixation and sulfate reduction (McGlathery et al. 1998; Eyre et al. 2011, Cole and McGlathery 2012). Many studies have found that seagrasses in both temperate and tropical environments increased the benthic fluxes of ammonium and nitrate, phosphorous, O<sub>2</sub>, and DIC when compared to non-vegetated sites (e.g. McGlathery et al. 1998, Eyre et al. 2011, Hume et al. 2011; Duarte et al. 2010) which can provide more nutrients for either seagrasses, epiphytes, or benthic microalgal communities. Seagrasses will also change the availability of O<sub>2</sub> within the sediments, as seagrass roots exude O<sub>2</sub> at the growing root tips, providing hotspots for aerobic microbial

activity to occur at depths that would generally be anoxic (Frederiksen and Glud 2006).

Increased oxygenation combined with higher organic material can lead to increased sediment respiration in seagrass meadows relative to unvegetated sediments (Apostolaki et al. 2010, Hume et al. 2011).

### *Carbon budgets*

Oxygen metabolism can be used as a proxy for CO<sub>2</sub> metabolism, and understanding the metabolic state of a system can help determine the relative effect on regional or even global cycling of CO<sub>2</sub>. Some studies suggest that seagrasses can have a large role in enhancing the uptake of CO<sub>2</sub> from the oceans (Short et al. 2007) by producing large quantities of recalcitrant organic matter in their roots, rhizomes, and leaf tissues (Enriquez et al. 1993). This suggests seagrasses have a high capacity for sequestering carbon, yet the high rates of sediment respiration associated with the presence of seagrasses may cause seagrass meadows to be net heterotrophic on a daily or annual basis (Barron et al. 2004). Although 37% of seagrass meadows have been found to be net heterotrophic on a global scale (Duarte et al. 2010), seagrass meadows still have a large capacity to be a carbon sink (Duarte et al. 2011). Many studies of seagrass carbon balances suggest that the import of carbon through deposition or the stripping of organic matter from the water column (Hendriks et al. 2008) exceeds the carbon consumption by the meadows, resulting in carbon burial into the sediments although the systems may have a net heterotrophic ecosystem metabolism (Duarte et al. 2010, 2011).

## Motivation

The Virginia Coast Reserve (VCR) Long Term Ecological Research site is the location of a successful seagrass restoration project. The coastal bays of the VCR experienced a complete loss of seagrass in the late 1920s through a slime mold followed by a hurricane in 1933 (Cottam and Munro 1954). Since 2001, a large-scale restoration effort has successfully restored over 1700 ha of seagrass to these coastal bays, and the meadows are continuing to expand (Orth et al. 2006, 2010, 2012). There have been increasing trends in summer shoot density and sediment organic content with time since seeding (McGlathery et al. 2012). This suggests that ecosystem metabolism will be altered as well, although only one other study has looked at changes in ecosystem metabolism at the VCR with a state change from unvegetated sediments to seagrass meadows. Hume et al. (2011) compared ecosystem metabolism measured at the VCR in 2007, when the meadow was 6 years old, using the eddy correlation technique and found that the presence of seagrass increased ecosystem metabolism. However, they only compared seagrass vegetated and unvegetated sediments rather than multiple different aged meadows. They also only collected data during the mid-to-late summer, so the data cannot be used to estimate annual metabolism. Barron et al. (2004) found that *Cymodocea nodosa* meadows became more heterotrophic with colonization due to increases in sediment respiration that were attributed to increases in sediment organic matter pools. However, compilations of data available in the literature suggest that *C. nodosa* meadows are frequently found to be heterotrophic (Duarte et al. 2010), so the effect of meadow age found by Barron et al. (2004) on ecosystem metabolism may not be significant. As seagrass restoration projects increase worldwide, it is important to



understand the relative effects of seagrass colonization on net ecosystem metabolism as a component of carbon cycling.

## **Research Questions**

*Chapter 1: How well do eddy correlation measurements integrate heterogeneous fluxes and how quickly will rapid changes in the  $O_2$  flux be registered in eddy correlation fluxes?*

In this chapter, I investigate the effects of heterogeneous benthic fluxes within the footprint of the eddy correlation instrument, as well as the response time to rapid changes in  $O_2$  fluxes using 3-dimensional numerical modeling techniques. Previously, eddy correlation measurements were assumed to be representative of ecosystem-scale  $O_2$  fluxes as they integrate over a very large area that can be on the order of  $100\text{ m}^2$  depending on environmental conditions and measurement height (Berg et al. 2007). However, the unique distribution of the contribution of fluxes within the footprint to the total measurement is such that the majority of the flux contribution comes from a smaller area within the footprint (Berg et al. 2007). Thus it is important to understand whether this distribution affects our interpretation of eddy correlation fluxes as measurements may be skewed towards one community type or another depending on placement of the instrument. Through numerical modeling techniques, I show that eddy correlation measurements can be affected by heterogeneous fluxes and the error associated with heterogeneity is dependent on measurement height, sediment surface roughness, and heterogeneity patch size. I also show that there can be a significant time lag between a rapid change in  $O_2$  flux at the sediment surface and when the flux reaches the

measurement height that is dependent on sediment surface roughness, measurement height, and water velocity. The results of this study are in review at *Limnology and Oceanography: Methods*.

*Chapter 2: What are the primary drivers of ecosystem production and respiration in seagrass meadows and how do they change seasonally?*

The second chapter of this thesis examines the primary drivers of ecosystem production and respiration, including light, temperature, and flow using the eddy correlation technique in an established *Zostera marina* L. meadow at the Virginia Coast Reserve (VCR). While the general effects of these drivers on *Z. marina* plants are understood through experimental manipulations, the meadow-scale response is less clear as the technology to obtain large-scale, in situ measurements has only recently been developed. Hume et al. (2011) used the eddy correlation technique at the same site to determine ecosystem metabolism during the summer and found that O<sub>2</sub> metabolism was highly correlated to light and flow conditions. In this chapter, I expand on that study by documenting seasonal variation in ecosystem O<sub>2</sub> metabolism as light, flow, and temperature changed over the course of a year. I found that the relative influence of these drivers on O<sub>2</sub> metabolism varied seasonally. For example, flow was increasingly important in stimulating respiration with the most stimulation in June and none in February that corresponded to the seasonal trends in shoot density and temperature. I also found that there was significant coupling between ecosystem gross primary production and respiration on hourly, daily, and seasonal timescales suggesting that there may be multiple positive feedback processes occurring. The results of this study are to be submitted at *Marine Ecology Progress Series*.

*Chapter 3: How does ecosystem metabolism change with seagrass colonization?*

In the third chapter of this thesis, I examine the effects of seagrass restoration on ecosystem metabolism through seasonal measurements across a chronosequence of seagrass colonization. The VCR is the site of an extremely successful *Z. marina* restoration project which began in 2001, and regular seeding continued until 2008 providing a chronosequence of sites where time since seeding is known. The sites compared in this study are bare (0 years since seeding), young vegetated (5 years since seeding), and older vegetated (11 years since seeding). I found that ecosystem metabolism, as measured by gross primary production and respiration, increased with *Z. marina* meadow age likely due to increased biomass of both autotrophic and heterotrophic organisms. I also found through modeling techniques that there were fundamental differences in annual net ecosystem metabolism at the 5 year and 11 year sites where the 5 year site was strongly net autotrophic while the 11 year site was net heterotrophic. This is likely an indication of increasing biomass and meadow expansion at the 5 year site while the 11 year site may be maintaining a critical biomass. In addition, annual net ecosystem metabolism was not different at the bare and 11 year sites indicating that carbon imported in excess of what supported the unvegetated sediments is not likely used as a source for respiration. Thus, through returning seagrass to this system, this restoration has altered the magnitude of metabolism in the lagoons but not the balance. The results of this study are to be submitted at Limnology and Oceanography.

## References

- Aalderink, R. H. and R. Jovin. (1997). Estimation of the photosynthesis/irradiance curve parameters from light and dark bottle experiments. *Jour. of Plankton Res.* 19(11): 1713 – 1742.
- Barron, C., N. Marba, J. Terrados, H. Kennedy, and C. M. Duarte. (2004). Community Metabolism and Carbon Budget along a Gradient of Seagrass (*Cymodocea nodosa*) Colonization. *Limnol. Oceanogr.* 49(5): 1642 – 1651.
- Berg, P., H. Roy, and P. L. Wiberg. (2007). Eddy correlation flux measurements: The sediment surface area that contributes to the flux. *Limnol. Oceanogr.* 52(4): 1672 – 1684.
- Binzer, T., K. Sand-Jensen, and A. Middleboe. (2006). Community photosynthesis of aquatic macrophytes. *Limnol. Oceanogr.* 51(6): 2722 – 2733.
- Caine, E., A. (1980). Ecology of two littoral species of caprellid amphipods (Crustacea) from Washington, USA. *Mar. Biol.* 56:327 – 335.
- Cottam, C., Munro, D.A., 1954. Eelgrass status and environmental relations. *J. Wildlife Manage.* 18: 449–460.
- Cole, L. W. and K. J. McGlathery. 2012. Dinitrogen fluxes from restored seagrass meadows. *Mar. Ecol. Prog. Ser.* 448: 235-246.
- Congdon, R. A. and A. J. McComb. (1979). Productivity of *Ruppia*: Seasonal changes and dependence on light in an Australian estuary. *Aquatic Botany.* 6:121 – 132.
- Dillon, C. R. (1971). A comparative study of the primary productivity or estuarine phytoplankton and macrobenthic plants. PhD thesis, Univ. North Carolina. 112 p.

- Duarte, C. M., N. Marba, E. Gacia, J. W. Fourqurean, J. Beggins, C. Barron, and E. T. Apostolaki. (2010). Seagrass community metabolism: Assessing the carbon sink capacity of seagrass meadows. *Global Biogeochem. Cycles*. 24: GB4302.
- Duarte, C. M., H. Kennedy, N. Marba, and I. Hendriks. (2011). Assessing the capacity of seagrass meadows for carbon burial: Current limitations and future strategies. *Ocean and Coastal Management*. In Press. 1 – 11.
- Enríquez, S., C. M. Duarte, and K. Sand-Jensen. (1993). Patterns in decomposition rates among photosynthetic organisms: the importance of detritus C:N:P content. *Oecologia*. 94(4): 457 – 471.
- Eyre, B. D., D. Maher, J. M. Oakes, D. V. Erler, and T. M. Glasby. (2011). Differences in benthic metabolism, nutrient fluxes, and denitrification in *Caulerpa taxifolia* communities compared to uninvaded bare sediment and seagrass (*Zostera capricorni*) habitats. *Limnol. Oceanogr.* 56(5): 1737 – 1750.
- Frederiksen, M. S. and R. N. Glud. (2006). Oxygen dynamics in the Rhizosphere of *Zostera marina*: A Two-Dimensional Planar Optode Study. *Limnol. Oceanogr.* 51(2): 1072 – 1083.
- Fonseca, M. S., and J. S. Fisher. (1986). A comparison of canopy friction and sediment movement between four species of seagrass with reference to their ecology and restoration. *Mar. Ecol. Prog. Ser.* 29: 15 – 22.
- Gacia, E., H. Kennedy, C. M. Duarte, J. Terrados, N. Marba, S. Papadimitriou, and M. Fortes. (2005). Light-dependence of the metabolic balance of a highly productive Philippine seagrass community. *Jour. of Exp. Mar. Biol. and Ecol.* 316: 55 – 67.

- Goodman, J. L., K. A. Moore, and W. C. Dennison. (1995). Photosynthetic responses of eelgrass (*Zostera marina* L.) to light and sediment sulfide in a shallow barrier island lagoon. *Aquatic Botany*. 50: 37 – 47.
- Hansen, J. C. R. and M. A. Reidenbach. (2012). Wave and tidally driven flows in eelgrass beds and their effect on sediment resuspension. *Mar. Ecol. Prog. Ser.* 448: 271 – 287.
- Harlin, M. M. (1973). Transfer of products between epiphytic marine algae and host plants. *J. Phycol.* 9:243 – 248.
- Hemminga, M. and C. Duarte (2000). *Seagrass Ecology*. Cambridge University Press. New York, NY.
- Hendriks, I. E., T. Sintes, T. J. Bouma, and C. M. Duarte. (2008). Experimental assessment and modeling of the effects of seagrass *Posidonia oceanica* on flow and particle trapping. *Mar. Ecol. Prog. Ser.* 356: 163 – 173.
- Höffle, H., M. S. Thomsen, and M. Holmer. (2011). High mortality of *Zostera marina* under high temperature regimes but minor effects of the invasive macroalgae *Gracilaria vermiculophylla*. *Est. Coastal and Shelf Sci.* 92: 35 – 46.
- Hume, A., P. Berg, and K. McGlathery. (2011). Dissolved oxygen fluxes and ecosystem metabolism in an eelgrass (*Zostera marina*) meadow measured with the eddy correlation technique. *Limnol. Oceanogr.* 56(1): 86 – 96.
- Long, M. H., K. J. McGlathery, J. C. Zieman, and P. Berg. (2008). The role of organic acid exudates in liberating phosphorus from seagrass-vegetated carbonate sediments. *Limnol. and Oceanogr.* 53(6):2616 – 2626.

- Masini, R. J. and C. R. Manning. (1997). The photosynthetic responses to irradiance and temperature of four meadow-forming seagrasses. *Aquatic Botany*. 58: 21 – 36.
- Mazzella, L. and R. S. Alberte. (1986). Light adaptation and the role of autotrophic epiphytes in primary production of the temperate seagrass, *Zostera marina* L. *J. Exp. Mar. Biol. Ecol.* 109: 165 – 180.
- McGlathery, K. J., S. Risgaard-Petersen, and P. B. Christensen. (1998). Temporal and spatial variation in nitrogen fixation activity in the eelgrass *Zostera marina* rhizosphere. *Mar. Ecol. Prog Ser.* 168:245 – 258.
- McGlathery K.J., Sundback, K, I.C. Anderson. 2007. Eutrophication in shallow coastal bays and lagoons: the role of plants in the coastal filter. *Mar. Ecol. Prog. Ser.* 348: 1-18
- McGlathery, K. J., L. K. Reynolds, L. W. Cole, R. J. Orth, S. R. Marion, and A. Schwartzchild. (2012). Recovery trajectories during state change from bare sediment to eelgrass dominance. *Mar. Ecol. Prog. Ser.* 448:209 – 221.
- Meling-López, A. E., and S. E. Ibarra-Obando. (1999). Annual life cycles of two *Zostera marina* L. populations in the Gulf of California: contrasts in seasonality and reproductive effort. *Aquatic Botany*. 65(1-4): 59 – 69.
- Moncreiff, C. A., M. J. Sullivan, and A. E. Daehnick. (1992). Primary production dynamics in seagrass beds of Mississippi Sound: the contributions of seagrass, epiphytic algae, sand microflora, and phytoplankton. *Mar. Ecol. Prog. Ser.* 7:161 – 171.
- Mook, D. (1977). Studies on fouling invertebrates in the Indian River, Florida 2: Effects of *Modulus modiolus* (Prosobranchia: Modulidae). *Nautilus*. 91:134 – 136.

- Olesen, B. and K. Sand-Jensen. 1993. Seasonal acclimation of eelgrass *Zostera marina* growth to light. *Mar. Ecol. Prog. Ser.* 94: 91 – 99.
- Orth, R. J., T. J. B. Carruthers, W. C. Dennison, C. M. Duarte, J. W. Fourqurean, K. L. Heck, A. R. Hughes, G. A. Kendrick, W. J. Kenworthy, S. Olyarnik, F. T. Short, M. Waycott, and S. Williams. (2006b). A Global Crisis for Seagrass Ecosystems. *BioScience*. 56(12): 987 – 996.
- Ouisse, V., A. Mingé, and D. Davoult. (2011). Community-level carbon flux variability over a tidal cycle in *Zostera marina* and *Z. noltii* beds. *Mar. Ecol. Prog. Ser.* 437: 79 – 87.
- Penhale, P. A. and W. O. Smith, Jr. 1977. Excretion of Dissolved Organic Carbon by Eelgrass (*Zostera marina*) and its Epiphytes. *Limnol. Oceanogr.* 22(3): 400 – 407.
- Sand-Jensen, K. (1977). Effect of epiphytes on eelgrass photosynthesis. *Aquatic Botany*. 3:55 – 63.
- Sand-Jensen, K., T. Binzer, and A. L. Middleboe. (2007). Scaling of photosynthetic production of aquatic macrophytes – a review. *Oikos*. 116: 280 – 294.
- Short, F., T. Carruthers, W. Dennison, and M. Waycott 2007. Global seagrass distribution and diversity: a bioregional model. *Jour. of Exp. Marine Biol. and Ecol.* 350: 3 – 20.
- Staehr, P. A. and J. Borum. (2011). Seasonal acclimation in metabolism reduces light requirements of eelgrass (*Zostera marina*). *Jour. of Exp. Marine Biol. And Ecol.* 407: 139 – 146.



Van Montfrans, J., R. L. Wetzel, and R. J. Orth. (1984). Epiphyte-Grazer Relationships in

Seagrass Meadows: Consequences for Seagrass Growth and Production.

*Estuaries*. 7(4): 298 – 309.

Waycott, M., C. M. Duarte, T. J. B. Carruthers, R. J. Orth, W. C. Dennison, S. Olyarnik,

A. Calladine, J. W. Fourqurean, K. L. Heck Jr., A. Randall Hughes, G. A.

Kendrick, W. J. Kenworthy, F. T. Short, and S. L. Williams. (2009). Accelerating

loss of seagrasses across the globe threatens coastal ecosystems. *PNAS*. 106(30):

12377 – 12381.

**Chapter 1 : The effects of spatial and temporal variability at the sediment surface  
on aquatic eddy correlation flux measurements.**

**Acknowledgements**

Support for this study was provided by the University of Virginia and the National Science Foundation through grants from the Chemical Oceanography program (OCE-0536431 and OCE-1061364) and Division of Environmental Biology (DEB-0917696 and DEB-0621014).

**Abstract**

The eddy correlation technique has become a widely used approach to measure ecosystem scale fluxes in aquatic benthic environments; however, there are few theoretical studies designed to guide deployment planning, the characterization of flux variability, or how to correctly interpret measured fluxes. Here, a 3-dimensional numerical model for the turbulent transport and mixing in the near-bottom water was used to examine how well variations in vertical flux due to heterogeneities in the benthic community are integrated in eddy correlation measurements. The results showed that an appropriate choice of measuring height above the sediment surface is crucial to obtain an accurate average of the vertical flux from heterogeneous benthic communities. Through regression analysis of modeling results, a set of simple analytical expressions were derived for this threshold measuring height as a function of two parameters: heterogeneity patch size and sediment surface roughness. The same model was also used to examine the time lag between when a change in vertical flux occurs at the sediment surface and when it reaches the measuring point. The results showed that this response time varies by several orders of magnitude depending on flow velocity, sediment surface roughness, and measuring height. Simple analytical expressions were also derived for the response time. Overall, the findings indicate that both the spatial variability in benthic communities and the response to temporal changes are important factors that should be considered in planning eddy correlation measurements and interpreting eddy correlation fluxes.

## Introduction

Eddy correlation (EC), sometimes termed eddy covariance, has been used since the early 1950s (Swinbank 1951) as an approach to measure fluxes of mass, energy, and momentum in the atmospheric boundary layer. The technique was recently modified for the aquatic environment by Berg et al. (2003) to measure fluxes of dissolved O<sub>2</sub> across the sediment-water interface, and has since been used in a wide variety of environments including riverine systems, permeable sediments, lake sediments, the deep oceans, arctic fjords, seagrass meadows, under ice sheets, the continental shelf, and coral reefs (Berg et al. 2003, Kuwae et al. 2006, Berg and Huettel 2008, Brand et al. 2008, McGinnis et al. 2008, Berg et al. 2009, Glud et al. 2010, Lorrai et al. 2010, McGinnis et al. 2011, Hume et al. 2011, Long et al. 2012, Reimers et al. 2012; Long et al. 2013). These sites included both uniform and heterogeneous benthic communities and EC measurements were made from a wide range of different measuring heights (8 – 80 cm). However, little information is given on why these measurement heights were chosen or how different measuring heights may affect the flux.

The size and shape of the footprint of EC measurements was determined by Berg et al. (2007) through a 3-dimensional (3D) numerical tracer modeling study. Berg et al. (2007) showed that while the footprint can be very large (50 – 100 m<sup>2</sup>), the uneven distribution of the flux signal causes a large percentage of the signal to be from a smaller area within the footprint. As a result of this distribution, the maximum contribution to the flux signal typically arises from a location ~1 to 7 m upstream of the instrument depending on environmental conditions and measurement height (Berg et al. 2007). When EC is used to derive ecosystem-scale fluxes, this uneven distribution within the

footprint may cause inaccurate interpretations of the measured fluxes when the benthic community is heterogeneous. For example, Fig. 1 illustrates a conceptual heterogeneous benthic community with patchy vegetated and unvegetated sediments. As the fluxes would vary across this benthic community, it is important to understand if eddy correlation measurements taken in different locations (illustrated as different footprint ovals) would accurately represent the entire benthic ecosystem or if the fluxes measured may be skewed towards one component of the community or another depending on instrument placement. This is the first topic investigated in this study.

During EC deployments, physical drivers of production and respiration are often measured simultaneously (Glud et al. 2010, Hume et al. 2011, Long et al. 2012). For an accurate interpretation of the fluxes measured, it is also necessary to understand whether there may be any significant time lag between measurements of these controlling variables and the fluxes estimated with the EC instrument. The 90% response time is defined as the time lag between when a change in vertical flux occurs at the sediment surface and when it reaches the measuring point. This time lag has not yet been quantified, thus most previous studies using the EC technique have assumed an instantaneous response in measured fluxes with changes in the controlling variables. For example, the benthic O<sub>2</sub> flux may change rapidly as a result of varying light conditions at the sediment surface (e.g. Hume et al. 2011); however, this change in flux may take time to reach the measurement height and result in data inaccurately correlated in relationships. This is the second topic studied in this paper. In this way, our results complement a recent study by Holtappels et al. (2013) who showed that dynamic changes

in mean water velocity and mean water column  $O_2$  concentration can impact measured EC fluxes.

In summary, to further improve the interpretation of EC data, we have quantified the following characteristics of aquatic EC measurements: 1) the threshold measurement heights at which variability in fluxes due to heterogeneity in the benthic community is well integrated, and 2) the time lag between a change in flux at the sediment surface and its observation at the measurement height. From numerous simulations using a 3D numerical model for turbulent mixing of a tracer in the near bottom water, we derive simple correlations for these key characteristics. We finally present an example based on a previously published EC data using our correlations to estimate appropriate measurement heights and response times for a specific site.

## **Materials and Procedures**

### *Numerical Solution*

The numerical solution used in this study was adapted from Berg et al. (2007) who produced a detailed map of the footprint of the EC technique. The original model relies on a 3D mathematical formulation for the transport and dispersion of a conservative solute in turbulent flow where separate parameterizations for the turbulent diffusion and molecular diffusion are used. As no analytical solution to this model exists, it is solved using a numerical control volume approach (Carnahan et al. 1969). The original model assumes that while turbulent diffusion and molecular diffusion contribute to mixing in the direction of the mean current, the x direction (Fig. 1.1), advection is

significantly greater. Thus, downstream effects of fluxes from the benthic surface do not affect upstream conditions. This allows the 3D solution to be solved as a series of 2D solutions in the y-z direction (Fig. 1.1). At each time step, the solutions are solved using the “implicit alternating direction method” (Douglas 1955, Peaceman and Rachford 1955, Carnahan et al. 1969). In order to minimize the total number of calculations, symmetry in the x-z plane (Fig. 1.1) is utilized so that a solution is only found for  $y \geq 0$ . Also, to incorporate long footprints (e.g. 90 m along the x axis, Berg et al 2007), grid sizes in the x-direction are significantly larger than that of the y-direction. Finally, to obtain a detailed description of vertical variation, a fine grid is used for the z-direction.

### *Heterogeneous fluxes*

The original model for the analysis of the footprint (Berg et al. 2007) was altered to include the effect of benthic heterogeneities on EC flux measurements. The calculation domain was significantly reduced in both grid size in the x and y-directions (2 cm x 2 cm grids) and number of grid cells to minimize calculation times by using additional symmetry lines illustrated in Fig. 1.2A as dashed lines. The lower boundary condition was defined as a series of square patches to represent a heterogeneous benthic surface containing fluxes of different proportions (Fig. 1.2A). The upper boundary condition was given as a constant flux equal to the integration of the lower boundary condition. The upstream boundary condition (“inlet”) parameterized using values calculated at the downstream boundary (“outlet”), creating an infinite loop that allows the solution to run to steady state. A solution to the 1-dimensional formulation of the tracer release from a homogenous sediment surface was used as the initial conditions in every control volume to further minimize the total number of calculations to reach steady state. A wide range of



field conditions were used in the simulations and are given in Table 1.1. These include 52 different pairs of sediment surface roughness ( $z_0$ ) and friction velocity ( $u_*$ ) calculated from the mean flow velocity at 15 cm above the bottom ( $\bar{U}$ ) for each set of heterogeneity patch sizes ( $X$ ), summing to a total of 276 separate steady state simulations

The numerical solution provided fluxes in three directions across the boundaries of all control volumes within the calculation domain. Distributions of fluxes across both the x and y direction – an example of which is given in Fig. 1.2B – were used to determine the maximum variation of vertical fluxes from the average flux for each heterogeneous surface at different heights in the z-direction. At a certain height above the lower boundary which varied with  $z_0$  and  $X$ , all variability vanished due to turbulent mixing and vertical fluxes for each control volume equaled the average vertical flux from the entire benthic surface. At this height and above, effects of individual bottom heterogeneities were no longer detectable and the vertical transport simplified to a 1-dimensional relationship. At heights below this threshold, vertical fluxes were not well integrated. By analyzing the results of each model simulation, threshold heights were identified where the vertical fluxes varied less than 5, 10, or 20% from the averaged benthic flux ( $h_5$ ,  $h_{10}$ , and  $h_{20}$ ).

### *Response Time*

The 90% response time ( $T_{90}$ ) in EC measurements is defined as the time elapsed from when an abrupt change in benthic flux occurs until 90% of the change is registered at a given measuring height. The magnitude of  $T_{90}$  was examined using the 3D numerical model described above where all model parameters except the lower boundary condition were identical to those described previously. The lower boundary was defined as a

uniform benthic surface with a flux of 1 out of every grid cell. The model was run until a steady state solution was reached and then the flux from the benthic surface was doubled and rerun to steady state. From each simulation, values of  $T_{90}$  were extracted at the measuring heights 5, 10, 15, 20, 30, and 45 cm above the sediment. Model runs were performed for the range of  $z_0$  and  $u_*$  given in Table 1.1 for a total of 52 separate simulations.

### *Regression Analysis*

For each parameter tested, simple correlations were determined using a two-step regression analysis (Berg et al. 2007). For estimation of  $h_5$ ,  $h_{10}$ , and  $h_{20}$ , the threshold heights were first correlated with  $z_0$  and the coefficients from the initial fit were then correlated with  $X$ .  $T_{90}$  was initially correlated to  $u_*$  for each simulation based on a log-profile of flow (Stull 1988), and the coefficients were then correlated to the measurement height ( $h$ ).

### *Example from Glud et al. 2010*

A site image and data from Glud et al. (2010) was used to give an example of the use of the correlations provided in this study. An image (station 4) from Glud et al. (2010) shows a heterogeneous site in a sub-arctic fjord located off the coast of Greenland with coarse sands interspersed with large rocks covered in calcareous algae. A characteristic heterogeneity patch size was determined by choosing 8 randomly distributed points on the image and measuring the horizontal lengths of the uniform benthic surface surrounding the points. As no information was available in Glud et al.

(2010) on  $z_0$ , a sensitivity analysis was done using a range of roughness values that were 5 – 30% of the characteristic patch size.

## **Assessment**

### *Numerical solution*

The numerical solution was tested to insure assumptions based on minimizing the calculation domain as well as grid independence were fulfilled. Larger calculation domains were tested in the z-direction to ensure the calculation domain extended high enough in the water column so that the numerical solution was truly 1-dimensional. Grid independence, defined as whether the numerical solution was impacted by reducing the grid size, was also ensured for the larger grid size of 2 cm x 2 cm in the x and y-directions in additional simulations using a finer grid of 1 cm x 1 cm, which gave the same result as the standard grid solution within 0.42%.

### *Heterogeneity*

The modeled horizontal fields of the vertical flux were strongly correlated with sediment surface roughness ( $z_0$ ), heterogeneity patch size (X) and measurement height (h). An example of one model run, based on  $X = 102$  cm and  $z_0 = 1.32$  cm, is shown in Fig. 1.2. Fig. 1.2C, D, E, and F show the vertical fluxes in the planes 5, 10, 15, and 45 cm above the bottom, respectively, illustrating that the heterogeneities in vertical fluxes are not fully integrated until 45 cm above the sediment surface. Wide ranges of  $z_0$ , X, and mean velocity ( $\bar{U}$ ) were prescribed in model runs in order to simulate typical field

conditions and can be found in Table 1.1. Similar to Berg et al. (2007), the vertical flux integration within the calculation domain was independent of  $\bar{U}$ .

As the vertical flux field was found to be independent of all variables other than  $z_0$ ,  $X$ , and  $h$ , correlations for  $h_5$ ,  $h_{10}$ , and  $h_{20}$  were determined in a two-step process where functions were fitted first to  $z_0$  and then the coefficients of the original functions were fitted to  $X$ . As an example, Fig. 1.3A shows all values of  $h_5$  as a function of  $z_0$  on a log axis (all  $r^2 > 0.999$ ). The fitting function  $h_5 = a + b(z_0)^c$  was used for all six different patch sizes tested. The coefficients were then fitted with the following functions and can be seen in Fig. 1.3B for  $h_5$ :  $a = a_1X + b_1$  and  $b = a_2X^{b_2}$ . The coefficient  $c$  was found to be constant for all correlations (Fig. 1.3B) of a given percent error (0.430, 0.458, and 0.487 for  $h_5$ ,  $h_{10}$ , and  $h_{20}$ , respectively). This two-step process produced the following empirical relationships for the threshold measuring height with a user selectable maximum error of 5, 10, or 20%:

$$h_5 = 2.01X^{0.534}z_0^{0.430} + 0.0840X - 0.903 \quad (1)$$

$$h_{10} = 1.80X^{0.505}z_0^{0.458} + 0.0634X - 0.702 \quad (2)$$

$$h_{20} = 1.54X^{0.478}z_0^{0.487} + 0.0440X - 0.516 \quad (3)$$

where  $X$  is patch length in cm and  $z_0$  is sediment surface roughness in cm. A visual test of the empirical relationships against the more robust numerical solution is shown in Fig. 1.3C for  $h_5$  and the average difference between the two solutions was found to be  $0.4 \pm 0.6$ ,  $0.8 \pm 0.7$ , and  $1.0 \pm 0.8\%$  for fits  $h_5$ ,  $h_{10}$ , and  $h_{20}$ , respectively (SE,  $n = 52$ ). The goodness of fit was tested statistically using a two sample Kolmogorov-Smirnov (K-S) test between the numerical model and the simple fits for each height (Massey 1951), and

there were no significant differences between the numerical model and the simple fits (K-S stat = 0.0556, 0.0556, and 0.0370;  $p = 1.000$  for Eqs. 1, 2, and 3, respectively).

### *Response Time*

An example of the simulated time series for a  $z_0 = 1.0$  cm and  $\bar{U} = 10$  cm s<sup>-1</sup> is given in Fig. 1.4, where the 90% response time ( $T_{90}$ ) is generated as the time interval at which the normalized flux estimated reached 0.9 (from 0 at time zero) for each measuring height above the benthic surface. Values of  $T_{90}$  were found to be correlated with  $\bar{U}$ ,  $z_0$ , and  $h$ . Through trial and error, it was found that the combined effect of  $z_0$  and  $\bar{U}$  can be merged into one variable, the friction velocity ( $u_*$ ), defined as (Stull 1988):

$$u_* = \frac{\bar{U}\kappa}{\ln\left(\frac{h}{z_0}\right)} \quad (4)$$

where  $h$  is the measurement height above the bottom in cm,  $\bar{U}$  is mean velocity at height  $h$  in cm s<sup>-1</sup>,  $z_0$  is sediment surface roughness in cm, and  $\kappa$  is Von Karmann's constant.

Using a similar multi-step fitting process as previously described (Fig. 1.5A and B) a simple correlation was determined to estimate  $T_{90}$  as a function of  $u_*$  and  $h$ :

$$\log T_{90} = 2.87 - 1.22(0.92^h) - \log u_* \quad (5)$$

The average difference between the simple fit and the numerical solution was  $1.3 \pm 2.7\%$  (SD,  $n = 324$ ). The goodness of fit is shown in Fig. 1.5C and was tested statistically using a two sample K-S test (Massey 1951), and there was no significant difference between the two datasets (K-S stat = 0.0154,  $p = 1.00$ ).

*Example from Glud et al. 2010*

The heterogeneity patch size (Station 4 in Glud et al. 2010) was determined to be  $11 \pm 2$  cm (SE,  $n = 8$ ). Using Eq. 1, 4, and 5, with  $z_0$  defined from 0.5 – 3.0 cm,  $h_5$  ranged from 5.5 – 11 cm, and  $T_{90}$  ranged from 4.3 – 11.5 min.

## **Discussion**

This study reveals how aquatic EC measurements can be affected by heterogeneous benthic communities and temporal changes in the benthic flux. In determining ecosystem scale fluxes, these biases can be minimized if the set of simple guidelines derived in this study are followed when planning EC deployments and when the results are interpreted.

Generally, EC instruments are deployed above the roughness layer of the sediment surface and in the log layer of flow which typically extends up to 1 m above the seafloor (Boudreau and Jørgensen, 2001). It is often assumed that with this approach, the footprint of the EC technique will be large enough to incorporate benthic heterogeneities and that the fluxes measured will be representative of the benthic community as a whole. However, this study shows that due to the uneven distribution of the flux signal within the footprint, benthic fluxes measured in heterogeneous environments can be skewed towards one patch community type or another. For example, this could be significant if the site under study had patchy algal mats (e.g. Fig 1.1) or a seagrass meadow with bare sediments interspersed. In these cases, if deployments were not properly planned to incorporate the benthic heterogeneity, biological interpretations of measured EC fluxes

may differ depending on proximity of the instrument to one benthic community or another.

The effect of heterogeneity was found to be correlated with heterogeneity patch size ( $X$ ), measurement height ( $h$ ), and sediment surface roughness ( $z_0$ ). The effects of  $X$  and  $h$  are straightforward in that with larger patch sizes, more mixing is needed to integrate the solution well, requiring measurements higher above the sediment surface (e.g. Fig. 1.2). The effect of  $z_0$  is more complex because  $z_0$  changes the amount of turbulence in the flow (Stull, 1988). Threshold values for  $h_5$ ,  $h_{10}$ , and  $h_{20}$  increase with  $z_0$  (Eq. 1, 2, and 3) because increased mixing associated with larger roughness elements make flux variations on the sediment surface penetrate higher in the water column. Thus, the effects of flux heterogeneity would be more pronounced and the instrument would need to be deployed higher above the bottom to compensate.

The interpretation of EC fluxes in dynamic environments can be difficult due to non-steady state conditions (Holtappels et al. 2013). Data interpretation can be complicated by changes in mean  $O_2$  concentration as well as current velocities (Holtappels et al. 2013) and we show benthic flux variance in time can further affect EC measurements. Often, the controls on production or respiration, such as light or flow, can vary drastically over short periods of time (e.g. Hume et al. 2011). As these controlling variables may change on a time scale of minutes and the benthic community response may be nearly instantaneous, it is important to know how fast such changes are registered at the point where EC measurements are recorded. The 90% response time ( $T_{90}$ ) is an estimate of the total time elapsed for 90% of a rapid change in benthic flux to reach the measurement height. Under extreme conditions for EC measurements (very high flows,

rough sediment surfaces, and small measurement heights),  $T_{90}$  can be near instantaneous ( $\sim 6$  s, Fig 1.5); however, these field conditions are rare. Conventionally, many EC measurements have been recorded in 10–20 min bursts with individual flux estimates produced from each burst (Berg et al. 2003, Kuwae et al. 2006, Berg and Huettel 2008, Berg et al. 2009, Lorrai et al. 2010, Glud et al. 2010, McGinnis et al. 2011, Hume et al. 2011, Long et al. 2012, Reimers et al. 2012, Long et al. 2013, Berg et al. in press). Under the majority of field conditions, with relatively rough sediment surfaces (e.g.  $z_0 = 0.01$  cm) and middle range flow conditions (e.g.  $\bar{U} = 5 \text{ cm s}^{-1}$ ),  $T_{90}$  was found to be shorter than this integration period. This suggests that interpretations of published EC fluxes are accurate. However, under some realistic conditions that are not ideal (smooth sediment surfaces, low flows, and high measurement heights),  $T_{90}$  may be longer than the integration period of the EC data, indicating that this response time must be accounted for when dynamic fluxes are interpreted.

The parameters used in the correlations to determine the threshold measurement heights for  $h_5$ ,  $h_{10}$ , and  $h_{20}$ , and  $T_{90}$  can be determined using several techniques. A simple field survey or image analysis can be used to determine  $X$ , the heterogeneity patch size. Values of  $z_0$  and  $u_*$  are more complex, but can be estimated using the high resolution EC data (Berg et al. 2007) where Reynold's stress and thus  $u_*$  can be extracted from the 3D velocity field (*see* Berg et al. 2007).

Below, we present an example of how to use the derived correlations for measuring heights that ensure appropriate integration of fluxes from heterogeneous sediments (Eq. 1) and to estimate  $T_{90}$  (Eq. 4, 5) from the data available. Field data used as input were taken from Glud et al. (2010) where the heterogeneity patch size was



estimated from a photograph to be  $11 \pm 2$  cm (SE,  $n = 8$ ),  $\bar{U}$  was estimated to be  $\sim 2$  cm s<sup>-1</sup>, and  $z_0$  was estimated to range from 0.5 – 3.0 cm, as no data for this parameter were available. Using Eq. 1, 4, and 5, with  $z_0$ ,  $X$ , and  $\bar{U}$  values estimated for this study site,  $h_5$  ranged from 5.5 – 11 cm, and  $T_{90}$  ranged from 4.3 – 11.5 min. These first order estimates suggest that regardless of the roughness chosen for the site, the measuring height used by Glud et al. (2010) ( $h = 8$ -10 cm) was high enough above the benthic surface to incorporate heterogeneous fluxes into their measurements. Also, for the range of  $z_0$  used in this estimate,  $T_{90}$  for their study site was well within the length of a single flux calculation ( $T_{90} < 14.5$  min), indicating that most of a sudden change in benthic flux would be recorded in the 14.5 min integration time of one flux calculation.

In this study, and in the earlier footprint study by Berg et al. (2007), unidirectional current flow was assumed in all calculations and the presence of surface waves was considered negligible. However, in many cases, significant wave action has been found at shallower sites where the EC technique has been applied (Berg and Huettel 2008, Reimers et al. 2012, Long et al. 2013). The effects of wave action on the footprint, the technique's ability to integrate over heterogeneous surfaces, and the 90% response time should be included in future modeling studies to further improve the interpretation and understanding of aquatic EC measurements in waves.

### **Comments and Recommendations**

This modeling study represents a simplistic approach to determining the effects of spatial and temporal variability at the sediment surface on aquatic eddy correlation flux measurements. While we realize that the ideal conditions that must be assumed in a mechanistic modeling exercise do not always exist in natural field situations, the derived

simple correlations still provide guidance in preparation of EC deployments and interpretation of EC data. Specifically, we recommend using these equations to select appropriate measuring heights for given study site. However, the equations for  $h_5$ ,  $h_{10}$ , and  $h_{20}$  will provide measurement heights that may not be ideal or possible, such as very close to the sediment surface (i.e. 5 cm or below) where we would not recommend attempting deployments. We also recommend using equations to determine  $T_{90}$  for dynamic fluxes when EC data are interpreted. Site selection and deployment planning are important components of using the EC technique, and at sites that are heterogeneous, this study shows that there may be a tradeoff between a fast response time and a full integration of heterogeneous fluxes to estimate an ecosystem scale flux.

## References

- Berg, P., H. Roy, F. Janssen, V. Meyer, B. B. Jørgensen, M. Huettel, and D. de Beer. 2003. Oxygen uptake by aquatic sediments measured with a novel non-invasive eddy-correlation technique. *Mar. Ecol. Prog. Ser.* 261: 75 – 83.
- Berg, P., H. Roy, and P. L. Wiberg. 2007. Eddy correlation flux measurements: The sediment surface area that contributes to the flux. *Limnol. Oceanogr.* 52(4): 1672 – 1684.
- Berg, P. and M. Huettel. 2008. Monitoring the seafloor using the noninvasive eddy correlation technique: Integrated benthic exchange dynamics. *Oceanography*. 21(4):164 – 167.
- Berg, P., R. N. Glud, A. Hume, H. Stahl, K. Oguri, V. Meyer, and H. Kitazato. 2009. Eddy correlation measurements of oxygen uptake in deep ocean sediments. *Limnol. Oceanogr: Methods*. 7: 576 – 584.
- Berg, P., M. Long, M. Huettel, J. E. Rheuban, K. J. McGlathery, R. W. Howarth, A. E. Giblin, and R. Marino. In Press. Eddy correlation measurements of oxygen fluxes in permeable sediments exposed to varying current flow and light. *Limnol. Oceanogr.*
- Boudreau, B. P. and B. B. Jørgensen. 2001. The benthic boundary layer: transport processes and biogeochemistry. Oxford University Press.
- Brand, A., D. F. McGinnis, B. Wehrli, and A. Wuest. 2008. Intermittent oxygen flux from the interior into the bottom boundary of lakes as observed by eddy correlation. *Limnol. Oceanogr.* 53(5): 1997 – 2006.
- Carnahan, B., H. A., Luther, and J. O. Wilkes. 1969. Applied numerical methods. Wiley.

- Dade, W. B., A. J. Hogg, and B. P. Boudreau. 2001. Physics of flow above the sediment-water interface, p. 3-43. *In* B. P. Boudreau and B. B. Jørgensen [eds.], The benthic boundary layer. Oxford Univ. Press.
- Douglas, J. 1955. On the numerical integration of  $\partial^2 u / \partial x^2 + \partial^2 u / \partial y^2 = \partial u / \partial t$  by implicit methods. *J. Soc. Indust. Appl. Math.* 3: 42-65.
- Glud, R. N., P. Berg, A. Hume, P. Batty, M. E. Blicher, K. Lennert, and S. Rysgaard. 2010. Benthic O<sub>2</sub> exchange across hard bottom substrates quantified by eddy correlation in a sub-Arctic fjord. *Mar. Ecol. Prog. Ser.* 417: 1 – 12.
- Holtappels, M., R. N. Glud, D. Donis, B. Liu, A. Hume, F. Wenzhöfer, and M. M. M. Kuypers. 2013. Effects of transient bottom water currents and oxygen concentrations on benthic exchange rates as assessed by eddy correlation measurements. *J. Geophys. Res. Oceans.* 118: 1 – 13.
- Hume, A., P. Berg, and K. McGlathery. 2011. Dissolved oxygen fluxes and ecosystem metabolism in an eelgrass (*Zostera marina*) meadow measured with the eddy correlation technique. *Limnol. Oceanogr.* 56(1): 86 – 96.
- Kuwae, T., K. Kamio, T. Inoue, E. Miyoshi, and Y. Uchiyama. 2006. Oxygen exchange flux between sediment and water in an intertidal sandflat, measured *in situ* by the eddy-correlation method. *Mar. Ecol. Prog. Ser.* 307: 59 – 68.
- Long, M. H., D. Koopmans, P. Berg, S. Rysgaard, R. N. Glud, and D. H Sogaard. 2012. Oxygen exchange and ice melt measured at the ice-water interface by eddy correlation. *Biogeosciences.* 9(6): 1957 – 1967.

- Long, M.H., P. Berg, D. de Beer, and J. Zieman. 2013. In situ coral reef oxygen metabolism: an eddy correlation study. *PloS ONE* 8(3): e58581. [DOI:10.1371/journal.pone.0058581].
- Lorrai, C., D. F. McGinnis, A. Brand, and A. Wuest. 2010. Application of oxygen eddy correlation in aquatic systems. *Jour. Atm. And Oceanic Tech.* 27: 1533 – 1546.
- Massey, F. J. 1951. The kolmogorov-smirnov test for goodness of fit. *Jour. of the Amer. Stat. Assoc.* 46(253): 68–78.
- McGinnis, D. F., P. Berg, A. Brand, C. Lorrai, T. J. Edmonds, and A. Wüest. 2008. Measurements of eddy correlation oxygen fluxes in shallow freshwaters: Towards routine applications and analysis. *Geophys. Res. Lett.*, 35, L04403
- McGinnis, D. F., S. Cherednichenko, S. Sommer, P. Berg, L. Rovelli, R. Schwarz, R. Glud, and P. Linke. 2011. Simple, robust eddy correlation amplifier for aquatic dissolved oxygen and hydrogen sulfide flux measurements. *Limnol. and Oceanogr.: Methods.* 9: 340 – 347.
- Peaceman, D. W., and H. H. Rachford. 1955. The numerical solution of parabolic and elliptic differential equations. *J. Soc. Indust. Appl. Math.* 3: 28 – 41.
- Reimers, C. E., H. T. Ozkan-Haller, P. Berg, A. Devol, K. McCann-Grosvenor, and R. D. Sanders. 2012. Benthic oxygen consumption rates during hypoxic conditions on the Oregon continental shelf: Evaluation of the eddy correlation method. *Jour. of Geophys. Res.* 117: 1 – 18.
- Stull, R. B. 1988. The mathematical theory of turbulence. Springer-Verlag.
- Swinbank, W. C. 1951. The measurement of vertical transfer of heat and water vapor by eddies in the lower atmosphere. *Jour. of Meteor.* 8(3): 135 – 145.

**Figures**

**Figure 1.1** Conceptual model of heterogeneity effects.

Conceptual heterogeneous benthic community with theoretical eddy correlation footprints. Measuring points are given as a dot and flow is from left to right.

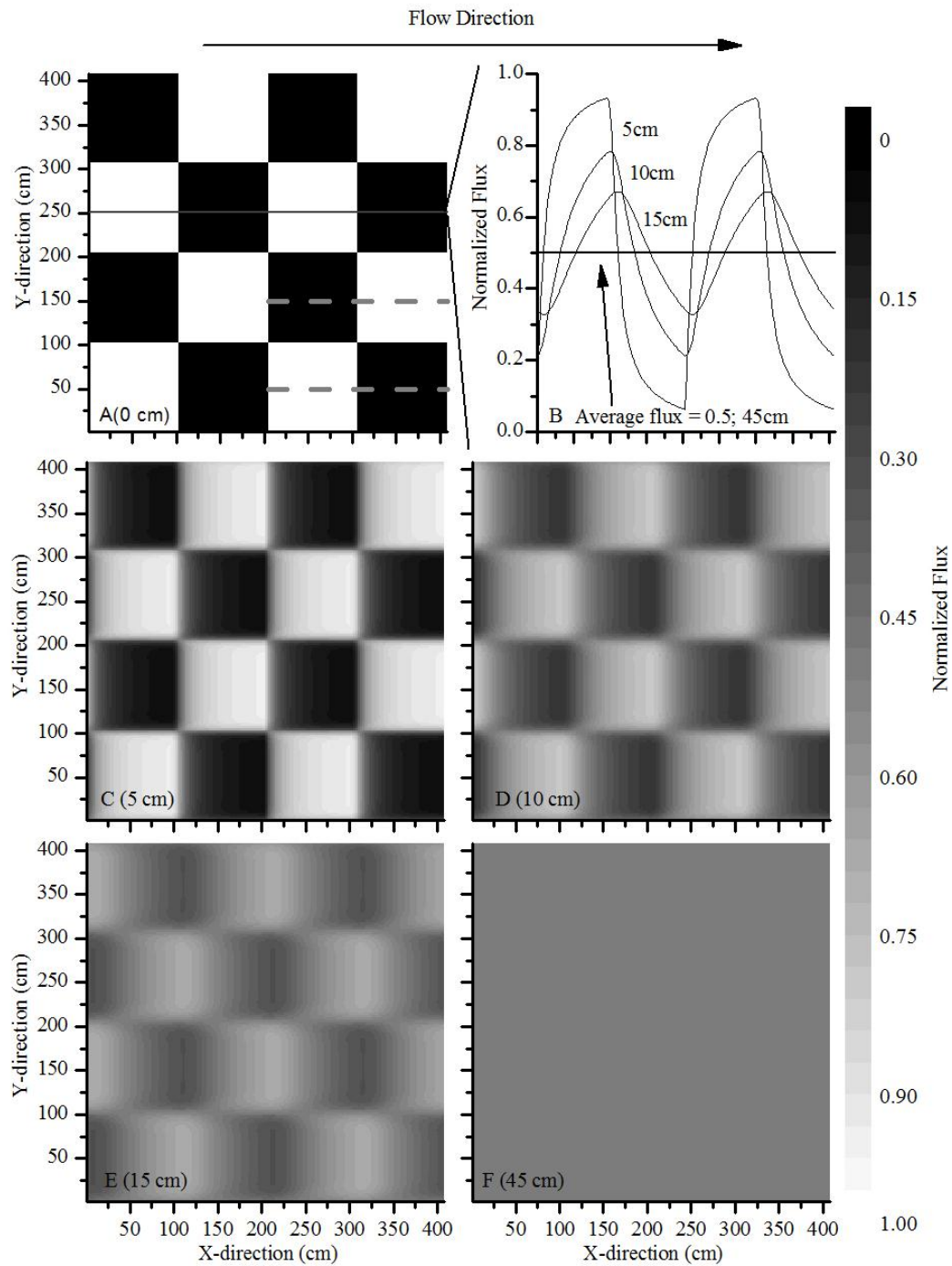


**Figure 1.2** Example model results.

(A) Checkerboard pattern of spatial flux heterogeneity on the sediment surface as seen from above. Flow direction is from left to right. Dashed lines show symmetry lines utilized to minimize calculation domain. (B) Vertical flux calculated at different

measuring heights along the line marked in panel A. For this surface heterogeneity (102 x 102 cm) and roughness (1.32 cm), a fully integrated flux of 0.5 was first obtained for a measuring height of ~45 cm. (C – F) Two-dimensional flux distributions at each horizontal plane 5, 10, 15, and 45 cm above the sediment surface, respectively. Legend for panels A and C – F is located on the right.



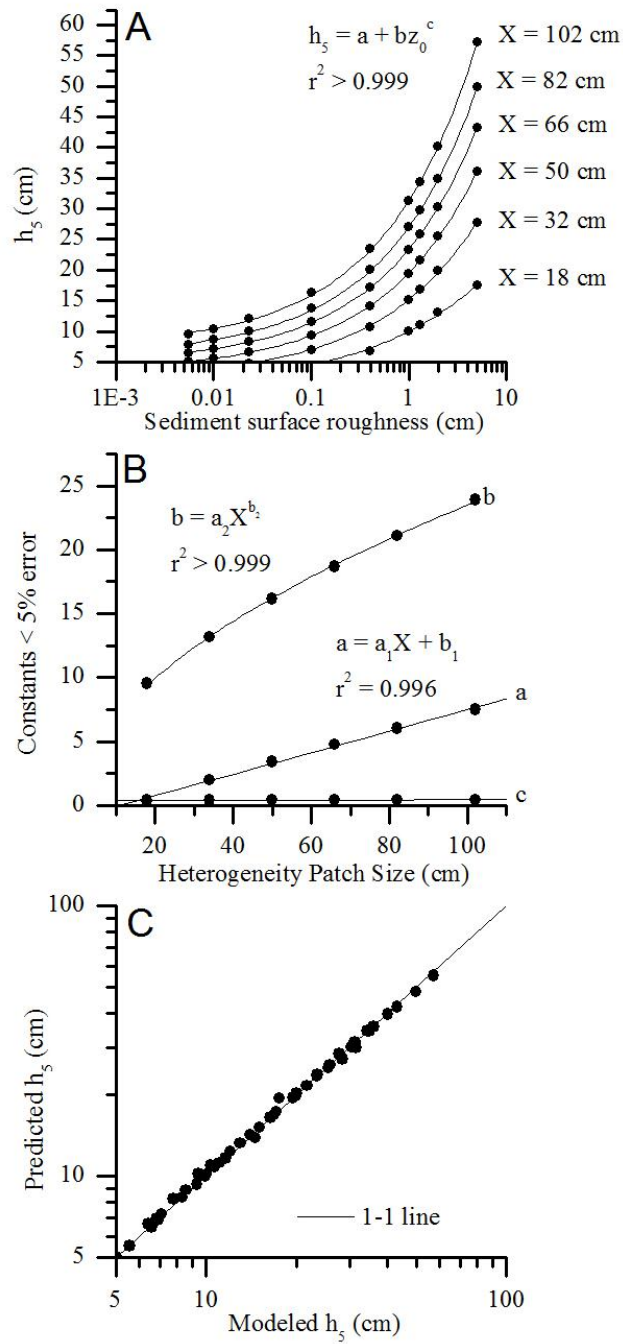


**Figure 1.3** Regression analysis for flux heterogeneity.

(A) Minimum measuring height ( $h_s$ ) required over a heterogeneous benthic surface to ensure < 5% error in flux measurements as a function of sediment surface roughness ( $z_0$ ).

Fits were generated using the curves from panel A and then the constants were used to fit with patch length to generate the final curves (Eq. 1, 2, and 3). (B) Constants a and b

fitted as a function of heterogeneity patch size ( $X$ ). Constant  $c$  is given as the average value. (C) Predicted  $h_5$  vs. modeled  $h_5$  shown with the 1-1 line. Predicted  $h_5$  is not significantly different from modeled  $h_5$  according to a two-sample Kolomogorov-Smirnov goodness of fit test (K-S stat = 0.556,  $p = 1.00$ ).

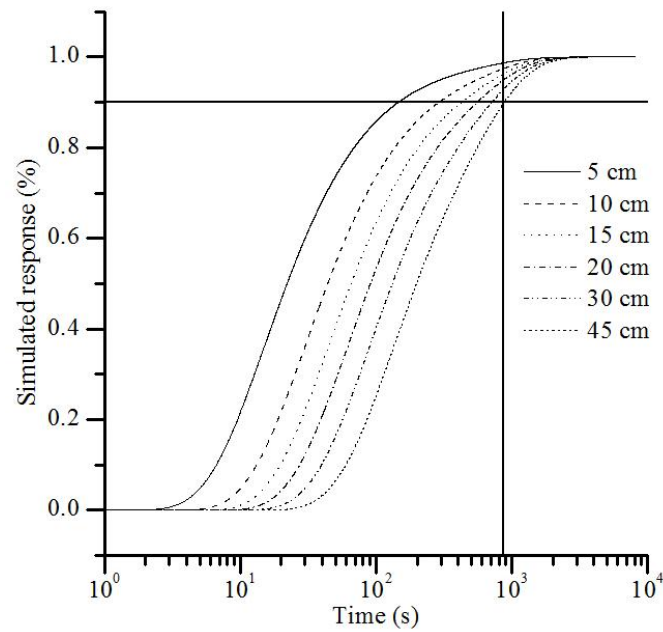


**Figure 1.4** Example model run for response time.

Example model runs for 90% response time tests with  $z_0 = 0.1$  cm and  $\bar{U} = 10$  cm s<sup>-1</sup>.

Timeseries was recorded at heights of 5, 10, 15, 20, 30, and 45 cm above the bottom after doubling the benthic flux and the horizontal line represents the 90% instrument response.

Vertical line represents typical 870 s timeseries for calculation of one flux.

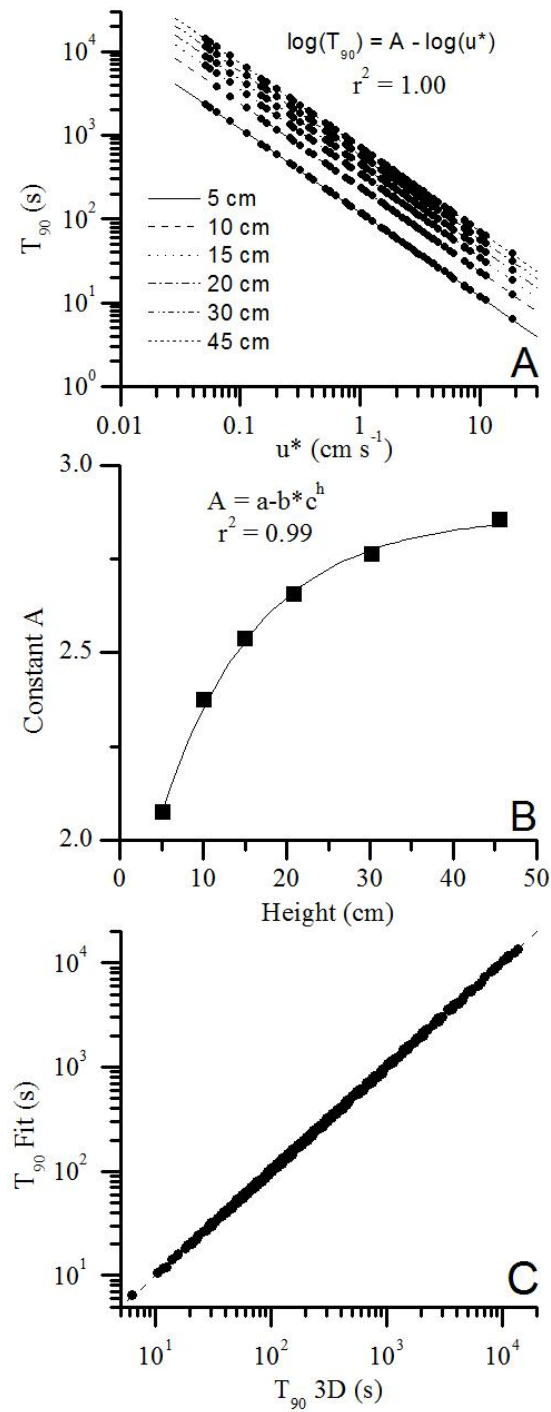


**Figure 1.5** Regression analysis for response time.

(A) Fit of 90% response time ( $T_{90}$ ) against friction velocity (Eq. 4,  $u^*$ ) for different heights above the sediment surface. (B) Constant  $A$  fitted against measurement height to determine final fit (Eq. 5). (C) Simple fit plotted against the complex numerical model to

show goodness of fit. Dashed line is 1-1 line. A two sample K-S test showed no significant differences between the 3D model and the simple fit (KS stat = 0.0154,  $p = 1.00$ ,  $n = 324$ ).

**Table 1.1** Model input parameters.

Input parameters used in model runs.  $\bar{U}$  represents mean velocity at 15 cm above the benthic surface,  $z_0$  represents sediment surface roughness, and  $u_*$  represents the friction velocity, calculated using Eq. 4. X represents patch side length and width in cm. The model was run using all combinations of  $z_0$ ,  $u_*$ , and X, adding up to a total of 276 and 52 separate simulations for heterogeneity and response time, respectively.

$\bar{U}$ (cm s <sup>-1</sup> )						
	1	5	10	20	30	50
$z_0$ (cm)	$u_*$ (cm s <sup>-1</sup> )					
0.00558	-	0.260	0.519	1.038	1.558	2.596
0.0100	-	0.280	0.561	1.121	1.682	2.803
0.0229	0.063	0.316	0.632	1.265	1.897	3.161
0.100	0.082	0.409	0.818	1.637	2.455	4.091
0.400	0.113	0.566	1.131	2.262	3.394	5.656
1.00	0.151	0.757	1.514	3.028	4.542	7.570
1.32	0.169	0.843	1.687	3.374	5.061	8.435
2.00	0.203	1.017	2.035	4.070	6.105	10.174
5.00	0.373	1.866	3.732	7.464	11.196	18.660
X (cm)	18	32	50	66	82	102

**Chapter 2 : Seasonal oxygen metabolism in restored *Zostera marina* L. (eelgrass)****meadows measured by eddy correlation**

**Acknowledgements**

Support for this study was provided by the University of Virginia and the National Science Foundation through grants from the Chemical Oceanography program (OCE-0536431 and OCE-1061364) and the Division of Environmental Biology to the VCR-LTER (DEB-0917696 and DEB-0621014).



**Abstract**

Oxygen metabolism was measured seasonally using eddy correlation in a restored eelgrass (*Zostera marina* L.) meadow 10 – 11 years after initial seeding in the coastal bays of the Virginia Coast Reserve. The high temporal resolution of the eddy correlation measurements showed strong correlations with light and current velocity, indicating that these variables are important drivers of oxygen metabolism on an hourly to daily timescale. A hysteresis effect was observed during October and August, with a different photosynthetic response to light during the morning than the afternoon indicating that there may be an increase in respiration throughout the day. The magnitudes of daily gross primary production and respiration were well correlated, yet varied seasonally reflecting a tight coupling on two different timescales: day-to-day variation in light and current flow, and seasonal changes in temperature. Average gross primary production and respiration were also tightly coupled to shoot density as an important driver of areal biomass and photosynthesis. Annual net ecosystem metabolism based on measurements for all four seasons was  $1.3 \pm 5.1 \text{ mol O}_2 \text{ m}^{-2} \text{ yr}^{-1}$  (SE, n = 17) indicating a balance between respiration and gross primary production.

## Introduction

Seagrass meadows are significant contributors to marine carbon (C) sequestration due to both high rates of net primary production (Duarte et al. 2010) and C burial (Duarte et al. 2011, Mcleod et al. 2011, Fourqurean et al. 2012). The baffling effect of the seagrass canopy enhances sedimentation of particles in the water column and reduces sediment resuspension (Fonseca and Fisher 1986, Gacia et al. 2001, Hansen and Reidenbach 2012) and much of the C buried in seagrass sediments is of allochthonous origin (Kennedy et al. 2010). High rates of primary production and respiration (Barron et al. 2004, Eyre et al. 2011, Hume et al. 2011) are supported by high nutrient uptake rates, and seagrass meadows act as a coastal filter that improves local water quality (McGlathery et al. 2007). Given new information on the effect of seagrass meadows on rates of C sequestration (Mcleod et al. 2010, Duarte et al. 2011, Fourqurean et al. 2012), a detailed understanding of ecosystem metabolism is important as a key component of C cycling in these coastal systems.

*Zostera marina* L. has a broad geographical range (Short et al. 2007) and individual sites show strong acclimation to seasonal variations in light and temperature (Moore et al. 1997, Staehr and Borum 2011). Seagrasses increase photosynthetic efficiency and pigment concentration in response to lower light (Masini and Manning 1997) and decrease respiratory requirements with lower temperatures (Moore et al. 1997). The Virginia coastal bays are close to the lower latitudinal limit for *Z. marina* (Short et al. 2007), and seagrasses are sensitive to high summer temperatures due to higher light requirements associated with increased respiration (Moore et al. 1997, 2012). In the Virginia coastal bays, seagrass production and distribution is limited by

temperature stress at shallow depths and light stress at deeper depths (Carr et al. 2010, McGlathery et al. 2012). Because of this sensitivity to temperature, large losses and regrowth of above and belowground biomass can be observed (Orth and Moore 1986, Moore 2004, 2012) which are expected to have significant effects on ecosystem metabolism.

Compared to unvegetated sites, seagrass meadows have been shown to stimulate both production and respiration (Barron et al. 2004, Eyre et al. 2011, Hume et al. 2011). However, on a net basis, ecosystem metabolism in *Z. marina* meadows is widely variable with both net autotrophy and heterotrophy reported for different locations (Duarte et al. 2010). This suggests that on a broader scale, *Z. marina* meadows may have a net metabolic balance between ecosystem production and respiration (Duarte et al. 2010) but also warrants a deeper understanding and better quantification of the drivers of metabolism in these communities. Here, we report measurements of benthic ecosystem metabolism in a restored *Z. marina* meadow at the Virginia Coast Reserve (VCR). This site is characterized by a large-scale ecosystem state change from bare to vegetated sediments that occurred as a result of restoration via seeding beginning in 2001 (McGlathery et al. 2012, Orth et al. 2012).

Based on results by Hume et al. (2011), summertime ecosystem metabolism at this site can be very dynamic and is highly correlated to light and flow conditions. We expand on this study to assess seasonal variation in metabolism as temperature and light vary over the course of a year (Moore et al. 1997, Staehr and Borum 2011) and to estimate annual net metabolism of the seagrass meadows. Barron et al. (2004) found that seagrass meadows became more heterotrophic with time since colonization as a result of

higher rates of ecosystem respiration with increased biomass and sediment organic content. From these results and based on the recovery trajectories in McGlathery et al. (2012) we hypothesized that after 10–11 years since seeding, this meadow would be annually net heterotrophic.

As in Hume et al. (2011), we determined seagrass metabolism using the eddy correlation technique (Berg et al. 2003). This approach is an improvement over traditional flux incubations as it has a much higher temporal resolution and is noninvasive to the benthic environment (Berg et al. 2003). In addition, this method measures ecosystem-scale processes as it integrates over a large sediment surface area, termed the footprint, which may be several orders of magnitude larger than traditional core and chamber techniques (Berg et al. 2007). Seagrass meadows can vary spatially on scales of <1 to 10's of m<sup>2</sup> (Townsend and Fonseca 1998, Frederiksen et al. 2006), thus methods with small footprints may not integrate the ecosystem-scale processes accurately.

## Methods

### *Study site*

The study site was located in the shallow subtidal lagoons of the Virginia Coast Reserve (VCR Long-Term Ecological Research site) between the Delmarva Peninsula and the barrier island chain. The study site, South Bay (37° 15'43.6356N, 75° 48'54.547"W), is characterized by a large-scale *Z. marina* restoration via seeding that occurred in the early 2000s, and has resulted in over 1700 ha of dense seagrass meadows

as of 2011 (Orth et al. 2006, 2010, McGlathery et al. 2012). This site is approximately 1.3 m at mean sea level with a 1 m tidal range, and is relatively protected from high wave energy by the barrier islands. Organic content measured at this site in July 2011 and 2012 as mass loss on ignition at 500 °C was  $2.8 \pm 0.3\%$  and  $2.6 \pm 0.3\%$  (SE, n = 5 McGlathery unpublished data).

### *Data Collection*

Based on temperature, data were collected during four major seasonal periods for *Z. marina* (Orth and Moore, 1986): fall regrowth after summer heat stress, low winter growth, early summer peak growth, and late summer heat stress. Data were collected in late July/August 2011, October 2011, February 2012, June 2012, and August 2012.

Benthic oxygen (O<sub>2</sub>) fluxes were measured with the eddy correlation technique (Berg et al. 2003) that has been used and validated in traditionally difficult environments for measuring benthic fluxes such as rocky hard substrates, seagrass meadows, and permeable sediments (Glud et al. 2010, Hume et al. 2011, Berg et al. in press). The eddy correlation system consists of an acoustic Doppler velocimeter (ADV, Nortek-AS) coupled to a fast responding (90% response < 0.3s) Clark-type O<sub>2</sub> microsensor designed to minimize stirring sensitivity (< 2%, Unisense), and a submersible pico-amplifier (GEOMAR, *see* McGinnis et al. 2011). The ADV was deployed such that the sensors record data at 32 – 64 Hz and were mounted to a stainless steel tripod designed to limit disturbances to natural flow. The ADV records data continuously for 14.5 min and stops for 0.5 min, resulting in 4 flux estimates per h. The eddy correlation system was adjusted so the measuring volume was above the canopy (~30 cm), and care was taken to ensure

the instrument was leveled and the x-axis oriented along the mean current direction. To avoid breaking the microsensor tip when the seagrass blades extend vertically at low current flow (Hume et al. 2011), blades were clipped in an area directly under the microsensor that was not part of the flux footprint (Berg et al. 2007). Twenty-four h deployments were performed in succession for up to one week during each season, with 1 – 2 h gaps between deployments to download data and change O<sub>2</sub> microsensors. However, microsensors are very fragile and often break mid deployment, and this resulted in fewer 24 h periods of data than deployments made.

Environmental parameters that affect O<sub>2</sub> fluxes were also measured during deployments. These included photosynthetically active radiation (PAR) reaching the canopy which was recorded every 15 min using a submersible planar 2 $\pi$  Odyssey PAR sensor (Dataflow Systems). This sensor was calibrated to a LI-193SA (LI-COR Biosciences) scalar 4 $\pi$  PAR sensor (Long et al. 2012b). Mean O<sub>2</sub> concentration was recorded using either an optode (Hach Systems) in a waterproof housing or a submersible miniDOT O<sub>2</sub> optode (PME) mounted at the measuring height of the eddy correlation instrument. Both sensors recorded O<sub>2</sub> concentration and temperature every 15 min. Mean current velocity, water depth, and current direction were derived from the ADV data. Shoot density was measured at the end of each deployment periods in August 2011/2012, October 2011, and June 2012 by counting all shoots located within replicate (n = 4 – 10) 0.25 m<sup>2</sup> quadrats haphazardly thrown within the footprint of the eddy correlation instrument. Due to cold water temperatures in February 2012, shoot density was counted within 8 haphazardly thrown 0.125 m<sup>2</sup> quadrants.

*Data analysis*

Benthic O<sub>2</sub> fluxes were extracted using EddyFlux2.0 software (Berg, unpublished) from data averaged to 16 Hz from raw 64 or 32 Hz eddy correlation data after careful data quality control to remove sections of O<sub>2</sub> data where the microsensors were impacted by floating debris or fouled. In the flux extraction over a 15 min period, the fluctuations of vertical velocity and O<sub>2</sub> concentration were defined by linear detrending (*see* Berg et al. 2009, Lorrai et al. 2010, Hume et al. 2011 for specifics on flux extraction). When eddy correlation fluxes are extracted from raw data, rotation of the velocity field has been deemed important if the instrument is tilted relative to the sediment surface (Chipman et al. 2012, Reimers et al. 2012). However, caution must be taken when rotating the velocity data when significant surface waves are present (Reimers et al. 2012) or when the mean current velocity is very small. Here, fluxes were extracted with both rotated and unrotated velocity fields and differences in the underlying distributions were tested using a two-sample Kolmogorov-Smirnov (K-S) test (Massey 1951) to determine if there were significant differences between the two extraction methods. A significant difference was only found for one deployment during August 2012 ( $p > 0.05$  for all other individual deployments,  $n = 20$ ). This deployment was only 4 h and was dominated by wave motions. Thus fluxes based on unrotated velocity data were used.

The benthic eddy flux is derived from an O<sub>2</sub> mass balance for a control volume bounded vertically by the measuring height and the sediment surface (Berg et al. 2003, Hume et al. 2011). In the absence of horizontal gradients and noticeable O<sub>2</sub> production or respiration in the bottom water, the mass balance expresses that the eddy flux is equal to

the benthic flux minus any storage of O<sub>2</sub> within the water column contained in the control volume (Berg et al. 2003, Hume et al 2011). Usually, this storage is neglected (Berg et al. 2003, Glud et al. 2010, Hume et al. 2011), but a correction can be defined as:

$$J_{benthic} = J_{EC} - \int_0^h \frac{dC}{dt} dz \quad (1)$$

where  $J_{benthic}$  is the benthic flux,  $J_{EC}$  is the measured eddy flux,  $h$  is the measuring height and  $dC/dt$  is the temporal change in mean O<sub>2</sub> concentration within the control volume. The latter can be approximated by the O<sub>2</sub> recorded at the measuring height. Because we encountered particularly large changes in mean O<sub>2</sub> concentration over the diurnal cycle and because we used a relatively large measuring height (i.e. 30cm), this correction was applied in all our flux calculations.

After initial flux extractions, data were processed as in Hume et al. (2011), where 15 min fluxes were grouped to determine hourly averaged fluxes and associated standard errors. These hourly averages were then grouped into light data where PAR > 1.0  $\mu\text{mol photons m}^{-2}\text{s}^{-1}$  and dark data, where PAR < 1.0  $\mu\text{mol photons m}^{-2}\text{s}^{-1}$  for use in regression analyses. For continuous 24 h deployments, ecosystem respiration (R), gross primary production (GPP) and net ecosystem metabolism (NEM) were determined as in Hume et al. (2011). In the few cases where hourly values were missing, for example due to sensor fouling or breakage, values were interpolated using regressions from adjacent data. During August 2012 there were significant difficulties during all deployments with breaking or fouling of O<sub>2</sub> microsensors and no continuous 24 h deployments were available to calculate R, GPP, and NEM. For this one season, 15 min fluxes from all available data were combined to generate one continuous 24 h record to estimate seasonal



R, GPP, and NEM. This alternative approach was tested using data from August 2011 and the resulting rates were  $< 4\%$  different than averaging the available 24 h deployments, and well within one SE of the mean.

## Results

### *Eddy correlation analysis*

An example data set collected in June 2012 is shown in Fig. 2.1. 15 min fluxes are shown with light (Fig. 2.1D), flow in the x, y, and z directions and water depth (Fig. 2.1A), mean velocity and O<sub>2</sub> concentration (Fig. 2.1B), and the cumulative fluxes for each 15 min period (Fig. 2.1C). Data is missing between 23.0–24.5 and 30.0–30.25 due to fouling of the O<sub>2</sub> microsensor.

An example of fluxes calculated both with and without the storage term correction (Eq. 1) is given in Fig. 2. Over the 24 h period, mean O<sub>2</sub> concentration varied by more than 200%. This, combined with a relatively large measuring height of 30 cm resulted in fluxes calculated with the storage term correction that differed markedly from fluxes calculated without (Fig. 2.2B). Because this site was located within a large, continuous seagrass meadow, the recorded changes in mean O<sub>2</sub> concentration are believed to arise from local production and respiration. This prompted us to apply the storage correction to all our flux calculations. The significantly better correlation of the benthic flux to light illustrated in Fig. 2.2 supports this approach.

During June 2012, two EC instruments were placed ~6 m apart deployed at 30 cm above the sediment surface to determine variability in eddy fluxes within the seagrass

meadow (Fig. 2.3). Based on a first order estimate of footprint shape from Berg et al. (2007), the footprint widths were approximately 2 m, thus placement ensured no overlapping footprints. Flux data from the concurrent 24 h deployments were compared using a summation of all instantaneous fluxes throughout the day (Fig. 2.3). The cumulative fluxes showed the expected diurnal cycle with light and very good agreement between both instruments (Fig. 2.3).

#### *Ecosystem metabolism in eelgrass meadows*

Hourly averages of O<sub>2</sub> flux (Fig. 2.4) were highly variable throughout the year and showed a typical expected diurnal cycle driven mainly by light for each season. There was variability in both day and night fluxes between seasons as well as within the individual seasons. The high temporal eddy correlation data show that variation in metabolism within a single deployment was as high as variation between seasons (Fig. 2.4).

Night O<sub>2</sub> flux (respiration) was negatively correlated with flow during all seasons except February (Fig. 2.5). Data binned by mean flow velocity illustrates these relationships and linear regression analysis was used on both binned and unbinned data to show its significance (October:  $p = 0.035$  unbinned data,  $p = 0.012$ ,  $r^2 = 0.83$  binned data; June:  $p = 0.027$  unbinned data,  $p = 0.0069$ ,  $r^2 = 0.94$ ; August:  $p = 0.0075$  unbinned data,  $p = 0.0046$ ,  $r^2 = 0.95$  binned data). The slope of the regressions, representing the strength of stimulation with flow, changed seasonally, with the strongest effect observed during June.

A clear hysteresis effect was observed during October and August when fluxes throughout the day were plotted as a function of light (Fig. 2.6). Specifically, morning O<sub>2</sub>

fluxes were larger than fluxes of a similar irradiance in the afternoon. During these time periods, mean flow in the afternoon was not significantly different from morning ( $p = 0.834$ ,  $p = 0.330$ , respectively). During February and June, mean flow between morning and afternoon was significantly different at the  $\alpha = 0.1$  level ( $p = 0.043$ ,  $0.053$ , respectively).

Both average daily (Fig. 2.7) and seasonal (Fig. 2.8B) ecosystem R, GPP, and NEM rates were highly variable and there was a strong 1:1 coupling between GPP and R (Fig. 2.7). Seasonal grouping was found between GPP and R, indicating different couplings between GPP and R with different timescales (Fig. 2.7).

The highest shoot densities were observed during June and the lowest during February (Fig. 2.8A). Strong linear correlations between shoot density and rates of R ( $r^2 = 0.96$ ,  $p = 0.004$ ) and GPP ( $r^2 = 0.83$ ,  $p = 0.031$ ) were found. NEM was also variable (Fig 7B) between seasons, and average NEM rates were found to be both positive and negative, indicating a switch between autotrophy and heterotrophy during the year. In October, February, June, and August, average NEM  $\pm$  SE was  $-0.31 \pm 27.7$ ,  $6.4 \pm 7.6$ ,  $55.5 \pm 15.4$ , and  $-47.6 \pm 14.5$  mmol O<sub>2</sub> m<sup>-2</sup>d<sup>-1</sup>, respectively ( $n = 4, 3, 5$ , and  $5$ ). NEM was not significantly different from zero in October and February ( $p = 0.991$ ,  $p = 0.488$ , respectively), was significantly greater than zero in June ( $p = 0.037$ ) and was significantly less than zero in August ( $p = 0.030$ ). Annual average metabolic rates were, R:  $-73.1 \pm 10.4$ , GPP:  $74.5 \pm 11.4$ , and NEM:  $1.3 \pm 5.1$  mol O<sub>2</sub> m<sup>-2</sup>yr<sup>-1</sup> (SE,  $n = 17$ ).

## Discussion

This study represents the most detailed data set to date on seagrass whole ecosystem metabolism measured with the eddy correlation technique. This allows us to quantify seagrass metabolism and its seasonal variation down to a scale of hours over the year in a way that has not been possible previously using alternative methods (e.g. Fig. 2.1 and 2.4). Furthermore, the direct nature of eddy correlation measurements allows us to study and quantify the drivers of seagrass metabolism under naturally varying field conditions. Strong signals from eddy correlation fluxes are shown in linear cumulative fluxes (Fig. 2.1C) as well as good correlations were found with light (Fig. 2.1D) and flow (Fig. 2.1B). O<sub>2</sub> microsensors show very good agreement with stable field optodes, indicating good calibration and function (Fig. 2.1B). Eddy correlation flux measurements are usually assumed to be representative of the whole benthic ecosystem because the footprint for the technique is typically on the order of 100 m<sup>2</sup> at measuring heights such as the one used in this study (30 cm) and incorporates spatial heterogeneity (Berg et al. 2007). The good agreement between the side-by-side deployments of two eddy correlation instruments (Fig. 2.2) supports this perception, and indicates that we can use our measured metabolic rates as representatives for the *Z. marina* meadow as a whole.

During the day, light was the main driver of production (Fig. 2.1 and 2.4) with some variation likely due to current flow although no significant relationships between current flow and daytime O<sub>2</sub> fluxes were observed (data not shown). Isolation of individual drivers is more complex as both O<sub>2</sub> producing and consuming processes are occurring simultaneously. However, we would expect that increases in flow rates would increase O<sub>2</sub> metabolism by *Z. marina* communities through several processes during both

day and night. Increases in flow will reduce leaf boundary layers that allows for faster rates of nutrient uptake (Cornelisen and Thomas 2006) or gas exchange (Binzer et al. 2005). Higher turbulence through increased current flow can also increase canopy and sediment oxygenation through flushing, providing more O<sub>2</sub> for respiration. Finally, decreases in benthic boundary layers have also been shown to stimulate production through higher rates of metabolite release from tissues (Mass et al. 2010).

During October, June, and August the variability in night fluxes was driven largely by flow, likely due to stimulation of respiration (Fig. 2.5) (Hume et al. 2011) which has been shown for many shallow coastal systems (Precht and Huettel 2003, Long et al. 2013, Berg et al. in press). However, during winter, the lack of relationship between O<sub>2</sub> metabolism and flow may be due to low respiration at the low temperatures (Moore 1997). The observed seasonal changes in flow stimulation are likely the combined a result of temperature differences and changes in shoot density that affect flow and areal biomass. Numerous studies have documented that respiration increases with temperature (Wetzel and Penhale 1983, Moore et al. 1997, Moore 2004), explaining the increase in magnitude of fluxes observed with each season. This can be seen in the 10-fold larger fluxes measured in summer than in winter (Fig. 2.5) when there was a 20 °C difference in temperature between seasons.

Between June and August, the magnitude of fluxes observed during was very similar, as temperature ranges for both seasons were between 28–32 °C. However, there was a large difference in the slope of the regressions between respiration and flow during these two seasons and was likely the result of changing *Z. marina* shoot density (Fig. 2.5, 2.7A). Based on temperature and growth morphometrics, early summer is peak growth

season for *Z. marina* at the latitude of the VCR (Orth and Moore 1986, Moore 2004, Carr et al. 2010) and the highest shoot densities were observed during this season. Higher shoot densities cause more drag and dissipation of turbulence from flow and wave energy (Fonseca and Fisher 1986, Hansen and Reidenbach 2012) and the lower turbulence results in trapping of water within the canopy and buildup of boundary layers, so small increases in flow may have large effects on increasing rates of gas exchange (Binzer et al. 2005, Mass et al. 2010) and flushing of sediments (Precht and Huettel 2003, Berg et al. in press). At night, seagrasses translocate  $O_2$  from the water column to the sediments through their leaf tissues to support root and rhizome respiration as well as release  $O_2$  into the sediments (Binzer et al. 2005, Sand-Jensen et al. 2005). Binzer et al. (2005) found a logarithmic increase in tissue  $pO_2$  with flow which they attribute to increasing passive  $O_2$  uptake from reductions in diffusive boundary layers. This logarithmic relationship suggests that small increases in flow at low velocities may be more significant to  $O_2$  uptake by seagrasses than larger increases (Binzer et al. 2005). This process would result in the higher sensitivity of  $R$  to flow at higher shoot densities due to drastically reduced flow conditions combined with higher seagrass biomass (Fig. 2.5).

A hysteresis was observed during October and August with respect to light suggesting that there may be a coupling between production and respiration on the hourly timescale (Fig. 2.6, shown for October) where net metabolism during the morning was higher than the afternoon at a similar irradiance (Fig. 2.6). The lower rates of net production in the afternoon were likely the result of stimulation of respiration through the release and consumption of dissolved organic exudates (DOC) (Penhale and Smith 1977, Wetzel and Penhale 1979) or increased temperatures (Moore et al. 1997, Moore 2004,

Staeher and Borum 2011). During October, net production decreased by nearly 300 mmol O<sub>2</sub> m<sup>-2</sup>d<sup>-1</sup> at similar light values from morning to afternoon with an increase in temperature from only 16.3 to 17.8 °C (Fig. 2.6). This range is sub-optimal for *Z. marina*, e.g. < 25–28 °C, (Staeher and Borum 2011), and this temperature difference will not increase R relative to production as much as observed. Therefore, the hysteresis during October was likely a result of the buildup of DOC throughout the day stimulating heterotrophic R in the afternoon relative to the morning (Fig. 2.6). During August, when temperatures are above 28 °C, DOC stimulation of R is likely less important because temperature stress reduces seagrass photosynthesis and thus DOC production and temperature may be the main process. This is significant as direct measurements of daytime respiration can be very difficult to obtain. Most estimates of ecosystem R assume that daytime R is equal to nighttime R (e.g. Cole et al. 2000). However, this hysteresis suggests that R during the day may be higher than R at night which is supported by studies that have attempted to separate R from production and found that daytime R may be up to 4 fold higher than dark R (Glud 2008). During February and June it is not possible to separate these processes from effects of current flow, as mean velocity was significantly different between morning and afternoon.

Daily ecosystem metabolism showed tight coupling between GPP and R (Fig. 2.7) (Duarte et al. 2010, Hume et al. 2011); however, the seasonal variation in where these data fell on the 1:1 line indicated there were two separate timescale processes occurring. The short timescale represents mainly day-to-day variability in light and flow conditions, where sunny days may lead to higher GPP than cloudy days or high flow conditions may increase R (e.g. Fig. 2.5). Increases in GPP lead may lead to higher plant R of fixed

carbon during the day or exudation of excess labile DOC into sediments or from leaves (Penhale and Smith 1977, Wetzel and Penhale 1979) stimulating heterotrophic R. Increased R of labile DOC during the night can cause a release in nutrients which may then stimulate GPP resulting in two positive feedbacks between GPP and R.

The longer timescale represents seasonal differences in temperature and shoot density (Fig. 2.7). Because temperature stimulates both GPP and R (Moore et al. 1997, Moore 2004, Staehr and Borum 2011), warmer seasons would fall further down the 1:1 line (Figure 2.4, e.g. June and August). However, due to the covariance of shoot density and seasonal temperatures, differences in shoot density may explain the higher R in June relative to August. Seasonal average GPP and R estimates were strongly correlated to shoot density (Figure 2.8A) and may directly reflect seagrass metabolism, or the indirect effect of increasing seagrass biomass on the release of labile DOC (Penhale and Smith 1977, Wetzel and Penhale 1979) or increased nighttime sediment oxygenation through O<sub>2</sub> release into the rhizosphere (Frederiksen and Glud 2006) both of which may stimulate heterotrophic metabolism. Higher shoot density also suggests higher self-shading and leaf area indices which may allow for more efficient rates of light capture and thus production than at lower shoot densities (Zimmerman et al. 2003, Binzer et al. 2006, Sand-Jensen et al. 2007).

Estimates of O<sub>2</sub> metabolism can be used as a proxy to determine whether an ecosystem is net heterotrophic (source of CO<sub>2</sub>) or autotrophic (sink of CO<sub>2</sub>). Rates of R, GPP and NEM were highly variable depending on sampling season, indicating that the metabolic status of this seagrass meadow cannot be determined from a single sampling season (Murray and Wetzel 1987, Ziegler and Benner 1999). The average NEM switched



from net balanced during October and February, to net autotrophic during June and to net heterotrophic during August (Fig. 2.8B) and this pattern can be seen in the location of daily GPP and R relative to the 1:1 line (Fig. 2.7).

The *Z. marina* meadow we studied here is part of a successful restoration project (Orth et al. 2012) and the recovery trajectories over the 11 years since seeding suggest a return of important ecosystem services to the region (McGlathery et al. 2012). Shoot densities and rates of R, GPP, and NEM agreed well between August 2011 and August 2012 suggesting that after 11 years this meadow may be approaching quasi-steady state conditions. The annual balance found here between GPP and R indicates that this seagrass meadow has high internal recycling of nutrients and organic matter and over time with colonization, we expect that seagrass meadows in this area will become a prominent component of regional carbon cycling. Seagrasses have high capacities for carbon burial (Fourqurean et al. 2012) and improving the understanding of carbon cycling within seagrass meadows as we set out to do in this study will help us assess coastal carbon budgets on both a local and a global scale.

## References

- Barron, C., N. Marba, J. Terrados, H. Kennedy, and C. M. Duarte. 2004. Community metabolism and carbon budget along a gradient of seagrass (*Cymodocea nodosa*) colonization. *Limnol. Oceanogr.* 49(5): 1642 – 1651.
- Berg, P., H. Roy, F. Janssen, V. Meyer, B. B. Jørgensen, M. Huettel, and D. de Beer. 2003. Oxygen uptake by aquatic sediments measured with a novel non-invasive eddy-correlation technique. *Mar. Ecol. Prog. Ser.* 261: 75 – 83.
- Berg, P., H. Roy, and P. L. Wiberg. 2007. Eddy correlation flux measurements: The sediment surface area that contributes to the flux. *Limnol. Oceanogr.* 52(4): 1672 – 1684.
- Berg, P., R. N. Glud, A. Hume, H. Stahl, K. Oguri, V. Meyer, and H. Kitazato. 2009. Oxygen uptake by deep ocean sediments measured with the eddy correlation technique. *Limnol. Oceanogr: Methods.* 7: 576 – 584.
- Berg, P., M. Long, M. Huettel, J. E. Rheuban, K. J. McGlathery, R. W. Howarth, A. E. Giblin, and R. Marino. Eddy correlation measurements of oxygen fluxes in permeable sediments exposed to varying current flow and light. *Limnol. Oceanogr.* In Press.
- Binzer, T., J. Borum, and O. Pedersen. 2005. Flow velocity affects internal oxygen conditions in the seagrass *Cymodocea nodosa*. *Aquatic Botany.* 83: 239 – 247.
- Binzer, T., K. Sand-Jensen, and A. Middleboe. 2006. Community photosynthesis of aquatic macrophytes. *Limnol. Oceanogr.* 51(6): 2722 – 2733.

- Carr, J., P. D'Odorico, K. McGlathery, and P. Wiberg (2010), Stability and bistability of seagrass ecosystems in shallow coastal lagoons: Role of feedbacks with sediment resuspension and light attenuation, *J. Geophys. Res.*, 115, G03011
- Chipman, L., M. Huettel, P. Berg, V. Meyer, I. Klimant, R. Glud, and F. Wenzhoefer. 2012. Oxygen optodes as fast sensors for eddy correlation measurements in aquatic systems. *Limnol. Oceanogr.: Methods*. 10: 304 – 316.
- Cole, J. J., M. L. Pace, S. R. Carpenter, AND J. F. Kitchell. 2000. Persistence of net heterotrophy in lakes during nutrient addition and food web manipulations. *Limnol. Oceanogr.* 45:1718–1730
- Cornelisen, C. D. and F. I. M. Thomas. 2006. Water flow enhances ammonium and nitrate uptake in a seagrass community. *Mar. Ecol. Prog. Ser.* 312: 1 – 13.
- Duarte, C. M., N. Marba, E. Gacia, J. W. Fourqurean, J. Beggins, C. Barron, and E. T. Apostolaki. 2010. Seagrass community metabolism: Assessing the carbon sink capacity of seagrass meadows. *Global Biogeochem. Cycles*. 24: GB4302.
- Duarte, C. M., H. Kennedy, N. Marba, and I. Hendriks. 2011. Assessing the capacity of seagrass meadows for carbon burial: Current limitations and future strategies. *Ocean and Coastal Management*. In Press. 1 – 11.
- Eyre, B. D., D. Maher, J. M. Oakes, D. V. Erler, and T. M. Glasby. 2011. Differences in benthic metabolism, nutrient fluxes, and denitrification in *Caulerpa taxifolia* communities compared to uninvaded bare sediment and seagrass (*Zostera capricorni*) habitats. *Limnol. Oceanogr.* 56(5): 1737 – 1750.

- Fonseca, M. S., and J. S. Fisher. 1986. A comparison of canopy friction and sediment movement between four species of seagrass with reference to their ecology and restoration. *Mar. Ecol. Prog. Ser.* 29: 15 – 22.
- Fourqurean, J. W., C. M. Duarte, H. Kennedy, N. Marbà, M. Holmer, M. A. Mateo, E. T. Apostolaki, G. A. Kendrick, D. Krause-Jensen, K. J. McGlathery, and O. Serrano. 2012. Seagrass ecosystems as a globally significant carbon stock. *Nature Geoscience*. 5: 505 – 509.
- Frederiksen, M. S. and R. N. Glud. 2006. Oxygen dynamics in the Rhizosphere of *Zostera marina*: A Two-Dimensional Planar Optode Study. *Limnol. Oceanogr.* 51(2): 1072 – 1083.
- Gacia, E., H. Kennedy, C. M. Duarte, J. Terrados, N. Marba, S. Papadimitriou, and M. Fortes. 2005. Light-dependence of the metabolic balance of a highly productive Philippine seagrass community. *Jour. of Exp. Mar. Biol. and Ecol.* 316: 55 – 67.
- Glud, R. N. 2008. Oxygen dynamics of marine sediments. *Marine Biology Research*. 4(4): 243 – 289.
- Glud, R. N., P. Berg, A. Hume, P. Batty, M. E. Blicher, K. Lennert, and S. Rysgaard. 2010. Benthic O<sub>2</sub> exchange across hard bottom substrates quantified by eddy correlation in a sub-Arctic fjord. *Mar. Ecol. Prog. Ser.* 417: 1 – 12.
- Hansen, J. C. R. and M. A. Reidenbach. 2012. Wave and tidally driven flows in eelgrass beds and their effect on sediment resuspension. *Mar. Ecol. Prog. Ser.* 448: 271 – 287.

- Hume, A., P. Berg, and K. McGlathery. 2011. Dissolved oxygen fluxes and ecosystem metabolism in an eelgrass (*Zostera marina*) meadow measured with the eddy correlation technique. *Limnol. Oceanogr.* 56(1): 86 – 96.
- Long, M. H., D. Koopmans, P. Berg, S. Rysgaard, R. N. Glud, and D. H Sjøgaard. 2012. Oxygen exchange and ice melt measured at the ice-water interface by eddy correlation. *Biogeosciences*. 9: 1957 – 1967.
- Long, M. H., J. E. Rheuban, P. Berg, and J. C. Zieman. 2012b. A comparison and correction of light intensity loggers to photosynthetically active radiation sensors. *Limnol. Oceanogr.: Methods*. 10: 416 – 424.
- Lorrai, C., D. F. McGinnis, A. Brand, and A. Wüest. 2010. Application of oxygen eddy correlation in aquatic systems. *Jour. Atm. and Oceanic Tech.* 27: 1533 – 1546.
- Masini, R. J. and C. R. Manning. 1997. The photosynthetic responses to irradiance and temperature of four meadow-forming seagrasses. *Aquatic Botany*. 58: 21 – 36.
- McGinnis, D. F., S. Cherednichenko, S. Sommer, P. Berg, L. Rovelli, R. Schwarz, R. N. Glud, and P. Linke. 2011. Simple, robust eddy correlation amplifier for aquatic dissolved oxygen and hydrogen sulfide flux measurements. *Limnol. Oceanogr.: Methods*. 9: 340 – 347.
- Mass, T., A. Genin, U. Shavit, M. Grinstein, and D. Tchernov. 2010. Flow enhances photosynthesis in marine benthic autotrophs by increasing the efflux of oxygen from the organism to the water. *PNAS*. 107(6): 2527 – 2531.
- Massey, F. J. (1951). The Kolmogorov-Smirnov Test for Goodness of Fit. *Jour. of the Amer. Stat. Assoc.* 46(253): 68–78.

- McGlathery K.J., Sundback, K, I.C. Anderson. 2007. Eutrophication in shallow coastal bays and lagoons: the role of plants in the coastal filter. *Mar. Ecol. Prog. Ser.* 348: 1-18
- McGlathery, K. J., L. K. Reynolds, L. W. Cole, R. J. Orth, S. R. Marion, and A. Schwartzchild. 2012. Recovery trajectories during state change from bare sediment to eelgrass dominance. *Mar. Ecol. Prog. Ser.* 448:209 – 221.
- McLeod, E., G. L Chmura, S. Bouillon, R. Salm, M. Björk, C. M. Duarte, C. E. Lovelock, W. H. Schlesinger, and B. R. Silliman. 2011. A blueprint for blue carbon: toward an improved understanding of the role of vegetated coastal habitats in sequestering CO<sub>2</sub>. *Frontiers in Ecology and the Environment.* 9: 552–560
- Moore, K. A., R. L. Wetzel, and R. J. Orth. 1997. Seasonal pulses of turbidity and their relations to eelgrass (*Zostera marina* L.) survival in an estuary. *Jour. of Exp. Mar. Biol. and Ecol.* 215: 115 – 134.
- Moore, K.A. 2004. Influence of seagrasses on water quality in shallow regions of the lower Chesapeake Bay. *Journal of Coastal Research.* 45: 162-178.
- Moore, K. A. and J. C. Jarvis. 2008. Environmental factors affecting recent summertime eelgrass diebacks in the lower Chesapeake Bay: implications for long term persistence. *Journal of Coastal Research: Special Issue.* 55: 135 – 147.
- Moore, K. A., E. C. Shields, D. B. Parrish, and R J. Orth. 2012. Eelgrass survival in two contrasting systems: role of turbidity and summer water temperatures. *Mar. Ecol. Prog. Ser.* 448: 247 – 258.

- Orth, R. J and K. Moore. 1986. Seasonal and year-to-year variations in the growth of *Zostera marina* L. (eelgrass) in the lower Chesapeake Bay. *Aquatic Botany*. 24: 335 – 341.
- Orth, R. J., M. L. Luckenbach, S. R. Marion, K. A. Moore, and D. J. Wilcox. 2006. Seagrass recovery in the Delmarva Coastal Bays, USA. *Aquatic Botany* 84: 26 – 36.
- Orth, R. J., T. J. B. Carruthers, W. C. Dennison, C. M. Duarte, J. W. Fourqurean, K. L. Heck, A. R. Hughes, G. A. Kendrick, W. J. Kenworthy, S. Olyarnik, F. T. Short, M. Waycott, and S. Williams. 2006b. A Global Crisis for Seagrass Ecosystems. *BioScience*. 56(12): 987 – 996.
- Orth, R. J., S. R. Marion, K. A. Moore, and D. J. Wilcox. 2010. Eelgrass (*Zostera marina* L.) in the Chesapeake Bay Region of Mid-Atlantic Coast of the USA: Challenges in Conservation and Restoration. *Estuaries and Coasts*. 33: 139 – 150.
- Orth, R., J., K. A. Moore, S. R. Marion, D. J. Wilcox, and D. B. Parrish. 2012. Seed addition facilitates eelgrass recovery in a coastal bay system. *Mar. Ecol. Prog. Ser.* 448: 177 – 195.
- Penhale, P. A. and W. O. Smith, Jr. 1977. Excretion of Dissolved Organic Carbon by Eelgrass (*Zostera marina*) and its Epiphytes. *Limnol. Oceanogr.* 22(3): 400 – 407.
- Precht, E. and M. Huettel. 2003. Advective pore-water exchange driven by surface gravity waves and its ecological implications. *Limnol. Oceanogr.* 48(4): 1674 – 1684.
- Ralph, P. J., M. J. Durako, S. Enríquez, C. J. Collier, and M. A. Doblin. 2007. Impact of light limitation on seagrasses. *Jour. of Exp. Mar. Biol. and Ecol.* 350: 176 – 193.

- Reimers, C. E., H. T. Ozkan-Haller, P. Berg, A. Devol, K. McCann-Grosvenor, and R. D. Sanders. 2012. Benthic oxygen consumption rates during hypoxic conditions on the Oregon continental shelf: Evaluation of the eddy correlation method. *Jour. of Geophys. Res.* 117: 1 – 18.
- Sand-Jensen, K., O. Pedersen, T. Binzer, and J. Borum. 2005. Contrasting oxygen dynamics in the freshwater isoetid *Lobelia dortmanna* and the marine seagrass *Zostera marina*. *Annals of Botany*. 96: 613 – 623.
- Sand-Jensen, K., T. Binzer, and A. L. Middleboe. 2007. Scaling of photosynthetic production of aquatic macrophytes – a review. *Oikos*. 116: 280 – 294.
- Short, F., T. Carruthers, W. Dennison, and M. Waycott 2007. Global seagrass distribution and diversity: a bioregional model. *Jour. of Exp. Marine Biol. and Ecol.* 350: 3 – 20.
- Staehr, P. A. and J. Borum. 2011. Seasonal acclimation in metabolism reduces light requirements of eelgrass (*Zostera marina*). *Jour. of Exp. Marine Biol. And Ecol.* 407: 139 – 146.
- Waycott, M., C. M. Duarte, T. J. B. Carruthers, R. J. Orth, W. C. Dennison, S. Olyarnik, A. Calladine, J. W. Fourqurean, K. L. Heck Jr., A. Randall Hughes, G. A. Kendrick, W. J. Kenworthy, F. T. Short, and S. L. Williams. 2009. Accelerating loss of seagrasses across the globe threatens coastal ecosystems. *PNAS*. 106(30): 12377 – 12381.
- Wetzel, R. G. and P. A. Penhale. 1979. Transport of carbon and excretion of dissolved organic carbon by leaves and roots/rhizomes in seagrasses and their epiphytes. *Aquatic Botany*. 6: 149 – 158.



- Wetzel, R. L. and P. A. Penhale. 1983. Production ecology of seagrass communities in the lower Chesapeake Bay. *Mar. Technol. Soc. J.* 17: 22 – 31.
- Ziegler, S. and R. Benner. 1999. Dissolved organic carbon cycling in a seagrass-dominated lagoon. *Mar. Ecol. Prog. Ser.* 180: 149 – 160.
- Zimmerman, R. C. 2003. A biooptical model of irradiance distribution and photosynthesis in seagrass canopies. *Limnol. Oceanogr.* 48(1): 568 – 585.

## Figures

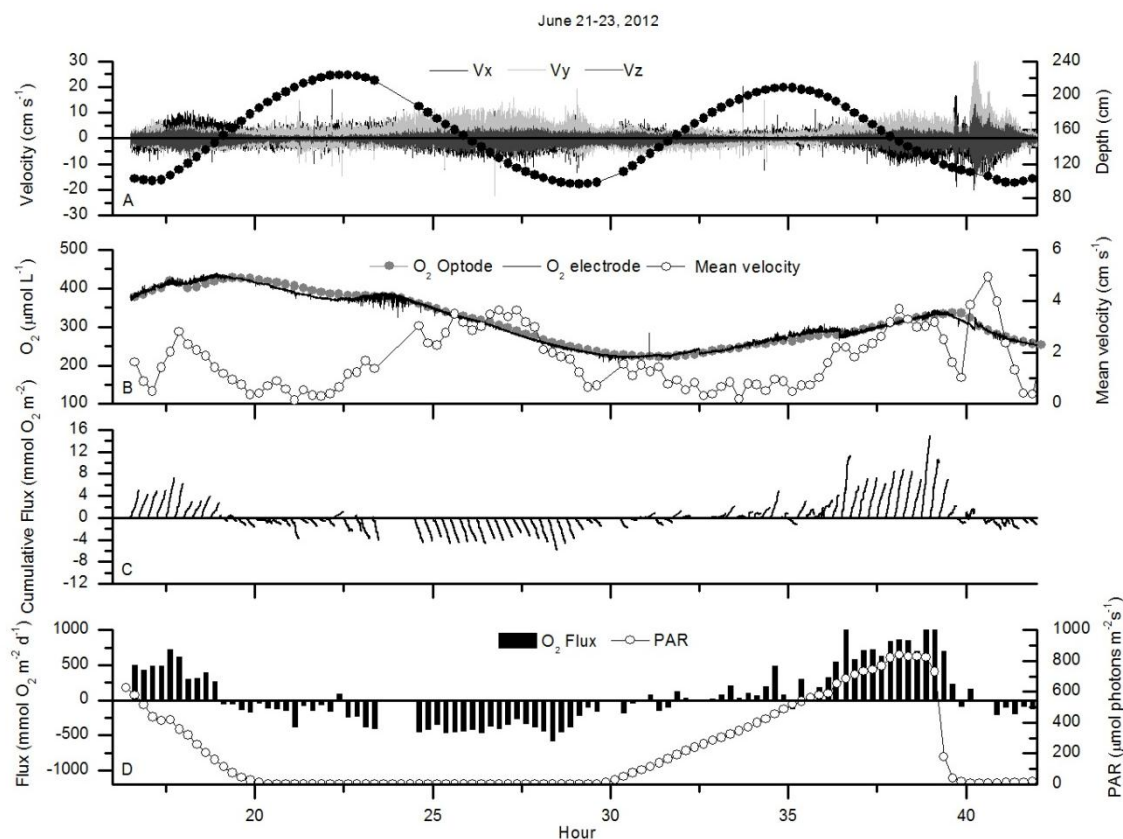


**Figure 2.1** Example deployment from June 2012.

Example eddy correlation deployment from June 2012. (A) Water velocity in x, y, and z directions and water depth. (B) O<sub>2</sub> concentration from the microsensor and a stable optode with mean current velocity. (C) Cumulative fluxes over each 15 min period. (D) 15 min O<sub>2</sub> fluxes shown with photosynthetically active radiation (PAR) reaching the canopy.

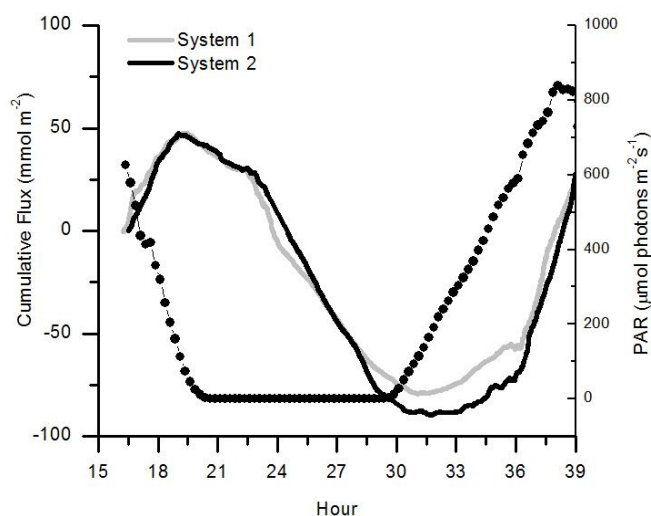


**Figure 2.2** Two eddy correlation instruments side-by-side.

Two eddy correlation instruments deployed in June 2012 side by side for 24 hours ~ 6 m apart with no overlapping footprints. Figure shows cumulative fluxes from both instruments over the 24 h period and photosynthetically active radiation (PAR).

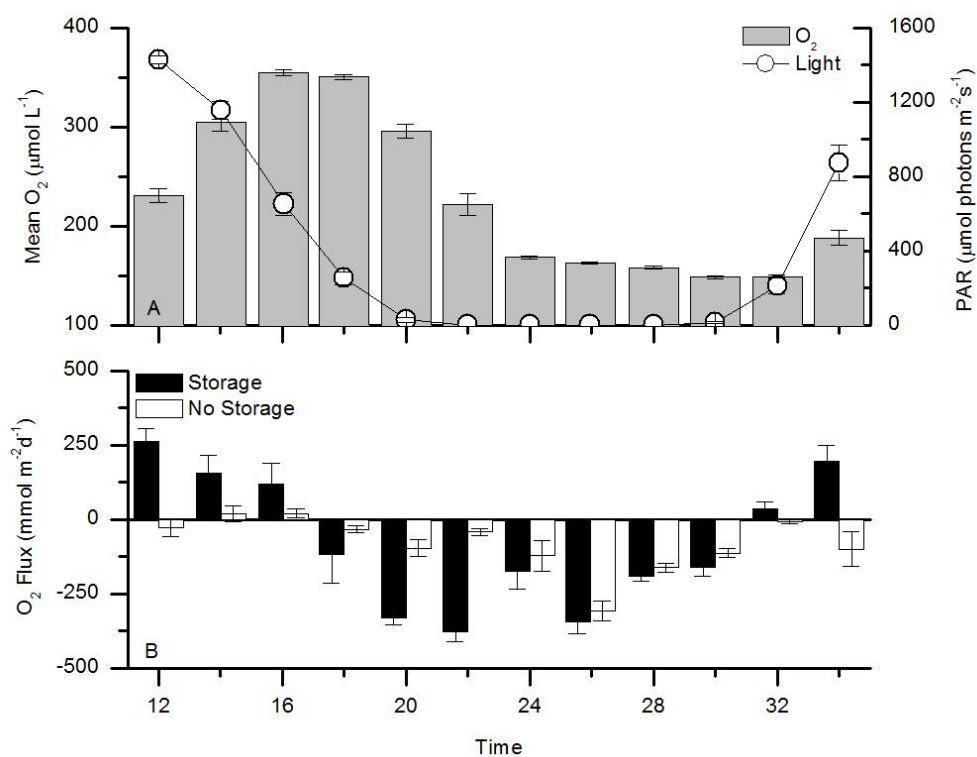


**Figure 2.3** Example use of storage in flux calculation.

Example from August 2011 of flux calculations with and without storage correction (Eq.

1) (A) Photosynthetically active radiation reaching the canopy and mean water column

$O_2$  concentration. (B) Comparison of flux extraction accounting for storage vs. no storage term.

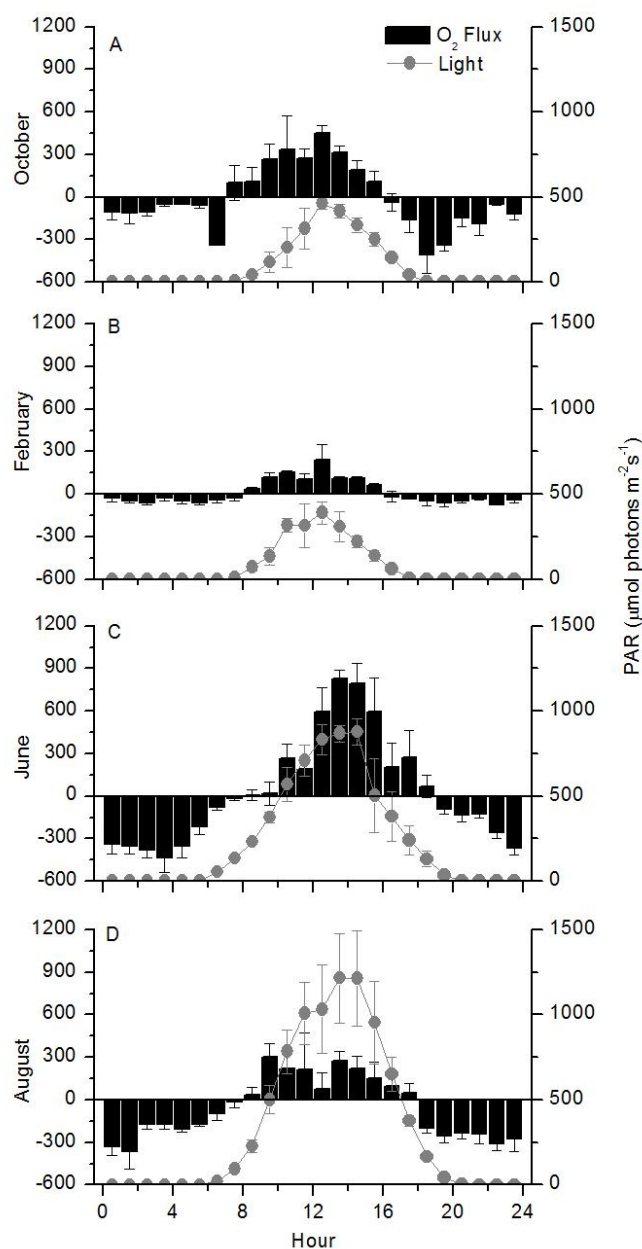


**Figure 2.4** Seasonal hourly fluxes and light.

Binned hourly average  $O_2$  fluxes and available photosynthetically active radiation for October, February, June, and August (A, B, C, and D, respectively). Error bars are standard error.

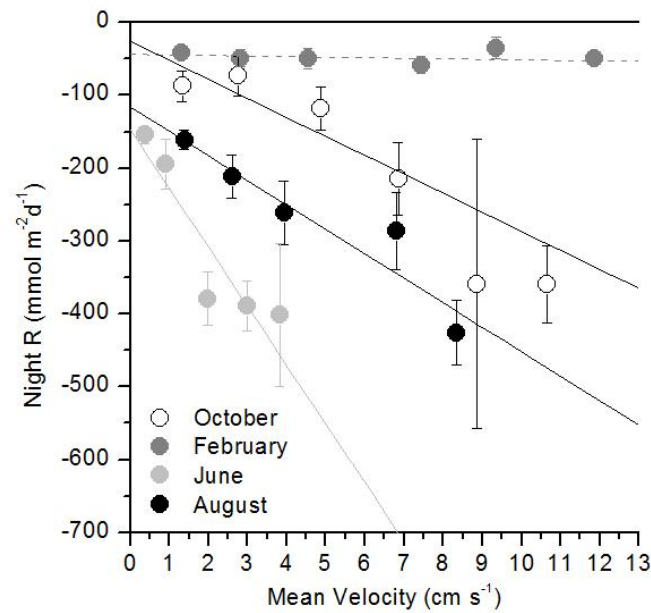


**Figure 2.5** Flow stimulation of night respiration.

Night respiration as a function of mean velocity for October, February, June, and August.

Data were binned to illustrate relationships and significant trends were found in October

( $p = 0.035$  unbinned data,  $p = 0.012$ ,  $r^2 = 0.83$  binned data), June ( $p = 0.027$  unbinned

data,  $p = 0.0069$ ,  $r^2 = 0.94$ ), and August ( $p = 0.0075$  unbinned data,  $p = 0.0046$ ,  $r^2 = 0.95$

binned data). Error bars are standard error.

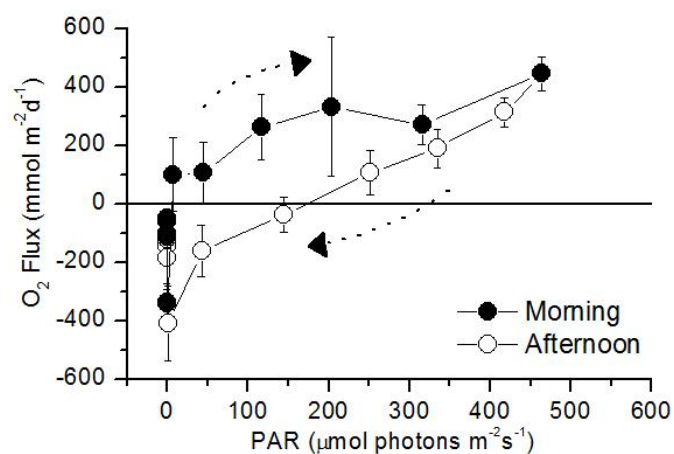


**Figure 2.6** Hourly average O<sub>2</sub> flux vs. light for October 2011.

Seasonal average oxygen flux binned by hour of day as a function of photosynthetically active radiation (PAR) for October. Error bars are standard error.

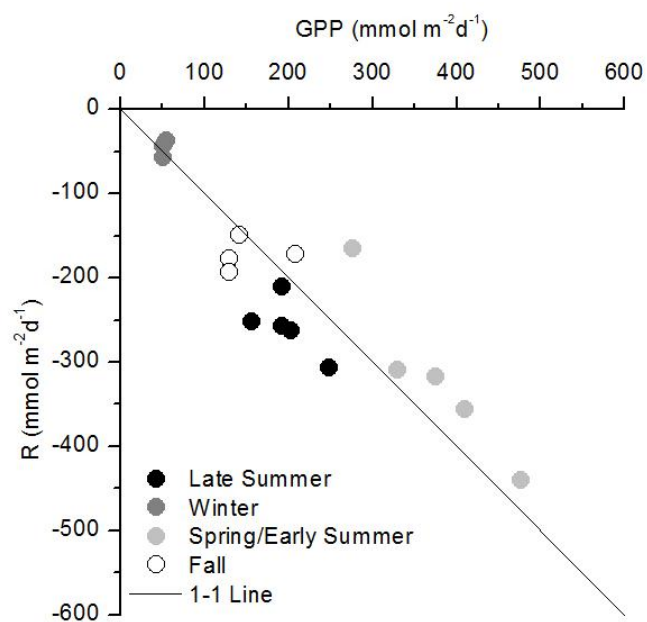


**Figure 2.7** Daily gross primary production vs. respiration.

Daily ecosystem gross primary production (GPP) vs. community respiration (R) for all sampling dates.



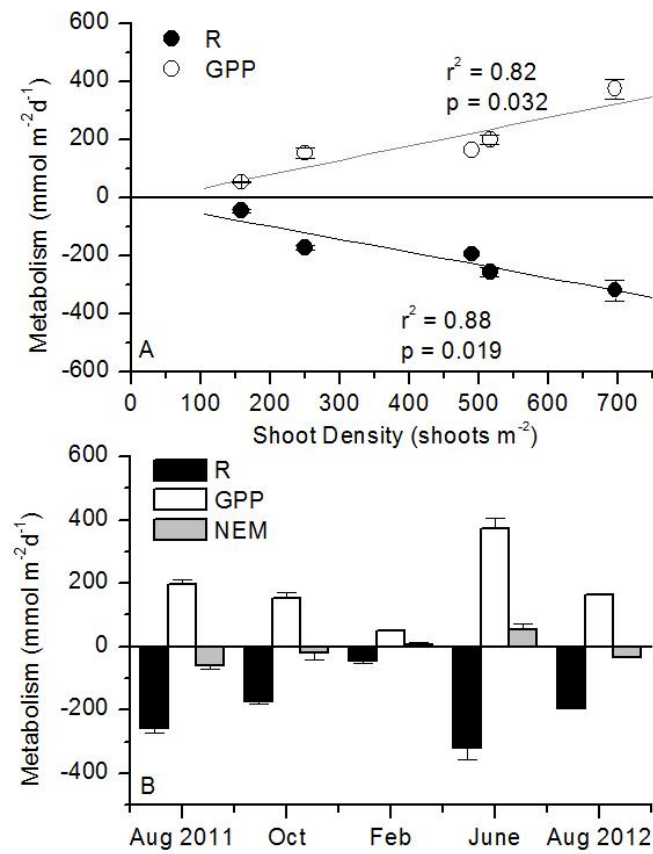


**Figure 2.8** Seasonal average metabolism and shoot density.

(A) Seasonal average gross primary production (GPP) and respiration (R) vs. shoot density. (B) Seasonal average R, GPP, and net ecosystem metabolism (NEM) during all sampling seasons ( $n = 5, 4, 3, 5, 1$  for August 2011, October, February, June, and August 2012, respectively). Error bars are standard error.

**Chapter 3 : Ecosystem metabolism along a colonization gradient of eelgrass (*Zostera marina* L.) measured by eddy correlation.**

**Acknowledgements**

Support for this study was provided by the University of Virginia and the National Science Foundation through grants from the Chemical Oceanography program (OCE-0536431 and OCE-1061364) and the Division of Environmental Biology to the VCR-LTER (DEB-0917696 and DEB-0621014).

## Abstract

Ecosystem metabolism was measured along a colonization gradient generated by a large-scale systematic *Zostera marina* L. restoration located in the Virginia coastal bays. This region experienced local extinction of seagrass during the early 1930s and recent restoration has generated an ecosystem state change from bare to vegetated sediments beginning in 2001. Ecosystem metabolism was measured seasonally using eddy correlation at three different sites representing different stages of seagrass colonization: unvegetated, young (seeded in 2007), and older (seeded in 2001). Ecosystem respiration (R) and gross primary production (GPP) increased in magnitude with meadow age. Hourly oxygen (O<sub>2</sub>) fluxes were highly correlated to light as the most important driver for production at the vegetated sites. However, no consistent trends with light were observed at the bare site. Ecosystem light compensation increased with temperature from 31 to 147 and 43 to 504  $\mu\text{mol photons m}^{-2}\text{s}^{-1}$  at the young and older seagrass sites, respectively. Photosynthesis-irradiance curves generated from hourly O<sub>2</sub> fluxes were used to produce a model for ecosystem metabolism based on incident light for every hour of the year to calculate a detailed flux record, and from that, an estimate of annual NEM. Annual NEM at the bare, 5 year, and 11 year sites was -7.6, 8.6, and -7.0  $\text{mol O}_2 \text{ m}^{-2}\text{yr}^{-1}$ , respectively. Although GPP and R were up to 10-fold larger at the older vegetated site relative to the bare site, the similar annual NEM among sites suggests that the ecosystem state change may not affect the metabolic balance at these sites.

## Introduction

Seagrass decline has been well documented worldwide (Orth et al. 2006, Waycott et al. 2009) and seagrass restoration via seeding or transplanting is used as a mechanism to reverse this trend and thus return important ecosystem services to coastal environments (McGlathery et al. 2012, Orth et al. 2012). Relative to unvegetated habitats, seagrasses can be globally significant to carbon (C) sequestration (Duarte et al. 2010, Mcleod et al. 2011, Fourqurean et al. 2012) through higher rates of primary productivity (Apostolaki et al. 2010, Hume et al. 2011) and sediment deposition (Gacia et al. 2005, Hansen and Reidenbach 2012). However, the capacity for a seagrass meadow to sequester C is dependent on rates of C burial as well as ecosystem production and respiration as an indicator of net autotrophy or heterotrophy (Duarte et al. 2010). As seagrass restoration is occurring worldwide, a detailed understanding of the effect of seagrass colonization on ecosystem metabolism is important as a key component of coastal C dynamics.

Seagrass restoration is expected to significantly alter coastal benthic ecosystem metabolism by changing benthic community structure. Seagrass meadows have increased productivity relative to unvegetated sediments (Barron et al. 2004, Holmer et al. 2004, Eyre et al. 2011) as they have higher primary producer and heterotrophic consumer biomass (Hemminga and Duarte 2000). In addition, changes in ecosystem structure through the development of a seagrass canopy can increase efficiency of light absorption on an ecosystem scale relative to unvegetated sites up to a point at which high densities may cause declines in photosynthesis as shading increases (Zimmerman et al. 2003, Binzer et al. 2006, Ralph et al. 2007). Finally, seagrass communities can alter the sediments through changes in flow conditions that create a depositional environment

(Gacia et al. 2001, Hansen and Reidnebach 2012), increase sediment organic content (Wetzel and Penhale 1983, Fourqurean et al. 2012, McGlathery et al. 2012), and change sediment oxygenation through release of oxygen from the roots and rhizomes (Binzer et al. 2005, Frederiksen and Glud 2006).

The coastal lagoons of the Virginia Coast Reserve (VCR) have been the site of a successful large-scale seagrass restoration project (Orth et al. 2010, 2012, McGlathery et al. 2012). These coastal bays historically were colonized by eelgrass (*Zostera marina* L.) but underwent an ecosystem state change in the late 1920s and early 1930s when *Z. marina* was completely removed from the system through natural causes by a slime mold (*Labrynthula zosterae*) followed by a hurricane in 1933 (Cottam and Munro 1954). Until the late 1990s, the lagoons were devoid of *Z. marina*, and between 2001 and 2008, a systematic restoration via seeding occurred and meadows have continued to expand by natural recruitment (Orth et al. 2006, 2012). The systematic restoration design provided a chronosequence in which the effects of seagrass colonization on the coastal lagoons can be observed (McGlathery et al. 2012).

Currently, the seagrass recovery trajectories of the coastal bays show increasing return of important ecosystem services with age (time since seeding). McGlathery et al. (2012) documented increased shoot density, areal productivity, sediment organic matter, carbon and nitrogen contents with age. This state change to seagrass dominance is expected to alter net ecosystem metabolism through changing above and belowground primary producer biomass, community structure (Barron et al. 2004), and increases in O<sub>2</sub> demand by heterotrophic organisms (Hemminga and Duarte 2000). In addition, subsequent measurements of shoot density, ecosystem metabolism, and carbon burial

data suggest this system has taken approximately 11 – 12 years to reach quasi-steady state conditions (Greiner et al. in review, Rheuban Chapter 2, McGlathery, unpublished data). Barron et al. (2004) found that net ecosystem metabolism decreased with time since seagrass (*Cymodocea nodosa*) colonization as a function of increasing rates of community respiration; however, their study site had unique characteristics of continuous burial by large subtidal sand dunes that may not be representative of other seagrass ecosystems.

In this study, we measured oxygen ( $O_2$ ) fluxes using the eddy correlation technique seasonally at three sites along a seagrass colonization gradient in order to determine how ecosystem metabolism changed with seagrass colonization. Based on seasonal  $O_2$  fluxes, we quantified ecosystem respiration (R), gross primary production (GPP), and net ecosystem metabolism (NEM) throughout the year. In addition, we provide a model based on light availability to estimate NEM continuously for one year to determine annual net metabolism for the different aged sites.

## Methods

*Study site* – the study site was located in the shallow lagoons of the Virginia Coast Reserve (VCR) Long Term Ecological Research (LTER) site, which are approximately 1 m deep at mean low water with a 1 m tidal range. Three sites were chosen within the lagoon system that represent different stages of seagrass colonization: bare sediment (no seeding), young meadows (seeded in 2007), and older meadows (seeded in 2001). The bare sediment site (hereafter labeled as bare) and the young meadow (hereafter labeled 5 year) were located in Hog Island Bay (37° 24'58.068"N, 75° 42'35.33"W and 37°

25°7.0788'N, 75°43'19.718'W for the bare and 5 year site, respectively), and the older meadow (hereafter labeled 11 year) was located about 20 km away in South Bay (37°15'43.6356N, 75°48'54.547'W). The bare site were colonized by benthic microalgae and had a sediment organic content of  $2.0 \pm 0.3$  % measured in July 2012 as mass loss on ignition at 500 °C (SE, n = 5, McGlathery, unpublished data) and permeability of  $5.8 \times 10^{-12} \text{ m}^2$ . The seagrass sites were originally seeded in 0.4 ha plots with 100,000 *Z. marina* seeds with organic content of  $1.7 \pm 0.1$  % and  $2.6 \pm 0.3$  % at the 5 and 11 year sites, respectively (average  $\pm$  SE, n = 5, McGlathery unpublished data). Other site characteristics including shoot density (shoots  $\text{m}^{-2}$ ), which can be a significant driver of ecosystem metabolism (Rheuban Chapter 2), and benthic chlorophyll concentrations as a proxy for benthic microalgal abundance ( $\text{mg m}^{-3}$ ) can be found in Table 3.1. Site characteristics from bare sites in these two lagoons were not significantly different which allows us to compare the effects of seagrass colonization directly (McGlathery et al. 2012).

*Data Collection* – Data were collected during four seasons for eelgrass based on temperature: fall regrowth after summer heat stress, low winter growth, spring/early summer peak growth season, and late summer heat stress (Orth and Moore 1986, Rheuban Chapter 2). Data were collected in late July/August 2011 at the 11 year site, and October 2011, February/March 2012, June 2012, and August 2012 at all three sites. The seasonal overlap (August 2011/2012) allowed us to check reproducibility in our data from year to year. Shoot density and benthic chlorophyll content were measured seasonally. Shoot density was measured by counting all shoots in situ located within 4 –



10 haphazardly thrown 0.25 m<sup>2</sup> quadrats. During February 2012, due to low temperatures and low shoot density, shoots were counted in 8 replicate 0.125 m<sup>2</sup> quadrants. Benthic chlorophyll was measured by collecting the top 1 cm of sediment in 8 replicate 10cm<sup>3</sup> syringe cores, and extracted in methanol/acetone as in McGlathery et al. (2012). Above and belowground biomass and seagrass morphology measurements from McGlathery (unpublished) were used from a larger annual survey in July 2011 and July 2012. Sediment permeability was measured at the bare site using a falling head permeameter.

Benthic O<sub>2</sub> fluxes were measured with the eddy correlation technique, which measures the vertical O<sub>2</sub> flux across the sediment-water interface (Berg et al. 2003, Glud et al. 2010, Hume et al. 2011). The eddy correlation instrument consists of an acoustic Doppler velocimeter (ADV, Nortek-AS), coupled to a fast responding (90% response < 0.3s) Clark-type O<sub>2</sub> microsensor designed to minimize stirring sensitivity (< 2%, Unisense Science) mounted on a submersible picoamp amplifier (Unisense Science or GEOMAR, *see* McGinnis et al. 2011). These sensors are self-contained and mounted on a stainless steel tripod designed to minimize disturbances to the natural flow. The O<sub>2</sub> microsensor is mounted such that the sensing tip is located just outside the measurement volume of the ADV, assuming a 1 cm<sup>3</sup> measurement volume, to minimize time lag between velocity and O<sub>2</sub> measurements. The measuring volume was adjusted such that it was located 31 cm, 26 cm, and 10 cm above the bottom at the 11 year, 5 year, and bare sites, respectively. These different measuring heights were chosen to ensure measurements were obtained above the seagrass canopy yet not exposed at low tide. Care was taken to ensure the instruments were level and oriented into the mean current direction at each site. The sensors recorded data continuously at 32–64 Hz for 14.5 min

bursts and stopped for 0.5 min, and a single flux was extracted from each 14.5 min data burst, producing 4 flux estimates per hour. The instruments recorded for 24 h with a 1–2 h gap between deployments to download data and replace O<sub>2</sub> microsensors as needed. Deployments at each site occurred continuously for 3–8 d during each sampling season for a total of 66 separate deployments. As the O<sub>2</sub> microsensors are fragile and often break mid-deployment, 37 complete 24 h datasets were collected to estimate daily metabolism.

Environmental drivers were also measured during deployments.

Photosynthetically active radiation (PAR) was recorded every 15 min at the measurement height using a submersible planar 2 $\pi$  PAR sensor (Odyssey Data Recording) calibrated to a LI-193SA 4 $\pi$  scalar PAR sensor (LI-COR Biosciences) as in Long et al. (2012). Mean O<sub>2</sub> concentration and temperature were recorded every 15 min by either a LDO probe (Hach Systems) mounted in a waterproof housing or a submersible optical DO datalogger (miniDOT, PME). Mean water velocity, current direction, and water depth were also extracted from the ADV data.

During June 2012, metabolism was also estimated from sediment core incubations and served as a validation of the eddy correlation fluxes. Six sediment cores (20 cm deep and 6 cm diameter) with overlying water and a large volume of seawater from the bare site were collected and kept on ice in the dark until returned to the lab. Sediment cores were bubbled with air and allowed to equilibrate overnight in an outdoor flowing seawater mesocosm to maintain in situ temperatures. After equilibration, the overlying water column was carefully siphoned off and replaced with seawater from the study site filtered using a GF/C (0.2  $\mu$ m) filter. Sediment cores were capped with lids in which magnetic stir bars were mounted and care was taken so that no air bubbles were

introduced into the cores. Six replicate sediment cores and 2 cores with only filtered seawater were incubated for 3 h in light at approximately  $600 \mu\text{mol photons m}^{-2}\text{s}^{-1}$  after which the mesocosm was covered and cores were incubated for 3 h in dark. Water samples were collected every 0.5 h and replaced with equal volume of filtered seawater from the site. DO was measured using an optical LDO probe (Hach Systems) and concentration changes were corrected for input of new filtered seawater to the cores.

*Data analysis* –  $\text{O}_2$  fluxes were extracted from 16 Hz data as in Hume et al. (2011) using EddyFlux2.0 (Berg, unpublished), where careful quality control was performed to ensure that  $\text{O}_2$  or velocity data were not impacted by floating debris, biofouling, or that sensor response times were not compromised. The  $\text{O}_2$  flux is calculated as:

$$\text{Flux} = \overline{\text{O}_2' u_z'} \quad (1)$$

where  $\text{O}_2'$  and  $u_z'$  are the fluctuating components of the  $\text{O}_2$  concentration and vertical velocity determined through the linear detrending method of Reynold's averaging (Berg et al. 2003, 2007, 2009) and over-bars indicate time averaging. The velocity field can be rotated if the instruments are tilted relative to the sediment surface (Berg et al. 2003, Lorrai et al. 2010, Reimers et al. 2012); however, caution must be taken if significant surface waves are present (Reimers et al. 2012). Therefore, fluxes were tested using a two-sample Kolomogorov-Smirnov (K-S) test (Massey 1951) to determine if rotation was important to the flux calculation. This non-parametric test observes differences in the underlying distribution of data rather than changes in the mean and thus is more applicable to this dataset than tests for means.  $\text{O}_2$  storage in the water column can be a significant component of the mass balance used for extracting the eddy flux (Hume et al.

2011). This term becomes more important when measurements are obtained higher in the water column or when large changes in mean O<sub>2</sub> concentration are observed (Rheuban Chapter 2). Thus, a correction for O<sub>2</sub> storage in the water column was applied to the data obtained at the seagrass sites where the measuring height was higher than 25 cm above the seafloor (Rheuban Chapter 2).

Hourly averages of O<sub>2</sub> fluxes with associated standard error were calculated from 15-min data as in Hume et al. (2011) and then grouped into light and dark data for regression analysis, where light is defined as PAR > 1.0 µmol photons m<sup>-2</sup>s<sup>-1</sup> and dark is defined as PAR < 1.0 µmol photons m<sup>-2</sup>s<sup>-1</sup>. Daily gross primary production (GPP), respiration (R), and net ecosystem metabolism (NEM) were estimated using the equations from Hume et al. (2011). If hourly values were missing due to fouled or broken O<sub>2</sub> microsenors, values were interpolated using regressions from adjacent data. These equations assume that respiration is constant during the day and night, which may lead to underestimation of GPP and R (e.g. Glud 2008); however, NEM will not be affected as NEM is calculated directly from the eddy flux measurements.

Metabolism from the sediment core incubations was calculated from the measured concentration changes over the incubation period. Respiration was calculated from dark incubations, NEM was calculated from light and dark incubations scaled for hours of daylight and darkness, and GPP was calculated as:

$$GPP = |R|h_d + NEMh_l \quad (2)$$

Photosynthetically active radiation (PAR) and O<sub>2</sub> flux values were used to determine photosynthesis-irradiance (P-I) relationships seasonally, where a hyperbolic

tangent function modified to account for a constant respiration was fit to the O<sub>2</sub> flux values (Jassby and Platt 1976):

$$Flux = A \tanh \frac{I}{B} - C \quad (3)$$

where A, B, and C are constants and I is available light. An annual model driven by light availability from a meteorological tower approximately 6.5 km away from the 11 year site and seasonal P-I relationships for both seagrass sites were used to determine hourly and daily NEM from November 2011 to October 2012. As consistent trends to light were not observed at the bare site, seasonal measured NEM was scaled by the length of each season to estimate NEM over the course of the year.

## Results

NEM varied significantly across seasons at the 5 year site (Figure 3.1, one-way ANOVA,  $F_6 = 16.5$   $p = 0.003$ ) and at the 11 year site (Figure 3.1, one-way ANOVA,  $F_{14} = 14.0$   $p = 0.0002$ ). Gross metabolism increased in magnitude with time since seeding during October and August (GPP and R, Figure 3.1A and D). During June, NEM at the 5 year site was significantly higher than the 11 year site ( $p = 0.0343$ ), while GPP and R were not significantly different. At the bare site, NEM was not significantly different across seasons (Figure 3.1,  $F_5 = 1.26$ ,  $p = 0.38$ ). During June, GPP was not significantly different from between sediment cores and the eddy correlation technique (Table 3.2), while R and NEM were significantly different (Table 3.2).

Rates of R and GPP also increased with time since seeding when comparing fluxes from the same site (Figure 3.2). NEM shifted from balanced (one-sample t-test,  $p$

= 0.11) to slight autotrophy at the  $\alpha = 0.1$  level ( $p = 0.09$ ) from bare to young vegetated in (as reported in Hume et al. 2011) to net heterotrophic during late summer in ( $p = 0.03$ , as reported in Rheuban Chapter 2).

Hourly fluxes from both the 11 and 5 year sites were well correlated to PAR during all seasons (Figure 3.3 and 3.4). Hyperbolic tangent functions (Eq. 3, modified from Jassby and Platt 1976) were fit to all data; however, from the 11 year site during October, June, and August, these functions converged to linear functions (Figure 3.3A, C, and D). Variability at the 5 year site was much higher, and P-I relationships had a hyperbolic tangent relationship during all seasons (Figure 3.4).

Using P-I relationships fit to the hourly fluxes, compensation irradiance, or the amount of light required for photosynthesis to equal respiration ( $I_{\text{comp}}$ ), was determined for each season at the 5 and 11 year sites (Figure 3.5). The compensation irradiance increased from 31 to 147  $\mu\text{mol photons m}^{-2}\text{s}^{-1}$  at the 5 year site and 43 to 504  $\mu\text{mol photons m}^{-2}\text{s}^{-1}$  at the 11 year site between February and August. This corresponded to an average increase in temperature from 12.3 to 27.9 and 9.3 to 30.5 °C at the 5 and 11 year sites, respectively. A log-linear relationship between  $I_{\text{comp}}$  and temperature was observed at both sites (Figure 3.5, 5 year:  $r^2 = 0.886$ ,  $p = 0.059$  and 11 year:  $r^2 = 0.991$ ,  $p = 0.0091$ ).

Incident PAR ( $\text{PAR}_{\text{incident}}$ ) measured at a meteorological station approximately 6.5 km away from the 11 year site was calibrated to PAR at the surface of the canopy ( $\text{PAR}_{\text{canopy}}$ ) at the 11 year site in October, February, and June (Figure 3.6). During the August 2011 sampling, the meteorological station PAR sensor was inactive, and during the August 2012 sampling, fouling due to particle settling or macroalgae limited the

number of  $PAR_{canopy}$  data available for calibration. The first-order exponential relationship between  $PAR_{incident}$  and  $PAR_{canopy}$  was similar during the 3 seasons of data available, and thus a single relationship ( $PAR_{canopy} = 910.96e^{(PAR_{incident}/-9371.51)} - 915.21$  Figure 3.6,  $r^2 = 0.82$ ) was used to calculate available light at the canopy throughout the year.

Using the P-I curves (Figures 3.3 and 3.4) and  $PAR_{canopy}$  (Figure 3.6), daily NEM was calculated throughout the year for the 5 and 11 year sites (Figure 3.7). Integrated daily  $PAR_{canopy}$  ranged from approximately  $200 \text{ mol photons m}^{-2}\text{d}^{-1}$  during winter to  $650 \text{ mol photons m}^{-2}\text{d}^{-1}$  during summer (Figure 3.7A). Daily NEM varied from -200 to 250  $\text{mmol O}_2 \text{ m}^{-2}\text{d}^{-1}$  at the 5 year site (Figure 3.7B) and -200 to 50  $\text{mmol O}_2 \text{ m}^{-2}\text{d}^{-1}$  at the 11 year site (Figure 3.7C). At the 5 year site, seasonal differences were found in NEM where early spring was net autotrophic for most days and other seasons were net heterotrophic for most days. At the 11 year site, NEM was more consistent and heterotrophic during late summer when temperatures were high. Measured and modeled seasonal NEM were not significantly different in October, February and June (Table 3.3).

Cumulating daily NEM over the year to estimate annual NEM showed clear differences between the 5 and 11 year sites (Figure 3.8). Cumulative annual NEM at the bare, 5 year, and 11 year sites was -7.6, 8.6, and -7.0  $\text{mol O}_2 \text{ m}^{-2}\text{yr}^{-1}$  ( $n = 366$ ), respectively.

## Discussion

### *Productivity and Respiration*

The effect of seagrass colonization on ecosystem metabolism was clear on multiple different timescales. Seasonal O<sub>2</sub> metabolism increased up to 10-fold with time since colonization, indicating that seagrass ecosystems are hotspots of both autotrophic and heterotrophic productivity (Figure 3.1). During October and August, GPP and R increased with time since seeding; however, during February and June, metabolism at the 11 year site was not different from 5 year site. These seasonal differences were likely a result temperature and shoot density dependency such that the low temperatures in February reduced O<sub>2</sub> metabolism at all sites and high production at both sites during June resulted GPP and R that were not significantly different. This general trend agrees well with increases in ecosystem metabolism from late summer 2007 as reported in an earlier eddy correlation study by Hume et al. (2011) and comparing to the 11 year site (6 years after initial seeding) (Figure 3.2). The increases in metabolism are likely a result of increasing shoot density with age as a proxy for seagrass biomass (Table 3.1). Rheuban (Chapter 2) found a strong correlation between rates of GPP and R with shoot density and attributed this relationship to several covarying factors. These factors include direct seagrass effects of increasing above and belowground biomass, or indirect effects such as increased efficiency of light absorption and thus photosynthesis with higher leaf area and community self-shading (Binzer et al. 2006, Sand-Jensen et al. 2007). Seagrasses also exude labile dissolved organic material from leaves as well as roots and rhizomes which can stimulate heterotrophic respiration in sediments (Penhale and Smith 1977, Wetzel and Penhale 1983). Seagrasses can increase sediment oxygenation through O<sub>2</sub> release into



the rhizosphere further stimulating respiration (Frederiksen and Glud 2006). Increases in rates of nitrogen fixation with age and shoot density (Cole and McGlathery 2012) may also stimulate ecosystem metabolism. In addition, seagrass meadows have higher biodiversity and populations of heterotrophic organisms relative to unvegetated sites (Hemminga and Duarte 2000), which further increases O<sub>2</sub> demand.

During all seasons, the bare site was either slightly net heterotrophic (June, August, Figure 3.1) or balanced (October, February, Figure 3.1) and concurrent sediment core incubations in June validate this result. The core incubations agreed well in order of magnitude and trophic state with the eddy correlation measurements; however, R and NEM based on eddy correlation were significantly larger than those from the sediment core incubations. The permeability of the bare site ( $5.8 \times 10^{-12} \text{ m}^2$ ) was at the suggested border above which current flow and wave energy drive advective O<sub>2</sub> exchange and below which exchange is dominated by diffusion (Huettel and Gust 1992). The disagreement between the two methods suggests that some advective processes during high flow and/or wave conditions may be stimulating the O<sub>2</sub> flux. This stimulation resulted in the larger R and thus lower NEM estimates from eddy correlation data than from core incubations as the former would capture these high flow and/or wave events (Berg and Huettel 2008, Berg et al. in press). The consistent average net heterotrophy disagrees with previous studies at the VCR lagoons that have shown unvegetated sediments were net autotrophic during at least part of the year (McGlathery et al. 2001, Tyler et al. 2003, Giordano et al. 2012). This may be a result of the methodological differences between sediment core incubations (used in the aforementioned studies) and

an in situ measurement from eddy correlation which may more directly reflect the true ecosystem metabolism.

The lack of light saturation in P-I relationships at the 11 year site (Figure 3.3), suggests community scale responses may be very different than that of individual plants which agrees with theoretical findings in the literature (Binzer et al. 2006, Ralph et al. 2007, Sand-Jensen et al. 2007). However, this has not yet been illustrated with measurements as the methodology to directly measure benthic ecosystem-scale, in situ photosynthesis has only recently been developed. Due to complex canopy structures in seagrass meadows, light absorption through the canopy can be highly efficient (Masini and Manning 1995, Ralph et al. 2007). During periods of high shoot density, the upper part of the canopy is likely light saturated at high light levels but through self-shading and efficient light absorption, the understory receives much lower irradiance (Short 1980, Zimmerman 2003, Binzer et al. 2006). Thus, ecosystem-scale measurements that integrate the production of the entire meadow as a whole may be very different than P-I relationships determined through isolating a part of the plant (Binzer et al. 2006, Sand-Jensen et al. 2007). In contrast to the P-I response seen at the 11 year site, the P-I curves from the 5 year site had the expected hyperbolic tangent relationship (Figure 3.4) with more light saturation observed during October and February (Figure 3.4A and B) than June and August (Figure 3.4C and D). The different ecosystem response to light between seasons and sites is likely due to differences in photosynthetic area. For example, based on an annual survey in July 2012, leaf area index (LAI) was  $1.17 \pm 0.25$  and  $3.08 \pm 0.53$   $\text{m}^2 \text{m}^{-2}$  (SE,  $n = 5$  and  $3$ ) at the 5 and 11 year site, respectively, indicating nearly 3-fold increase in photosynthetic area with age during this time of year (McGlathery,

unpublished). Using shoot density as a proxy for LAI, the higher LAI at the 11 year site during October, June, and August allows for more efficient light capture and photosynthesis than at the 5 year site (Binzer et al. 2006, Sand-Jensen et al. 2007) yielding P-I curves with less light saturation (Figure 3.3 and 3.4, A, C, and D). For example, the P-I response was steepest during June (Figure 3.3C and 3.4C) and shallowest during February (Figure 3.3B and 3.4B) which agrees well with measurements of shoot density (Table 3.1). This ecosystem scale response is important to consider when using P-I relationships to predict photosynthesis in seagrass communities. If this efficient light utilization is not taken into account, photosynthesis predictions will be drastically underestimated. For example, using photosynthesis characteristics from Dennison (1988) at 20 °C who used *Z. marina* leaf incubations to determine P-I relationships, maximum net photosynthesis was 67.7 mmol O<sub>2</sub> m<sup>-2</sup>d<sup>-1</sup>, while during June the maximum net photosynthesis observed was 1086.9 mmol O<sub>2</sub> m<sup>-2</sup>d<sup>-1</sup>, several orders of magnitude larger than estimated from a single leaf.

The amount of light required for photosynthesis to exceed respiration ( $I_{\text{comp}}$ ) is an important parameter to consider when planning seagrass restoration or assessing the capacity of a seagrass meadow to survive under limited light conditions. Plants cannot maintain a positive carbon balance if available light reaching the canopy is not greater than  $I_{\text{comp}}$  for the majority of the day (Gacia et al. 2005, Ralph et al. 2007, Moore et al. 2012). Light compensation increased 10-fold with temperature at both the 5 and 11 year sites (Figure 3.5) over the course of the year which was remarkably similar to that found by Moore et al. (1997) from chamber incubation methods. This is likely due to increases in sediment heterotrophic respiration with temperature (Murray and Wetzel 1987, Moore

et al. 1997) and increases in *Z. marina* respiratory requirements with temperature (Staeher and Borum 2011) as well as the covariance of biomass with temperature (Table 3.1, shoot density). Although these relationships were not statistically different, light compensation was always higher at the 11 year site than the 5 year site because of higher *Z. marina* belowground biomass with meadow age. For example, during an annual survey in July 2011, there was a more than 2-fold difference in belowground biomass between the 5 and 11 year meadows ( $36.0 \pm 14.2$  vs.  $84.6 \pm 20.6$  g m<sup>-2</sup>, SE, n = 3; McGlathery, unpublished data). Higher belowground biomass will increase respiratory O<sub>2</sub> demand and require more light for photosynthesis to exceed respiration.

#### *Modeling net ecosystem metabolism*

Since light is the major driver of the O<sub>2</sub> flux, P-I relationships as the ones shown in Figure 3.3 and 3.4 can be used to interpolate NEM throughout the year. Using concurrent PAR measurements from incident irradiance (PAR<sub>incident</sub>) and canopy irradiance (PAR<sub>canopy</sub>), a good calibration was obtained to allow us to estimate available light reaching the canopy throughout the year (Figure 3.6). It is likely that much of the scatter in this relationship would be improved if a more complex function were used that accounted for light attenuation from changing water depth due to tidal cycling or strong turbidity events from storms or wind as these events would be registered in the PAR<sub>canopy</sub> data but not necessarily the meteorological PAR<sub>incident</sub>. We could further increase our error by not accounting for spatial variability in turbidity between bays by using a relationship from the 11 year site to estimate PAR<sub>canopy</sub> at the 5 year site. However, the distributions of light data were not significantly different during any sampling season (two-sample K-S test, p = 0.530, 0.833, and 0.287 for October, February, and June,

respectively) indicating that using one curve for both sites is acceptable. Thus, this relationship provides a good estimate of average PAR available at the canopy as the main driver of production. For night respiration, the P-I curves average over all data where light  $< 1.0 \mu\text{mol photons m}^{-2}\text{s}^{-1}$ , thus hourly variability in flow stimulation of respiration at night (Rheuban Chapter 2) is not accounted for as no data for flow were available to use in the annual interpolation of NEM. However, the night respiration used to calculate the P-I curves incorporates considerable variability in mean flow conditions through tidal cycling. Thus, the modeled NEM accounts for changes in flow conditions by assuming average flow remains constant throughout the seasonal period.

The variation in daily in NEM (Figure 3.7) was different between the 5 year and 11 year site and likely related to different growth strategies with colonization. The 5 year site had higher daily NEM during peak growth period and was more often autotrophic than heterotrophic (April – June, Figure 3.7B and Figure 3.8). The strong daily autotrophy is likely an indication of rapid seagrass expansion and increases in both below and aboveground biomass at the 5 year site. This agrees well with measurements of shoot density and total biomass from McGlathery et al. (2012) who found a 4 year lag between seeding and a rapid increase in shoot density and biomass. In contrast, during peak growth season (April – June), the 11 year site was less autotrophic and much more frequently heterotrophic than the 5 year site when exposed to the same conditions. The 11 year site had a 2.5 fold higher belowground biomass than the 5 year site in July 2012 (McGlathery, unpublished), resulting in higher respiratory  $\text{O}_2$  demand which agrees well with seasonal average measurements of metabolism (Figure 3.1D and Figure 3.2). In addition, the 11 year site likely had higher abundance of heterotrophic organisms

(Hemminga and Duarte 2000) which may increase  $O_2$  demand. Finally,  $O_2$  demand can be further increased through the oxidation of reduced metabolites from anaerobic processes such as nitrogen fixation which increases with colonization and organic matter at these sites (Cole and McGlathery 2012).

The seasonal loss in biomass due to temperature stress during August can also be seen in the daily NEM at both the 5 and 11 year sites (Figure 3.7B and C, Figure 3.8). A drastic drop in daily NEM from approximately 200 to nearly 0  $mmol\ O_2\ m^{-2}d^{-1}$  and approximately 50 to -100  $mmol\ O_2\ m^{-2}d^{-1}$  at the 5 and 11 year sites, respectively, was seen during late summer. This agrees well with large losses in shoot density from June to August at both sites (Table 3.1) and also with other estimates of seagrass metabolism or temperature stress from similar latitudes (e.g. Wetzel and Penhale 1983, Orth and Moore 1986, Moore et al. 1997). Thus, this change in ecosystem net metabolism is likely a result of lower seagrass productivity due to a loss of photosynthetic biomass combined with a continued high  $O_2$  demand relative to photosynthesis either by belowground biomass or high populations of heterotrophic organisms remaining through the summer.

Cumulating daily NEM throughout the year (Figure 3.8) provides an estimate of annual NEM that accounts for significant daily variability in light and temperature conditions. After cumulating the full time series, a differences in annual NEM between the 5 year site and the bare and 11 year sites suggest different growth regimes with increasing seagrass colonization. The increasing heterotrophy with seagrass colonization is in good agreement with Barron et al. (2004), who found that NEM measured during a single summer sampling in a *Cymodocea nodosa* meadow decreased as a function of increasing ecosystem heterotrophic respiration with colonization. Summertime shoot

density has been consistent from 2010 – 2012 at the 11 year site (McGlathery et al. 2012, McGlathery unpublished) while shoot density at the 5 year site continued to increase from  $249.2 \pm 35.1$  (SE,  $n = 10$ ) shoots  $m^{-2}$  in 2010 to  $438.8 \pm 24.9$  in 2012 (SE,  $n = 10$ , McGlathery et al. 2012, McGlathery unpublished). This change in annual metabolism likely indicates an age threshold between 5 and 11 years where there is a functional shift from increasing *Z. marina* biomass to higher maintenance of belowground tissue. The net heterotrophy found at the 11 year site does not agree with annual rates using in situ enclosures measured by Murray and Wetzel (1987) in a *Z. marina* community at similar latitudes in the Chesapeake Bay to be annually net autotrophic. However, they estimated maximum annual  $O_2$  metabolism by only measuring during peak sunlight hours and did not account for daily variability in light which we show can affect day-to-day ecosystem trophic state (Figure 3.8). Enclosure incubations can also underestimate R and overestimate NEM at sites where flow is an important driver of R (Rheuban Chapter 2) due to lack of reproduction of in situ flow conditions (Berg and Huettel 2008, Berg et al. in press).

The very close agreement between annual NEM at the bare and 11 year sites suggests that the return of seagrass to this coastal system affects the magnitude but not the balance of ecosystem  $O_2$  metabolism. Rates of GPP and R increased by a maximum of nearly 10-fold showing that seagrass meadows are locations of high heterotrophic and autotrophic productivity which agrees well with Apolistaki et al. (2010) and Hume et al. (2011). Although gross metabolism was drastically increased by returning *Z. marina* to this ecosystem, the agreement between NEM at the bare and 11 year sites combined with the strong 1:1 coupling of daily GPP and R (Rheuban Chapter 2) suggests that the

increased C respired in this ecosystem is fixed on the same timescale. Export of material has likely increased in magnitude relative to the unvegetated site which may provide a substrate for metabolism in other areas, although the magnitude of this export and fate of this material is currently unknown. In addition, the 11 year site has significant carbon burial (Greiner et al. in review) and thus C import has increased due to the presence of seagrass. The good agreement between NEM at the bare and 11 year site suggests that the higher C imported into the sediments will not likely be used as a source for C respiration. If the increased C import is not mineralized through respiration, sediment carbon stocks may increase which further support the capacity of seagrass meadows to bury organic material on decadal to century timescales.



## References

- Aioi, K. (1980). Seasonal changes in the standing crop of the eelgrass (*Zostera marina* L.) in Odawa Bay, central Japan. *Aquat. Bot.* 8: 343-354.
- Apostolaki, E. T., M. Holmer, N. Marbà, and I. Karakassis. 2010. Reduced carbon sequestration in a Mediterranean seagrass (*Posidonia oceanica*) ecosystem impacted by fish farming. *Mar. Ecol. Prog. Ser.* 2: 49 – 59.
- Barron, C., N. Marba, J. Terrados, H. Kennedy, and C. M. Duarte. 2004. Community metabolism and carbon budget along a gradient of seagrass (*Cymodocea nodosa*) colonization. *Limnol. Oceanogr.* 49(5): 1642 – 1651.
- Berg, P., H. Roy, F. Janssen, V. Meyer, B. B. Jørgensen, M. Huettel, and D. de Beer. 2003. Oxygen uptake by aquatic sediments measured with a novel non-invasive eddy-correlation technique. *Mar. Ecol. Prog. Ser.* 261: 75 – 83.
- Berg, P., H. Roy, and P. L. Wiberg. 2007. Eddy correlation flux measurements: The sediment surface area that contributes to the flux. *Limnol. Oceanogr.* 52(4): 1672 – 1684.
- Berg, P. and M. Huettel. 2008. Monitoring the seafloor using the noninvasive eddy correlation technique: integrated benthic exchange dynamics. *Oceanography.* 21(4): 164 – 167.
- Berg, P., R. N. Glud, A. Hume, H. Stahl, K. Oguri, V. Meyer, and H. Kitazato. 2009. Oxygen uptake by deep ocean sediments measured with the eddy correlation technique. *Limnol. Oceanogr: Methods.* 7: 576 – 584.
- Berg, P., M. Long, M. Huettel, J. E. Rheuban, K. J. McGlathery, R. W. Howarth, A. E. Giblin, and R. Marino. Eddy correlation measurements of oxygen fluxes in

permeable sediments exposed to varying current flow and light. *Limnol.*

*Oceanogr.* In Press.

Binzer, T., K. Sand-Jensen, and A. Middleboe. 2006. Community photosynthesis of aquatic macrophytes. *Limnol. Oceanogr.* 51(6): 2722 – 2733.

Chipman, L., M. Huettel, P. Berg, V. Meyer, I. Klimant, R. Glud, and F. Wenzhoefer. 2012. Oxygen optodes as fast sensors for eddy correlation measurements in aquatic systems. *Limnol. Oceanogr.: Methods.* 10: 304 – 316.

Cottam, C., Munro, D.A., 1954. Eelgrass status and environmental relations. *J. Wildlife Manage.* 18: 449–460.

Cole, L. W. and K. J. McGlathery. 2012. Dinitrogen fluxes from restored *seagrass* meadows. *Mar. Ecol. Prog. Ser.* 448: 235-246.

Dennison, W. C., Alberte, R. S. (1982). Photosynthetic response of *Zostera marina* L. (eelgrass) to in situ manipulations of light intensity. *Oecologia.* 55: 137-144

Duarte, C. M., N. Marba, E. Gacia, J. W. Fourqurean, J. Beggins, C. Barron, and E. T. Apostolaki. 2010. Seagrass community metabolism: Assessing the carbon sink capacity of seagrass meadows. *Global Biogeochem. Cycles.* 24: GB4302.

Eyre, B. D., D. Maher, J. M. Oakes, D. V. Erler, and T. M. Glasby. 2011. Differences in benthic metabolism, nutrient fluxes, and denitrification in *Caulerpa taxifolia* communities compared to uninvaded bare sediment and seagrass (*Zostera capricorni*) habitats. *Limnol. Oceanogr.* 56(5): 1737 – 1750.

Fourqurean, J. W., C. M. Duarte, H. Kennedy, N. Marbà, M. Holmer, M. A. Mateo, E. T. Apostolaki, G. A. Kendrick, D. Krause-Jensen, K. J. McGlathery, and O. Serrano.

2012. Seagrass ecosystems as a globally significant carbon stock. *Nature Geoscience*. 5: 505 – 509.
- Frederiksen, M. S. and R. N. Glud. 2006. Oxygen dynamics in the rhizosphere of *Zostera marina*: a two-dimensional planar optode study. *Limnol. Oceanogr.* 51(2): 1072 – 1083.
- Gacia, E., H. Kennedy, C. M. Duarte, J. Terrados, N. Marba, S. Papadimitriou, and M. Fortes. 2005. Light-dependence of the metabolic balance of a highly productive Philippine seagrass community. *Jour. of Exp. Mar. Biol. and Ecol.* 316: 55 – 67.
- Giordano, J. C. P., M. J. Brush, and I. C. Anderson. 2012. Ecosystem metabolism in shallow coastal lagoons: patterns and partitioning of planktonic, benthic, and integrated community rates. *Mar. Ecol. Prog. Ser.* 458: 21 – 38.
- Glud, R. N., P. Berg, A. Hume, P. Batty, M. E. Blicher, K. Lennert, and S. Rysgaard. 2010. Benthic O<sub>2</sub> exchange across hard bottom substrates quantified by eddy correlation in a sub-Arctic fjord. *Mar. Ecol. Prog. Ser.* 417: 1 – 12.
- Hansen, J. C. R. and M. A. Reidenbach. 2012. Wave and tidally driven flows in eelgrass beds and their effect on sediment resuspension. *Mar. Ecol. Prog. Ser.* 448: 271 – 287.
- Hemminga, M. A. and C. M. Duarte. 2000. *Seagrass Ecology*. Cambridge University Press. New York, NY.
- Holmer, M., C. M. Duarte, H. T. S. Boschker, and C. Barron. 2004. Carbon cycling and bacterial carbon sources in pristine and impacted Mediterranean seagrass sediments. *Mar. Ecol. Prog. Ser.* 36: 227 – 237.

- Huettel, M. and G. Gust. 1992. Solute Release mechanisms from confined sediment cores in stirred benthic chambers and flume flows. *Mar. Ecol. Prog. Ser.* 82: 187 – 197.
- Hume, A., P. Berg, and K. McGlathery. 2011. Dissolved oxygen fluxes and ecosystem metabolism in an eelgrass (*Zostera marina*) meadow measured with the eddy correlation technique. *Limnol. Oceanogr.* 56(1): 86 – 96.
- Jassby, A. D. and T. Platt. 1976. Mathematical formulation of the relationship between photosynthesis and light for phytoplankton. *Limnol. Oceanogr.* 21(4): 540 – 547.
- Kentula, M. E. and C. D. McIntire. 1986. The autecology and production dynamics of eelgrass (*Zostera marina* L.) in Netarts Bay, Oregon. *Estuaries and Coasts.* 9(3): 188 – 199.
- Long, M. H., J. E. Rheuban, P. Berg, and J. C. Zieman. 2012. A comparison and correction of light intensity loggers to photosynthetically active radiation sensors. *Limnol. Oceanogr.: Methods.* 10: 416 – 424.
- Lorrai, C., D. F. McGinnis, A. Brand, and A. Wüest. 2010. Application of oxygen eddy correlation in aquatic systems. *Jour. Atm. and Oceanic Tech.* 27: 1533 – 1546.
- McGinnis, D. F., S. Cherednichenko, S. Sommer, P. Berg, L. Rovelli, R. Schwarz, R. N. Glud, and P. Linke. 2011. Simple, robust eddy correlation amplifier for aquatic dissolved oxygen and hydrogen sulfide flux measurements. *Limnol. Oceanogr.: Methods.* 9: 340 – 347.
- Mass, T., A. Genin, U. Shavit, M. Grinstein, and D. Tchernov. 2010. Flow enhances photosynthesis in marine benthic autotrophs by increasing the efflux of oxygen from the organism to the water. *PNAS.* 107(6): 2527 – 2531.

- Massey, F. J. (1951). The Kolmogorov-Smirnov Test for Goodness of Fit. *Jour. of the Amer. Stat. Assoc.* 46(253): 68–78.
- McGlathery, K. J., I. C. Anderson, and A. C. Tyler. 2001. Magnitude and variability of benthic and pelagic metabolism in a temperate coastal lagoon. *Mar. Ecol. Prog. Ser.* 216:1-15.
- McGlathery K.J., Sundback, K, I.C. Anderson. 2007. Eutrophication in shallow coastal bays and lagoons: the role of plants in the coastal filter. *Mar. Ecol. Prog. Ser.* 348: 1-18
- McGlathery, K. J., L. K. Reynolds, L. W. Cole, R. J. Orth, S. R. Marion, and A. Schwartzchild. 2012. Recovery trajectories during state change from bare sediment to eelgrass dominance. *Mar. Ecol. Prog. Ser.* 448:209 – 221.
- McLeod, E., G. L. Chmura, S. Bouillon, R. Salm, M. Björk, C. M. Duarte, C. E. Lovelock, W. H. Schlesinger, and B. R. Silliman. 2011. A blueprint for blue carbon: toward an improved understanding of the role of vegetated coastal habitats in sequestering CO<sub>2</sub>. *Frontiers in Ecology and the Environment.* 9: 552–560
- Moore, K. A., R. L. Wetzel, and R. J. Orth. 1997. Seasonal pulses of turbidity and their relations to eelgrass (*Zostera marina* L.) survival in an estuary. *Jour. of Exp. Mar. Biol. and Ecol.* 215: 115 – 134.
- Moore, K.A. 2004. Influence of seagrasses on water quality in shallow regions of the lower Chesapeake Bay. *Journal of Coastal Research.* 45: 162-178.
- Moore, K. A. and J. C. Jarvis. 2008. Environmental factors affecting recent summertime eelgrass diebacks in the lower Chesapeake Bay: implications for long term persistence. *Journal of Coastal Research: Special Issue.* 55: 135 – 147.

- Moore, K. A., E. C. Shields, D. B. Parrish, and R. J. Orth. 2012. Eelgrass survival in two contrasting systems: role of turbidity and summer water temperatures. *Mar. Ecol. Prog. Ser.* 448: 247 – 258.
- Murray, L. and R. L. Wetzel. 1987. Oxygen production and consumption associated with the major autotrophic components in two temperate seagrass communities. *Mar. Ecol. Prog. Ser.* 38: 231 – 239.
- Orth, R. J. and K. Moore. 1986. Seasonal and year-to-year variations in the growth of *Zostera marina* L. (eelgrass) in the lower Chesapeake Bay. *Aquatic Botany*. 24: 335 – 341.
- Orth, R. J., M. L. Luckenbach, S. R. Marion, K. A. Moore, and D. J. Wilcox. 2006. Seagrass recovery in the Delmarva Coastal Bays, USA. *Aquatic Botany* 84: 26 – 36.
- Orth, R. J., T. J. B. Carruthers, W. C. Dennison, C. M. Duarte, J. W. Fourqurean, K. L. Heck, A. R. Hughes, G. A. Kendrick, W. J. Kenworthy, S. Olyarnik, F. T. Short, M. Waycott, and S. Williams. 2006b. A Global Crisis for Seagrass Ecosystems. *BioScience*. 56(12): 987 – 996.
- Orth, R. J., S. R. Marion, K. A. Moore, and D. J. Wilcox. 2010. Eelgrass (*Zostera marina* L.) in the Chesapeake Bay Region of Mid-Atlantic Coast of the USA: Challenges in Conservation and Restoration. *Estuaries and Coasts*. 33: 139 – 150.
- Orth, R., J., K. A. Moore, S. R. Marion, D. J. Wilcox, and D. B. Parrish. 2012. Seed addition facilitates eelgrass recovery in a coastal bay system. *Mar. Ecol. Prog. Ser.* 448: 177 – 195.

- Penhale, P. A. and W. O. Smith, Jr. 1977. Excretion of Dissolved Organic Carbon by Eelgrass (*Zostera marina*) and its Epiphytes. *Limnol. Oceanogr.* 22(3): 400 – 407.
- Ralph, P. J., M. J. Durako, S. Enríquez, C. J. Collier, and M. A. Doblin. 2007. Impact of light limitation on seagrasses. *Jour. of Exp. Mar. Biol. and Ecol.* 350: 176 – 193.
- Reimers, C. E., H. T. Ozkan-Haller, P. Berg, A. Devol, K. McCann-Grosvenor, and R. D. Sanders. 2012. Benthic oxygen consumption rates during hypoxic conditions on the Oregon continental shelf: Evaluation of the eddy correlation method. *Jour. of Geophys. Res.* 117: 1 – 18.
- Sand-Jensen, K., T. Binzer, and A. L. Middleboe. 2007. Scaling of photosynthetic production of aquatic macrophytes – a review. *Oikos.* 116: 280 – 294.
- Short, F.T. 1980. A simulation model of the seagrass production system. In: Phillips, R.C., McRoy, C.P. (Eds.), *Handbook of Seagrass Biology: An Ecosystem Perspective*. Garland STPM Press, New York, pp. 275–295
- Staehr, P. A. and J. Borum. 2011. Seasonal acclimation in metabolism reduces light requirements of eelgrass (*Zostera marina*). *Jour. of Exp. Marine Biol. And Ecol.* 407: 139 – 146.
- Tyler, A. C., and K. J. McGlathery. 2003. Benthic algae control sediment-water column fluxes of organic and inorganic nitrogen compounds in a temperate lagoon. *Limnol. Oceanogr.* 48(6): 2125 – 2137.
- Waycott, M., C. M. Duarte, T. J. B. Carruthers, R. J. Orth, W. C. Dennison, S. Olyarnik, A. Calladine, J. W. Fourqurean, K. L. Heck Jr., A. Randall Hughes, G. A. Kendrick, W. J. Kenworthy, F. T. Short, and S. L. Williams. 2009. Accelerating

loss of seagrasses across the globe threatens coastal ecosystems. *PNAS*. 106(30): 12377 – 12381.

Wetzel, R. G. and P. A. Penhale. 1979. Transport of carbon and excretion of dissolved organic carbon by leaves and roots/rhizomes in seagrasses and their epiphytes. *Aquatic Botany*. 6: 149 – 158.

Wetzel, R. L. and P. A. Penhale. 1983. Production ecology of seagrass communities in the lower Chesapeake Bay. *Mar. Technol. Soc. J.* 17: 22 – 31.

Zimmerman, R. C. 2003. A biooptical model of irradiance distribution and photosynthesis in seagrass canopies. *Limnol. Oceanogr.* 48(1): 568 – 585.



## Figures

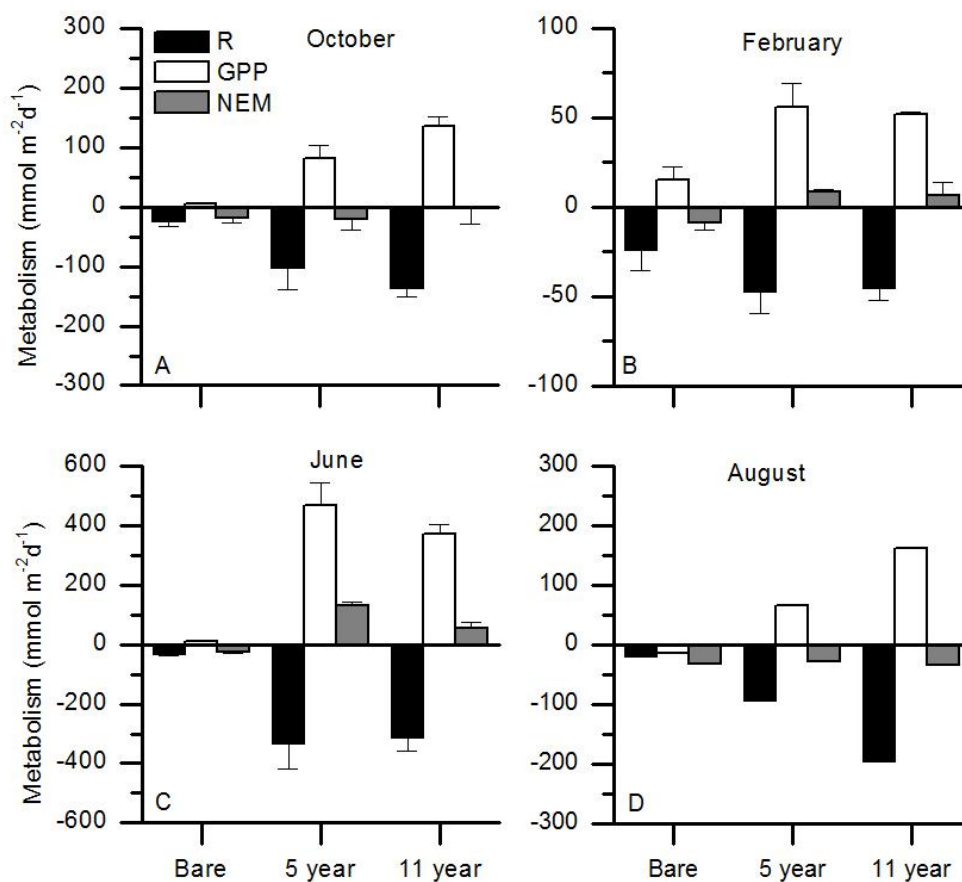


**Figure 3.1** Seasonal metabolism across sites.

(A – D) Average seasonal respiration (R), gross primary production (GPP), and net ecosystem metabolism (NEM) for October, February, June, and August respectively. Error bars are SE. August error bars are missing as this season was obtained by combining all data into one continuous 24 h record to estimate seasonal metabolism rather than averaging multiple days of data.

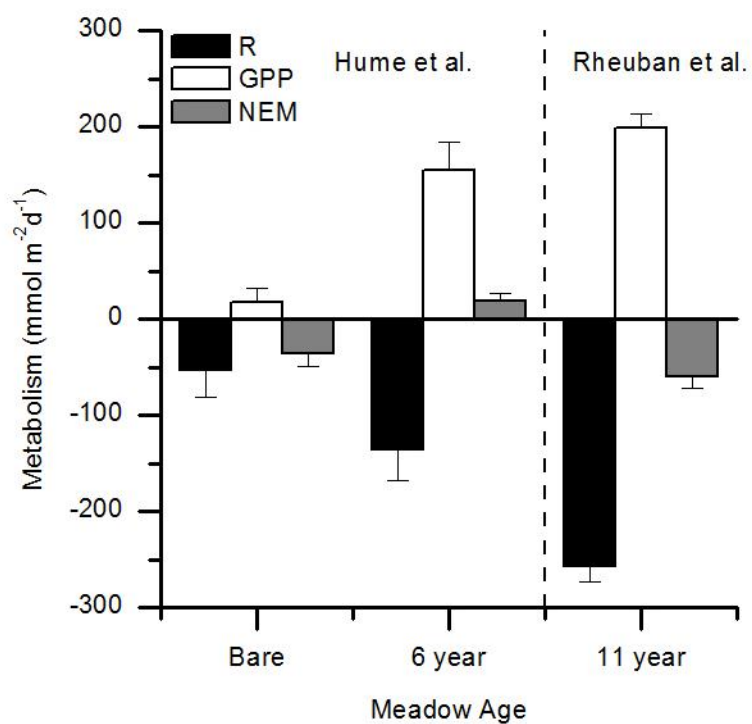


**Figure 3.2** Late summer metabolism from South Bay from Hume et al.

July/August metabolism from South Bay at three different age classes, bare, 6 years after seeding, and 11 years after seeding. Bare and 6 year data from Hume et al. (2011) and 11 year data from Rheuban et al. (in review). Error bars are SE.

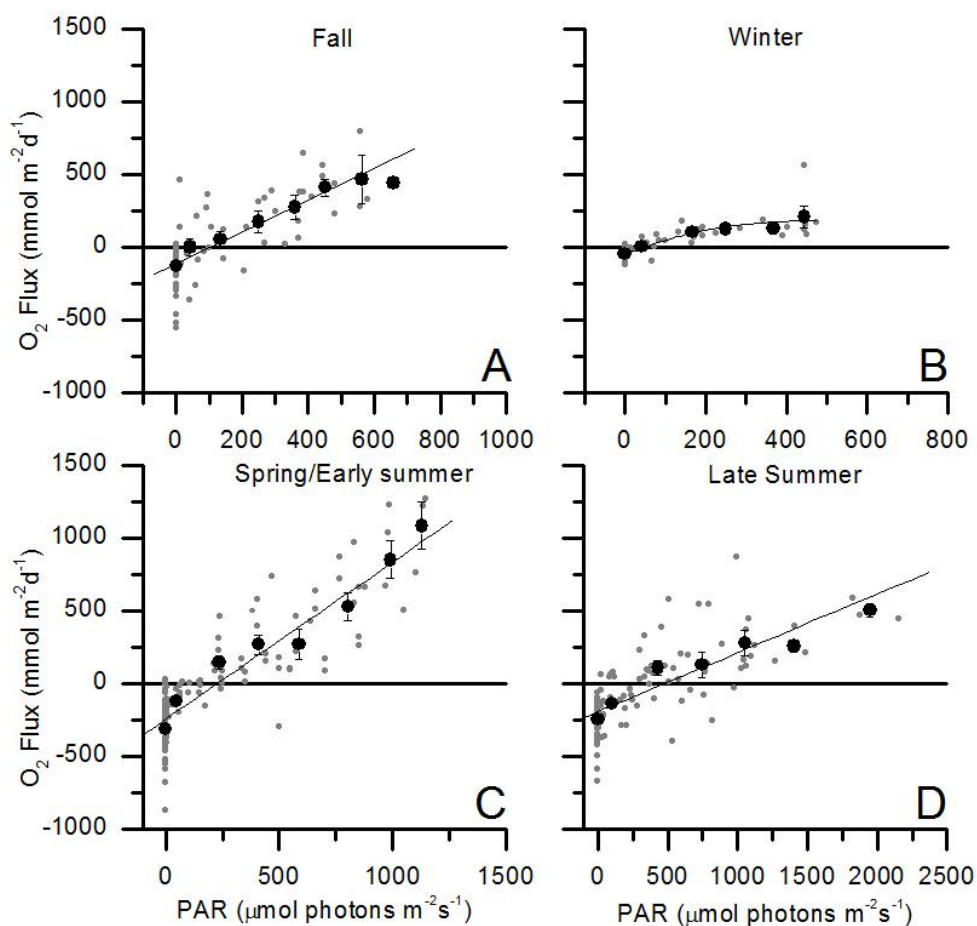


**Figure 3.3** Photosynthesis-irradiance curves from 11 year site.

(A – D) Photosynthesis-irradiance curves (Eq. 3) from the 11 year site in October, February, June, and August, respectively. Hyperbolic tangent functions from modified from Jassby and Platt (1976) were fit to the unbinned data. Data were binned to illustrate relationships.

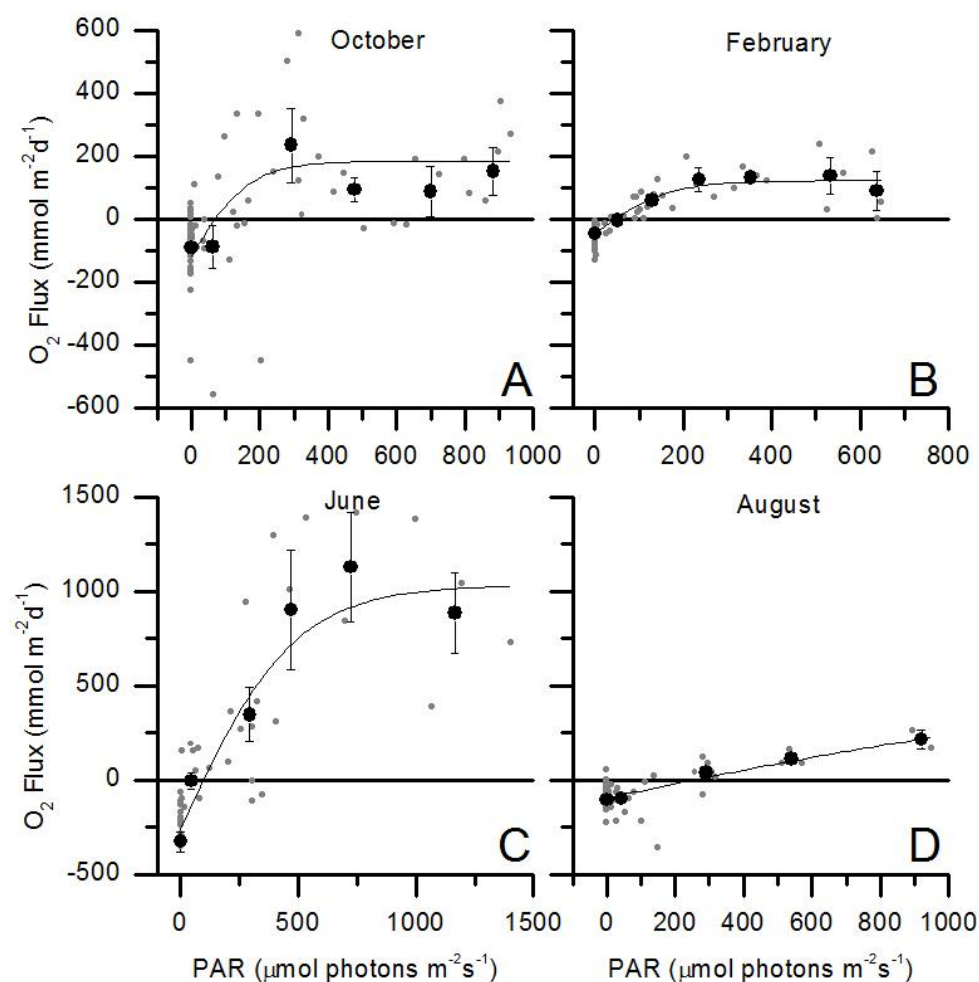


**Figure 3.4** Photosynthesis-irradiance curves from the 5 year site.

(A – D) Photosynthesis-irradiance curves (Eq. 3) from the 5 year site in October, February, June, and August, respectively. Hyperbolic tangent functions from modified from Jassby and Platt (1976) were fit to the unbinned data. Data were binned to illustrate relationships.

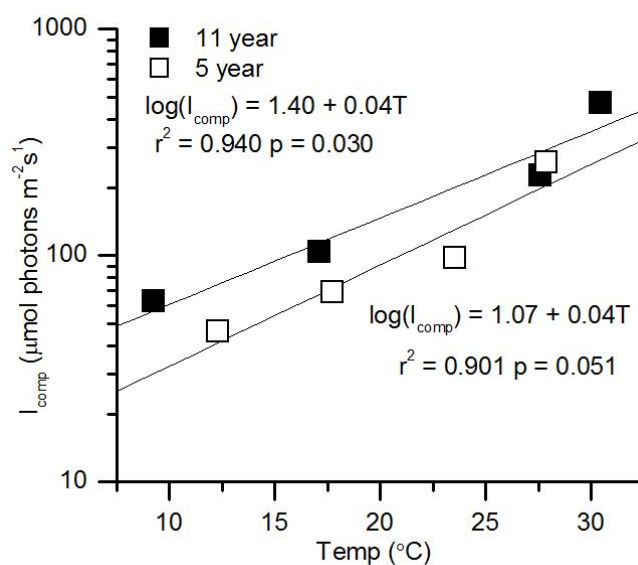


**Figure 3.5** Light compensation vs. temperature.

Compensation irradiance vs. temperature calculated from seasonal photosynthesis-irradiance relationships (Eq. 3) from 5 and 11 year sites.

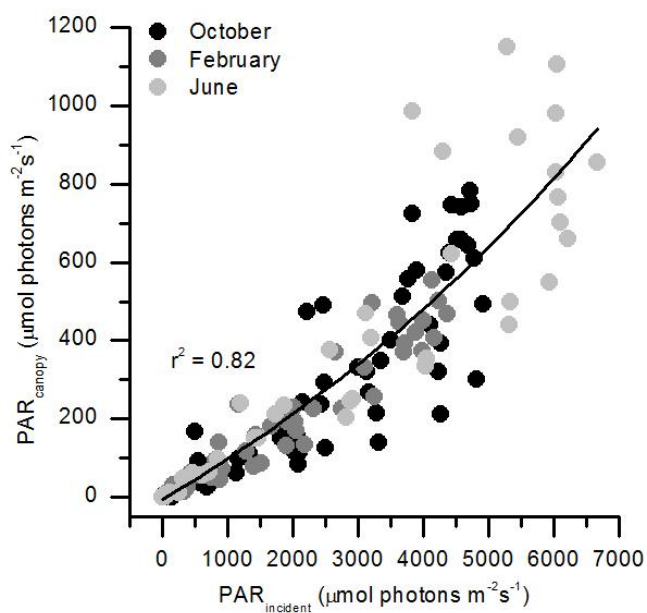


**Figure 3.6** Incident light vs. canopy light.

Photosynthetically active radiation (PAR) reaching the canopy ( $\text{PAR}_{\text{canopy}}$ ) vs. meteorological PAR ( $\text{PAR}_{\text{incident}}$ ) for October, February and June.

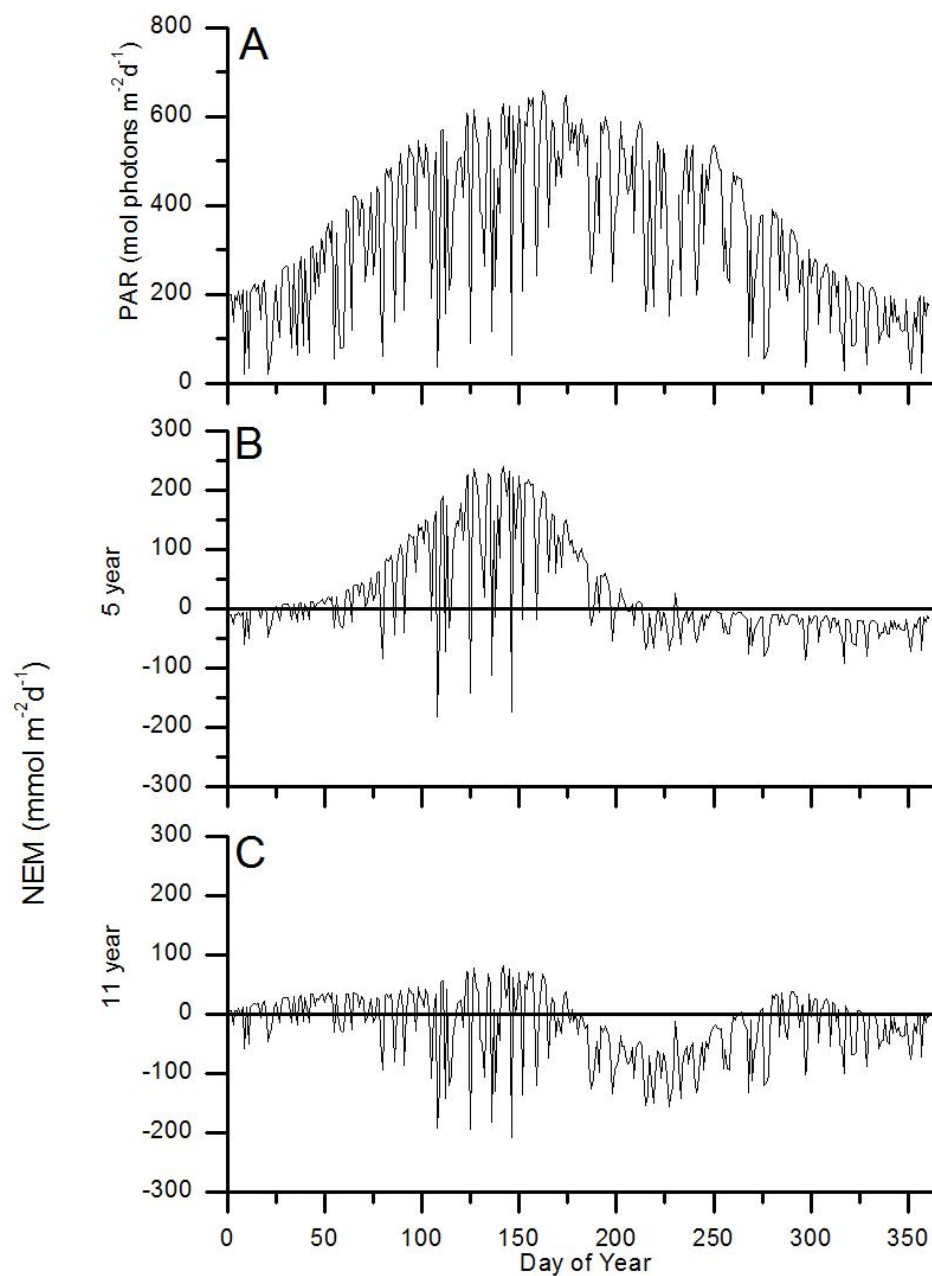


**Figure 3.7** Daily light and net ecosystem metabolism for 5 and 11 year sites.

(A) Integrated daily photosynthetically active radiation (PAR). (B – C) Modeled daily net ecosystem metabolism (NEM) from the 5 year (B) and 11 year (C) sites.

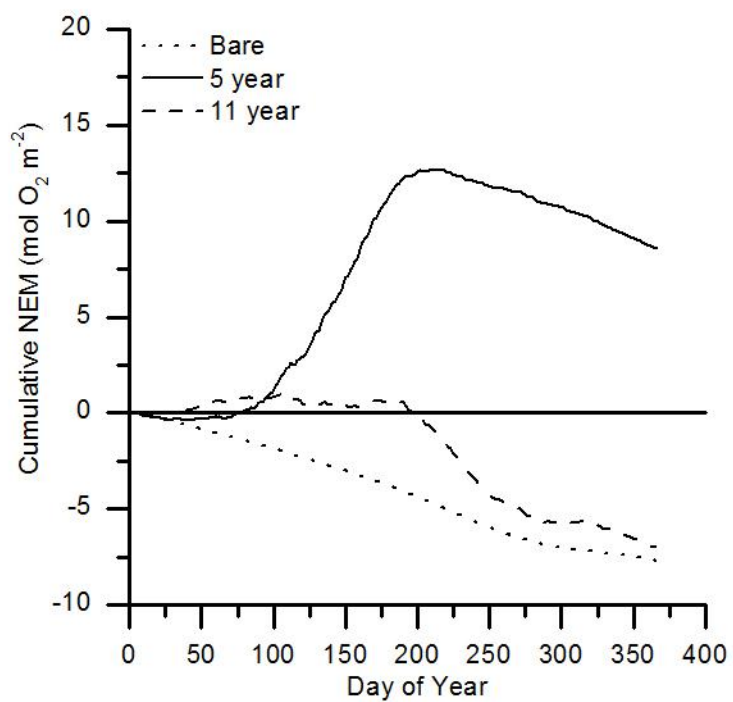


**Figure 3.8** Cumulative daily metabolism for all sites.

Cumulative daily modeled net ecosystem metabolism (NEM) for the bare, 5 year, and 11 year sites.



**Table 3.1** Site characteristics.

Site characteristics from the bare, 5 year, and 11 year site. Benthic chlorophyll (BChl) and phaeopigment (Phaeo) concentrations  $\pm$  SE ( $n = 8$ ) and seagrass shoot density (Den  $\pm$  SE) are given for each site. The number of samples varied by season and is shown in parentheses. The bare and 5 year sites were not sampled in August 2011.

Site		11-Aug	October	February	June	12-Aug
Bare	BChl	-	23.2 $\pm$ 3.8	18.7 $\pm$ 3.1	23.8 $\pm$ 3.3	28.6 $\pm$ 5.1
	Phaeo	-	34.9 $\pm$ 5.0	30.6 $\pm$ 5.5	34.5 $\pm$ 5.1	38.5 $\pm$ 3.7
5 year	BChl	-	38.2 $\pm$ 3.9	50.4 $\pm$ 7.3	31.7 $\pm$ 4.2	38.6 $\pm$ 5.9
	Phaeo	-	42.1 $\pm$ 5.4	48.1 $\pm$ 4.3	32.7 $\pm$ 2.6	37.0 $\pm$ 1.7
	Den	-	26 $\pm$ 2.5 (4)	196 $\pm$ 120.6 (8)	407.3 $\pm$ 78.4 (6)	224 $\pm$ 23.9 (8)
11 year	BChl	54.7 $\pm$ 6.9	43.8 $\pm$ 4.9	90.5 $\pm$ 27.2	50.7 $\pm$ 4.7	54.5 $\pm$ 7.2
	Phaeo	15.5 $\pm$ 3.6	34.8 $\pm$ 3.7	32.9 $\pm$ 5.5	34.8 $\pm$ 2.7	38.4 $\pm$ 4.3
	Den	516.4 $\pm$ 49.8 (10)	250.0 $\pm$ 18.2 (4)	158.2 $\pm$ 64.2 (8)	696 $\pm$ 106.7 (6)	490 $\pm$ 19.3 (8)

**Table 3.2.** Comparison of sediment cores and eddy correlation technique.

Comparison of sediment core and eddy correlation methods ( $\pm$ SE,  $n = 6$  and  $3$ , respectively) to calculate metabolism. The results of a two-sample t-test is given.

Method	R	GPP	NEM
Sediment Cores	$-19.2 \pm 1.9$	$4.0 \pm 1.7$	$-8.8 \pm 1.8$
EC	$-34.0 \pm 1.7$	$10.4 \pm 3.7$	$-23.6 \pm 4.1$
p	0.002	0.108	0.006

**Table 3.3** Measured vs. modeled seasonal NEM.

Measured vs. modeled seasonal NEM based on data where there were overlapping eddy correlation measurements with modeled data.

Site	Season	NEM eddy	NEM model	t (df)	p
11 year	October (2011)	$-20.3 \pm 22.6$	$2.2 \pm 21.2$	0.69 (6)	0.514
11 year	February (2012)	$6.0 \pm 7.3$	$5.2 \pm 9.6$	0.07 (4)	0.949
11 year	June (2012)	$55.9 \pm 15.4$	$9.6 \pm 10.7$	2.10 (4)	0.080
4 year	October (2011)	$-20.6 \pm 18.0$	$-26.1 \pm 3.3$	0.30 (6)	0.775
4 year	February (2012)	$8.3 \pm 1.4$	$17.9 \pm 9.9$	0.96 (4)	0.391
4 year	June (2012)	$132.4 \pm 11.2$	$148.2 \pm 71.0$	0.21 (2)	0.845

## Significance

The goal of this thesis was to address several issues regarding our understanding of the eddy correlation technique and its application to environmental systems, and to use this novel method to improve our knowledge of ecosystem metabolism in seagrass communities. As the eddy correlation technique is still relatively new, many aspects of this method are not well understood and may be difficult to measure directly in the field. For this reason, I used 3D numerical modeling to investigate the application of the eddy correlation technique in heterogeneous environments and the response time to rapid changes in O<sub>2</sub> flux. I showed that the eddy correlation measurements can integrate heterogeneous fluxes and incorporate rapid changes in O<sub>2</sub> fluxes, provided several guidelines based on site characteristics are followed. I also applied this technique to seagrass systems at the Virginia Coast Reserve and found that ecosystem metabolism in seagrass communities is highly variable, with hourly fluxes equally as variable as seasonal changes in ecosystem metabolism. I found seasonal variability in the relative importance of several of the drivers of O<sub>2</sub> metabolism such as light, flow, and temperature. Finally, I found that after ecosystem maturation, the seagrass restoration at the Virginia Coast Reserve has not likely altered the annual benthic net ecosystem metabolism in the coastal lagoons.

In the first chapter of this thesis, I found that eddy correlation measurements in heterogeneous or dynamic environments can accurately represent the ecosystem scale response if several guidelines are followed. I used a wide range of environmental variables such as sediment surface roughness, heterogeneity patch size, and water velocity in the model that may be characteristic of field conditions and found simple

correlations for eddy correlation users to utilize when planning and implementing deployments of eddy correlation instruments. The results of this study will be useful for the rapidly expanding group of eddy correlation users both in deployment planning as well as interpretation of data.

In the second chapter of this thesis, I found that the main drivers of ecosystem metabolism including light, temperature, and flow varied seasonally in their relative importance. I also found that multiple timescale feedback processes between production and respiration were occurring at the minute to hourly, daily, and monthly to seasonal timescales. I showed that there was high variability in O<sub>2</sub> fluxes on these different timescales, which is significant to other studies of ecosystem metabolism in seagrass communities. Because of these feedback processes, extrapolating measurements from several hours or even several days to longer timescales may not be appropriate in scaling exercises or determination of annual budgets. I also show that after 11 years, based on seasonal averaging, ecosystem metabolism in this meadow is net balanced. This is significant as, although the metabolic processes of this ecosystem are balanced, the capacity of this seagrass meadow to sequester and bury carbon (measured by Greiner et al. in review) shows that this ecosystem represents a regional net carbon sink.

In the third chapter of this thesis, I found through modeling hourly and daily net ecosystem metabolism, young *Z. marina* meadows were annually net autotrophic while older meadows were annually net heterotrophic, which was in contrast to the balance found in Chapter 2. This is important to consider as this modeling technique estimates daily metabolism throughout the year, while the seasonal averaging only accounts for longer timescale variability in O<sub>2</sub> metabolism. This suggests that longer records than

measured in Chapter 2 may be necessary to estimate a true seasonal average. The results of this chapter show that seagrass meadows are locations of high productivity and respiration relative to unvegetated sediments, likely through increases in both primary and secondary producer biomass. Although the older seagrass meadow was annually net heterotrophic, the similarity in annual net ecosystem metabolism between the older meadow and the bare sediments suggests that net carbon imported into this system in excess of what is imported to the unvegetated sediments is not mineralized through respiration. This further supports the capacity of seagrass meadows to sequester and store carbon over decadal timescales shown by Greiner et al. (submitted).

This thesis brings about more detailed questions regarding the effects of seagrass colonization on ecosystem metabolism. Through this work, I found that there was likely a colonization threshold where ecosystem metabolism reaches maximum autotrophy. However, I did not measure enough age classes to determine how soon after colonization this threshold would be reached. This work would be improved if more age classes were measured to determine when this threshold is reached where meadow expansion stops and maintenance of biomass begins.

## Appendix 1 – Water column metabolism

**Table A.1.1** Water column metabolism.

Water column metabolism in  $\text{mmol O}_2 \text{ m}^{-2} \text{ d}^{-1}$  from all sites and seasons measured through biological oxygen demand incubations in situ. GPP and NEM are calculated through weighting the dark and light incubations by hours of daylight.

Site	Season	R	SE	GPP	SE	NEM	SE	n
Bare	October	-109.3	50.2	17.9	20.3	-91.5	30.0	2
	February	-77.7	7.8	5.7	3.2	-72.0	10.9	2
	June	-45.9	23.4	70.6	14.5	24.7	8.9	2
	August (2012)	-39.9	11.7	118.5	4.3	78.6	16.1	2
4 year	October	-103.8	85.4	22.7	11.2	-81.1	74.1	2
	February	-48.3	0.8	1.9	4.0	-46.4	3.1	2
	June	-92.2	31.2	75.7	25.3	-16.5	56.6	2
	August (2012)	-90.0	32.2	69.5	8.4	-20.5	23.8	2
11 year	August (2011)	-74.5	20.7	82.1	14.0	9.7	15.6	3
	October	-49.9	20.1	28.6	7.2	-21.3	13.4	3
	February	-44.2	11.4	11.9	1.2	-32.3	12.4	3
	June	-21.2	15.5	47.4	2.4	26.2	13.2	2
	August (2012)	-11.6	3.0	61.3	6.1	49.8	7.0	3

Water column metabolism was measured through triplicate light and dark incubations in 300 mL biological oxygen demand (BOD) bottles. A large water sample was collected and an initial  $\text{O}_2$  concentration was determined using a LDO probe (Hach Systems) prior to filling BOD bottles. Bottles were carefully filled to avoid introducing new  $\text{O}_2$ , sealed, and dark bottles were covered with foil to exclude all light. Samples were incubated in situ for 1 – 2 hours during peak sunlight hours to estimate maximum water column productivity and respiration. Water column metabolism was determined by the

difference between the initial and final O<sub>2</sub> concentration. Daily R was calculated by assuming that respiration in the dark is constant throughout the day. GPP was calculated as:

$$GPP = |D|h_L + Lh_L$$

where D is hourly dark respiration, h<sub>L</sub> is hours of light, and L is hourly metabolism measured in light. Daily NEM was calculated by weighing light and dark metabolism by hours of daylight and darkness such that:

$$NEM = Dh_D + Lh_L$$

where h<sub>D</sub> is hours of darkness.

No significant trends were observed in water column metabolism measurements with temperature, shoot density, season, or site. I expected to see water column metabolism follow trends in shoot density and temperature as much of the water column chlorophyll is likely from resuspended benthic microalgae which would decrease with increasing shoot density. This system is fairly oligotrophic and thus water column phytoplankton concentrations are low. Also, I expected to see temperature stimulation of metabolism; however, no clear trends were found in the data. I believe if more days of data were available, there would be clearer trends.



## Appendix 2 – Benthic Chlorophyll A

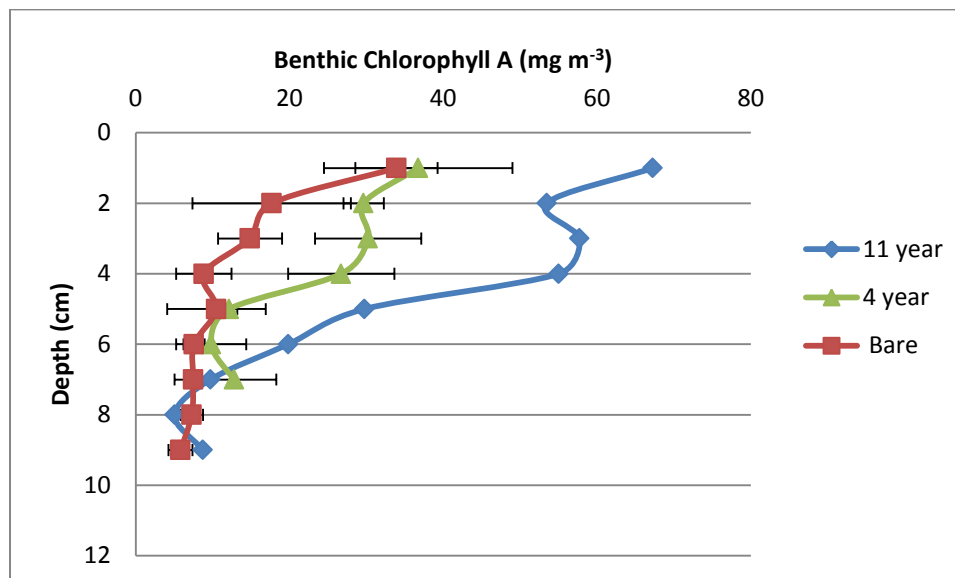


**Figure A.2.1** Benthic chlorophyll concentration with depth into sediment.

Benthic chlorophyll A concentration (mg m<sup>-3</sup>) as a proxy for benthic microalgal concentration is shown in Figure A.2.1 with depth into sediment. Two replicate 60 cc cores were taken from each site, returned to the lab in the dark and immediately frozen for later analysis. After freezing, cores were extruded and cut into 1 cm intervals and a 5 cc corer was used to collect sediment from the center of the core to minimize core effects. Sediment was processed as in McGlathery et al. (2012) through the 45:45 methanol:acetone spectrophotometric method (Lorenzen 1967; Pinckney and Zingmark 1994). Data from core 2 from the 11 year site were discarded as microalgae were visibly smeared throughout the core by the collection process.

ChlA concentration decreased with depth into sediment at all sites less light is available for microalgal growth deeper into the sediments. Overall chlA concentration increased with meadow age similar to the site characteristic data collected using only the

top 1 cm of sediment in the field. The increase in chlA concentration with age may be due to several factors including increasing nutrient availability and lower light levels. N<sub>2</sub> fixation has been found to increase with meadow age (Cole and McGlathery 2012), thus more nutrients may be available to support higher concentrations of benthic microalgae. However, using chlA concentration as a proxy for benthic microalgal concentration may be misleading as benthic microalgae are able to increase their chlorophyll concentration as a response to lower light availability. Thus, the increase in chlA concentration with age may be reflecting adaptation to lower light from shading under the canopy rather than increases in cell numbers.

### Appendix 3 – Waves

**Table A.3.1** Seasonal correlation of O<sub>2</sub> fluxes with wave height.

Linear regression analysis of hourly O<sub>2</sub> fluxes with significant wave height during day and night. Statistically significant relationships are shaded in gray.

Site	Season	<u>Day</u>		<u>Night</u>	
		r <sup>2</sup>	p	r <sup>2</sup>	p
11 year	August (2011)	5.3x10 <sup>-4</sup>	0.844	0.158	0.0075
	October	0.023	0.315	0.118	0.035
	February	0.150	0.024	0.002	0.786
	June	0.001	0.735	1.5x10 <sup>-4</sup>	0.932
	August (2012)	0.017	0.163	0.048	0.182
4 year	October	0.051	0.139	0.027	0.294
	February	0.004	0.781	0.076	0.12
	June	0.05	0.235	0.564	5.1x10 <sup>-4</sup>
	August (2012)	0.087	0.107	0.004	0.781
Bare	October	0.004	0.759	0.237	0.001
	February	0.013	0.615	0.017	0.547
	June	0.025	0.309	0.011	0.62
	August (2012)	0.036	0.026	0.013	0.226

Waves are expected to have a significant effect on O<sub>2</sub> metabolism through flushing of bottom water trapped within the seagrass canopy or through advective flushing of sediments. Sediment porewater can very rapidly become anoxic, limiting respiration. Advective transport from wave motions can significantly stimulate the O<sub>2</sub> flux through providing both organic material for mineralization and O<sub>2</sub> (Precht and Huettel 2003). Flushing of bottom water can stimulate production through a reduction in boundary layers that allow for faster rates of gas exchange and metabolite release (Mass et al. 2010). Here, I investigate the effects of wave energy using significant wave height

( $H_s$ ) as a proxy for wave energy.  $H_s$  was calculated from Wiberg and Sherwood (2008)

as:  $H_s = 4\sqrt{m_0}$  where  $m_0$  is the variance of the time series of surface water depth

measured from a pressure sensor.

Table A.2.1 shows the statistics for a linear regression analysis of significant wave height and the  $O_2$  flux for day and night  $O_2$  fluxes from all seasons and sites. Wave height was a statistically significant driver for the  $O_2$  flux only 6 out of the 26 datasets with no clear relationship between the time of year or site. I would expect to see wave height as an important driver at all the seagrass sites when the canopy is relatively dense (i.e. all data from the 11 year site and June and August from the 4 year site) as flushing of the canopy is expected to be an important process for gas exchange and  $O_2$  dynamics. I would also expect to see wave height as an important driver at the bare site during very high wind and wave events as sediment permeability may allow for some advective flushing ( $5.8 \times 10^{-12} \text{ m}^2$ ). However, the lack of clear trends between seasons or sites limits the analysis of wave energy. This may be a result of a bias of data collected during calm weather, as during events where wave energy is high, it is often difficult to collect eddy correlation data. During high energy events, algal material or seagrass blades are often suspended and moved around the lagoons, making it likely that the eddy correlation instrument is fouled or the microsensor breaks, limiting the amount of data that can be collected during these types of events.

## Appendix 4 – Data

**Table A.4.1** Daily fluxes from 11 year site.

R, GPP, NEM are daily fluxes calculated from 24 h datasets in  $\text{mmol O}_2 \text{ m}^{-2} \text{ d}^{-1}$ . Max and min are maximum and minimum measured hourly fluxes ( $\text{mmol O}_2 \text{ m}^{-2} \text{ d}^{-1}$ ), Temp is average temperature ( $^{\circ}\text{C}$ ), and PAR is integrated light throughout the day ( $\text{mol photons m}^{-2} \text{ d}^{-1}$ ). August \*\* is from August 2012 where daily data was not available due to fouling, thus August \*\* is the seasonal average, and 15 min max and min.

Season	R	GPP	NEM	Max	Min	Temp	PAR
August	-189.4	155.6	-33.8	870.3	-372.1	29.1	731.4
August	-256.9	192.0	-64.9	448.8	-417.4	29.5	892.4
August	-262.1	231.8	-30.3	546.0	-386.7	30.1	819.9
August	-187.7	173.8	-13.9	594.5	-589.7	31.2	959.8
August	-251.8	156.7	-95.1	376.0	-670.7	32.4	453.4
October	-150.2	115.7	-34.4	647.6	-519.5	20.0	182.8
October	-113.9	179.9	66.0	796.1	-274.4	19.9	238.2
October	-173.4	117.5	-55.9	564.6	-556.5	14.3	185.8
October	-106.9	129.9	23.1	484.6	-462.9	14.3	185.8
February	-57.7	50.8	-6.9	140.1	-122.3	10.0	176.7
February	-43.8	50.6	6.8	136.1	-77.6	9.4	119.8
February	-35.2	54.5	19.3	186.9	-92.9	8.5	211.8
June	-165.5	290.1	124.6	1225.5	-247.7	25.9	548.7
June	-318.1	360.7	42.6	1231.0	-515.8	27.2	657.4
June	-440.4	476.3	35.9	1271.9	-584.8	27.3	667.7
June	-309.6	330.0	20.3	875.3	-556.5	28.8	481.7
June	-343.6	401.9	58.3	977.8	-461.5	28.8	481.7
August **	-196.1	162.4	-33.6	1274.8	-616.4	27.7	331.7

**Table A.4. 2** Daily fluxes from 5 year site.

R, GPP, NEM are daily fluxes calculated from 24 h datasets in  $\text{mmol O}_2 \text{ m}^{-2} \text{ d}^{-1}$ . Max and min are maximum and minimum measured hourly fluxes ( $\text{mmol O}_2 \text{ m}^{-2} \text{ d}^{-1}$ ), Temp is average temperature ( $^{\circ}\text{C}$ ), and PAR is integrated light throughout the day ( $\text{mol photons m}^{-2} \text{ d}^{-1}$ ). August \*\* is from August 2012 where daily data was not available due to fouling, thus August \*\* is the seasonal average, and 15 min max and min.

Season	R	GPP	NEM	Max	Min	Temp	PAR
October	-204.4	148.6	-55.9	736.1	-963.7	19.9	189.0
October	-32.7	55.6	22.9	373.8	-134.9	16.7	424.6
October	-69.1	63.1	-6.0	215.6	-223.8	17.1	394.1
October	-102.8	59.2	-43.6	190.8	-170.3	17.2	234.3
February	-23.9	29.4	5.5	108.9	-46.3	8.8	88.1
February	-61.0	71.0	10.0	237.1	-103.1	13.1	189.8
February	-57.3	66.8	9.5	214.0	-127.8	15.0	383.6
June	-419.5	540.7	121.2	1416.5	-865.9	21.3	685.1
June	-245.5	389.1	143.6	1390.3	-353.8	25.9	264.6
August **	-54.6	45.0	-9.6	509.2	-415.5	27.9	347.7

**Table A.4.3** Daily fluxes from bare site.

R, GPP, NEM are daily fluxes calculated from 24 h datasets in  $\text{mmol O}_2 \text{ m}^{-2} \text{ d}^{-1}$ . Max and min are maximum and minimum measured hourly fluxes ( $\text{mmol O}_2 \text{ m}^{-2} \text{ d}^{-1}$ ), Temp is average temperature ( $^{\circ}\text{C}$ ), and PAR is integrated light throughout the day ( $\text{mol photons m}^{-2} \text{ d}^{-1}$ ). August \*\* is from August 2012 where daily data was not available due to fouling, thus August \*\* is the seasonal average, and 15 min max and min.

Season	R	GPP	NEM	Max	Min	Temp	PAR
October	-38.2	5.8	-32.4	45.9	-124.8	17.4	31.6
October	-7.2	4.9	-2.3	38.9	-29.0	14.5	196.9
October	-27.6	6.3	-21.4	40.0	-53.4	14.5	196.9
February	-12.6	7.8	-4.8	87.1	-51.8	14.0	158.9
February	-35.5	22.6	-12.9	36.2	-75.4	14.0	372.1
June	-30.8	13.2	-17.6	10.2	-55.2	20.9	314.4
June	-34.6	3.1	-31.4	47.7	-167.4	22.1	207.7
June	-36.5	14.9	-21.7	50.8	-51.3	23.4	242.9
August **	-19.6	-13.1	-32.7	55.7	-107.4	26.9	235.1